



Università  
Ca' Foscari  
Venezia

*Corso di Laurea magistrale  
(ordinamento ex D.M. 270/2004)  
in Scienze Ambientali*

Tesi di Laurea

Colloidal characterization and  
leaching testing to support safety  
assessment of nano-enabled  
products for the restoration of  
works of art

**Relatore**

Dott.ssa Elena Semenzin

**Correlatore**

Dott.ssa Elena Badetti

**Laureando**

Virginia Cazzagon  
Matricola 839247

**Anno Accademico**

2016 / 2017



<b>SOMMARIO</b>	<b>4</b>
<b>SUMMARY</b>	<b>6</b>
<b>MOTIVATION AND OBJECTIVES</b>	<b>8</b>
<b>THESIS' STRUCTURE</b>	<b>9</b>
<b>ABBREVIATIONS</b>	<b>10</b>
<b>1. MATERIALS AND METHODS</b>	<b>12</b>
1.1 DEFINITION AND PHYSICO-CHEMICAL PROPERTIES OF NANOMATERIALS	12
1.2 ENGINEERED NANOMATERIALS IN CONSERVATION SCIENCE	17
1.3 SAFETY ASSESSMENT	18
1.4 SAFETY ASSESSMENT IN NANORESTART PROJECT	21
1.5 CASE STUDY	24
1.5.1. <i>Cleaning formulations</i>	24
1.5.2. <i>Surface consolidations systems</i>	26
1.5.3. <i>Coatings for the protection of metal substrates</i>	27
1.6. COLLOIDAL CHARACTERISATION OF ENMS	29
1.6.1. <i>Dynamic Light Scattering</i>	30
1.6.2. <i>Centrifugal Separation Analysis</i>	32
1.7. BIBLIOGRAPHIC RESEARCH ABOUT LEACHING TESTING	35
<b>2. RESULTS AND DISCUSSION</b>	<b>37</b>
2.1. COLLOIDAL CHARACTERIZATION	37
2.1.1. <i>Cleaning formulations</i>	37
2.1.3. <i>Surface consolidation systems</i>	38
2.1.3. <i>Coatings for the protection of metal substrates</i>	43
2.2. LEACHING TESTS	47
2.2.1 <i>Bibliographic search</i>	48
2.2.1.1. <i>Coatings, paints and varnishes</i>	50
2.2.1.2. <i>Plastics and rubber</i>	55
2.2.2. <i>Experimental leaching test</i>	65
2.3. SAFETY ASSESSMENT	69
2.3.1. <i>Cleaning formulations</i>	69
2.3.2. <i>Surface consolidation systems</i>	70
2.3.3. <i>Coatings for the protection of metal substrates</i>	72
<b>3.CONCLUSIONS</b>	<b>75</b>
<b>9. REFERENCES</b>	<b>77</b>
<b>RINGRAZIAMENTI</b>	<b>91</b>

# Sommario

I prodotti a base di nanoparticelle sono state ampiamente utilizzati negli interventi di restauro di opere d'arte per via delle loro peculiari caratteristiche chimico-fisiche che favoriscono la loro interazione con il materiale da restaurare. Tuttavia, gli impatti sulla salute umana e sull'ambiente che potrebbero potenzialmente emergere dall'utilizzo di questi nuovi materiali risultano ancora poco delineati ed è per questo che è richiesta un'adeguata valutazione e gestione dei potenziali rischi associati.

In questo contesto, nell'ambito del progetto EU H2020 NANORESTART, sono state presentate formulazioni nanotecnologiche innovative per la conservazione e il restauro di opere d'arte moderne e contemporanee, sviluppate secondo un approccio Safe by Design (SbD).

La sicurezza delle nuove formulazioni è stata studiata dal gruppo di ricerca in cui è stato svolto questo lavoro di tesi, utilizzando da un lato l'approccio di auto-classificazione del Regolamento Europeo CLP per le miscele di sostanze chimiche, e dall'altro test ecotossicologici sperimentali *in vivo* ed *in vitro*, per poter così sviluppare rispettivamente la seconda e la terza fase dell'approccio SbD, ovvero 'screening hazard assessment' ed 'advanced hazard assessment'.

Nel presente studio, sempre a supporto dell' 'advanced hazard assessment', è stata condotta una caratterizzazione colloidale delle nuove formulazioni mediante Dynamic Light Scattering (DLS) e Centrifugal Separation Analysis (CSA) al fine di studiare il comportamento delle nanoparticelle incluse nelle nuove formulazioni, supportando così sia l'analisi degli effetti che quella dell'esposizione. Le dispersioni sono state analizzate tal quali e, in base al limite di rilevabilità degli strumenti, dopo diluizione nella specifica soluzione utilizzata per i test ecotossicologici. I risultati ottenuti hanno permesso di ricavare informazioni riguardanti il comportamento delle diverse formulazioni e la loro diversa stabilità nella fase di applicazione, ovvero quando la formulazione è applicata nell'opera d'arte dal restauratore.

Inoltre, sempre nell'ambito della fase di 'advanced hazard assessment' ma considerando invece la fase di post-applicazione (ovvero quando l'opera d'arte trattata è esposta a particolari condizioni ambientali), è stata condotta una ricerca bibliografica al fine di identificare una procedura sperimentale adeguata per l'identificazione e la quantificazione di possibili rilasci in ambiente dalle opere d'arte trattate. La procedura selezionata, che consiste in un test di immersione, è stata quindi applicata ad un caso di studio con l'obiettivo di simulare l'esposizione a condizioni ambientali (ad esempio pioggia) di opere d'arte in bronzo trattate con vernici protettive. Il test di immersione si è rivelato un metodo utile per identificare il rilascio di benzotriazolo (BTA) contenuto in due vernici

applicate su dischetti in bronzo, mentre, a causa della presenza di sostanze interferenti, non è stato possibile quantificarne la concentrazione.

Infine, i risultati ottenuti dalla seconda e dalla terza fase dell'approccio SbD sono stati integrati per derivare delle conclusioni sulla sicurezza chimica dei prodotti innovativi proposti ('safety assessment', quarta fase dell'approccio SbD). E' stato quindi possibile concludere che tali prodotti presentano una sicurezza chimica classificabile come "eccellente" o "molto buona", equivalente o migliore rispetto agli analoghi convenzionali già presenti sul mercato. Tuttavia, gli effetti cronici riscontrati e le indicazioni ottenute relativamente alla stabilità di tali prodotti e al possibile rilascio in ambiente di alcuni loro componenti, hanno evidenziato la necessità di prestare attenzione ai loro potenziali impatti sull'ambiente acquatico qualora dovessero essere utilizzati in quantità rilevanti (per usi più ampi rispetto a quello di nicchia relativo alla conservazione dei beni culturali).

# Summary

Nano-enabled products have been largely used in restoration interventions because of their physico-chemical characteristics that favour their interaction with the material to be conserved. However, the human health and environmental impacts that may potentially emerge from these new materials are still little known and an adequate assessment and management of potential risks is required.

In this context, in the frame of the EU H2020 NANORESTART project, innovative nano-enabled formulations for the conservation and restoration of modern and contemporary artworks, developed according to a Safe by Design (SbD) approach, have been presented. The safety of the new formulations was investigated by the research groups in which this thesis' work was carried out, by applying on one hand the EU CLP self-classification approach for mixtures and on the other hand experimental *in vivo* and *in vitro* ecotoxicological tests, in order to implement Step 2 'screening hazard assessment' and Step 3 'advanced hazard assessment' of the SbD approach, respectively.

In this thesis' work, as a support to the 'advanced hazard assessment', the colloidal characterization of the new formulations was performed by means of Dynamic Light Scattering (DLS) and Centrifugal Separation Analysis (CSA) techniques, in order to understand the behaviour of nanoparticles included in the formulations. The dispersions were analysed as produced and, according to the detection limit of the instruments, after dilution in the medium used for ecotoxicological testing. Information regarding the different behaviour of the formulations under dilutions and their stability in the application phase (i.e. when the formulation is applied by conservator to the work of art), were obtained.

Moreover, as an additional support to the 'advanced hazard assessment', but considering the products' post application stage (i.e. when the treated work of art is exposed to indoor or outdoor conditions) a literature review was carried out to identify a suitable experimental procedure for the identification and the quantification of possible product's releases into the environment from treated artworks. The selected procedure, consisting in an immersion test, was then applied to a case study simulating outdoor exposure of bronze works of art treated with a multilayer protective coating (active and passive coatings together) and exposed to environmental conditions (e.g. rain). The applied immersion test resulted to be a useful method to identify the release of a selected substance contained in the active coatings applied on bronze disks, in this case a corrosion inhibitor detectable by UV-Vis spectroscopy at low concentrations. Unfortunately, its quantification was not possible to determine due to the presence of interfering substances in the passive coating.

Finally, the results of Step 2 and 3 of the SbD approach were integrated to derive some conclusions on the chemical safety of the proposed innovative products (Step 4 'safety assessment' of the SbD approach). It was therefore possible to conclude that the proposed products have a "very good" to "excellent" chemical safety, equal or better than their conventional counterparts already present in the market. However, observed chronic effects, results obtained on products' stability as well as on environmental release of some components, highlighted the need to pay attention to their potential impacts on the aquatic environment once their production volume and use would grow (i.e. for a wider use than the niche of cultural heritage conservation).

# Motivation and objectives

The development of highly innovative techniques and technologies for artworks preservation and restoration is providing conservators with new engineered nanomaterials (ENM) and ENM-based formulations that can enhance performance and technical sustainability of art materials (Baglioni and Chelazzi, 2013). However, the human health and environmental impacts that may potentially emerge from these new materials and/or techniques are still little known and requires an adequate assessment and management of potential risks (Hassellöv *et al.*, 2008).

In this context, NANORESTART (NANOmaterials for the REStoration of works of ART) EU project was developed with the aim of assisting formulators in the early steps of development and refinement of these new products. In the project, the stepwise Safe-by-Design (SbD) framework for the sustainability assessment of nano-based products for restoration is proposed, taking into account the current EU legislative context as well as the specific features of the innovation process in the restoration field, which demands a high interaction between the product developers/formulators and the restorers ( Baglioni *et al.*, 2015; Ormsby *et al.*, 2016).

In order to investigate the safety of the innovative formulations, EU CLP self-classification approach for mixtures and experimental in vivo and in vitro eco-toxicological tests were applied by research groups in which this work was carried out, considering the Step 2 (screening hazard assessment) and Step 3 (advanced hazard assessment) of SbD framework.

Advanced hazard assessment, and more specifically the exposure assessment, was supported by this work of thesis, with the aim to get information regarding the application phase (i.e. when the formulation is applied by conservator to the work of art) and the post-application phase (i.e. when the treated work of art is exposed to indoor or outdoor conditions).

Therefore, the objectives of the present study were:

1. To perform a colloidal characterisation of the new formulations in order to support the advanced hazard assessment in the application phase
2. to define a suitable method of leaching test, after conducting a literature research, in order to support the advanced hazard assessment in the post-application phase
3. To combine results from the previous steps (i.e. the Step 2 and Step 3) deriving information regarding the Step 4, as the safety assessment.

# Thesis' structure

This work of thesis is divided into a methodological part, where the materials and methods of the study are presented, and an applicative one, in which the presented methodologies are applied to the case study and the results obtained are described and discussed.

Specifically, in chapter 1 the definition of nanomaterials and their application in conservation science is described (1.1, 1.2), and the safety assessment is illustrated (1.3, 1.4). This part is followed by the presentation of the case study and the families of products investigated (1.5), the description of the two techniques used for the colloidal characterisation, as DLS and CSA techniques (1.6), and finally the literature research on leaching tests conducted (1.7).

In chapter 2 results and discussion were showed, containing descriptions of the results obtained by the colloidal characterisation, dividing this chapter by the three families of products investigated (2.1), followed by the description of the adaptations of a case study of Zuin *et al.* 2014 and the leaching test conducted (2.2), and finally, safety assessment results were described dividing the chapter by three families of products (2.3), as performed in chapter 2.1.

The final chapter is a description concerned the conclusions.

# Abbreviations

AFM: Atomic Force Microscope

APS: Aerodynamic Particle Sizer

ASTM: American Society for Testing and Materials International

ATR-IR: Attenuated Total Reflection Infrared spectroscopy

CLP: Classification, Labelling and Packaging

CMC: Carboxymethyl cellulose

CPC: Condensation Particle Counter

CSA: Chemical Safety Assessment

CSA: Centrifugal Separation Analysis

DGT: Diffusive Gradient in Thin films

DLS: Dynamic Light Scattering

DMTA: Dynamic Mechanical Thermal Analysis

DNEL: Derived No Effect Level

DSC: Differential scanning calorimetry

EC: European Commission

EC: Effective Concentration

ECHA: European Chemicals Agency

EDS: Energy Dispersive Spectroscopy

EDX: Energy Dispersion X-ray Spectroscopy

EIS: Electrochemical Impedance Spectroscopy

ELPI: Electrical Low Pressure Impactor

ENMs: Engineered Nano-Materials

ENPs: Engineered Nano-Particles

ES: Exposure Scenario

FESEM: Field Emission Scanning Electron Microscopy

FMPS: Fast Mobility Particle Sizer

FTIR: Fourier Transform Infrared

GHS: Globally Harmonised System

HPLC: High Performance Liquid Chromatography

HR-SEM: High resolution Scanning Electron Microscopy

ICP-MS: Inductively Coupled Plasma Mass Spectrometry

ICP-OES: Inductively Coupled Plasma Emission Spectroscopy  
IEC: International Electrotechnical Commission  
ISO: International Organisation for Standardisation  
ITS: Integrated (or Intelligent) Testing Strategy  
LC-MS: Liquid Chromatography-Mass Spectrometry  
LC-MS/MS: Liquid Chromatography-Mass Spectrometry  
LSCM: Laser Scanning Confocal Microscopy  
MPS: Mini Particle Sampler  
NMs: Nanomaterials  
NMR: Nuclear Magnetic Resonance  
NOEC: No Observed Effect Concentration  
NOM: Natural Organic Material  
NPs: Nanoparticles  
NTA: Nanoparticle Tracking Analysis  
OC: Operational Conditions  
OECD: Organisation for Economic Co-operation and Development  
PNEC: Predicted No Effect Concentration  
RA: Risk Assessment  
RCF: Relative Centrifugal Force  
RCR: risk Characterisation Ratio  
REACH: Registration, Evaluation, Authorization of Chemicals  
RMM: Risk Management Measures  
ROS: Reactive Oxygen Species  
RPM: Rotation Per Minute  
SbD: Safe by Design  
SEM: Scanning Electron Microscopy  
SMPS: Scanning Mobility Particle Sizer  
TEM: Transmission Electron Microscopy  
TGA: Thermal gravimetric analysis  
TMP-ESEM: Turbo Molecular Pump Environmental Scanning Microscope  
VOC: Volatile Organic Compound  
XPS: X-ray Photoelectron Spectroscopy  
XRD: X-ray Diffraction

# 1. Materials and methods

## 1.1 Definition and physico-chemical properties of nanomaterials

Nanotechnologies are the set of technologies that enable the manipulation, control, and design of matter within the nanoscale range ( $10^{-9}$ -  $10^{-7}$  m) in order to develop new applications/products or enhance the capabilities of existing ones (Lynch *et al.*, 2014). Nanotechnologies includes nanomaterials (NMs), which in turn encompass nanoparticles (NPs), nanofibers, thin films, nanoporous materials and nanocomposites. NMs are defined by the European Commission as ‘a natural, incidental or manufactured material containing particles [...] and where, for 50 % or more of the particles in the number size distribution, one or more external dimensions is in the size range 1 nm - 100 nm’ (Piccinno *et al.*, 2012), while NPs as a ‘nano-object with all three external dimensions in the nanoscale’ (ISO, 2008).

According to this definition, NMs can therefore be classified into three main categories based on their source: natural, incidental and manufactured. Natural NMs are defined as materials that belong to the natural environment, without human modifications or processing (Sutherland, 2010). The second category of nanoscale objects to which humans and the environment could be exposed are the incidental NMs, which are inadvertently produced as a result of human activities. The third type of NMs are known as engineered nanomaterials (ENMs), which are purposefully produced by humans to exploit their properties in a variety of applications. As matter of fact, their unique physicochemical properties have exponentially increased the development of ENM-based consumer products (Piccinno *et al.*, 2012; Mitrano *et al.*, 2015), considering properties such as surface morphology, crystalline structure, water solubility and photocatalytic activity (Lynch *et al.*, 2014; Wohlleben *et al.*, 2015). This has led to the production of materials containing NPs in many industrial area, including cosmetics, paints and coatings, electronics, textiles and sport items, food packaging, and energy storage (Lynch *et al.*, 2014).

An explicative scheme of NMs characteristics have been reported by Lead and Smith (2009) and is represented in Figure 1.

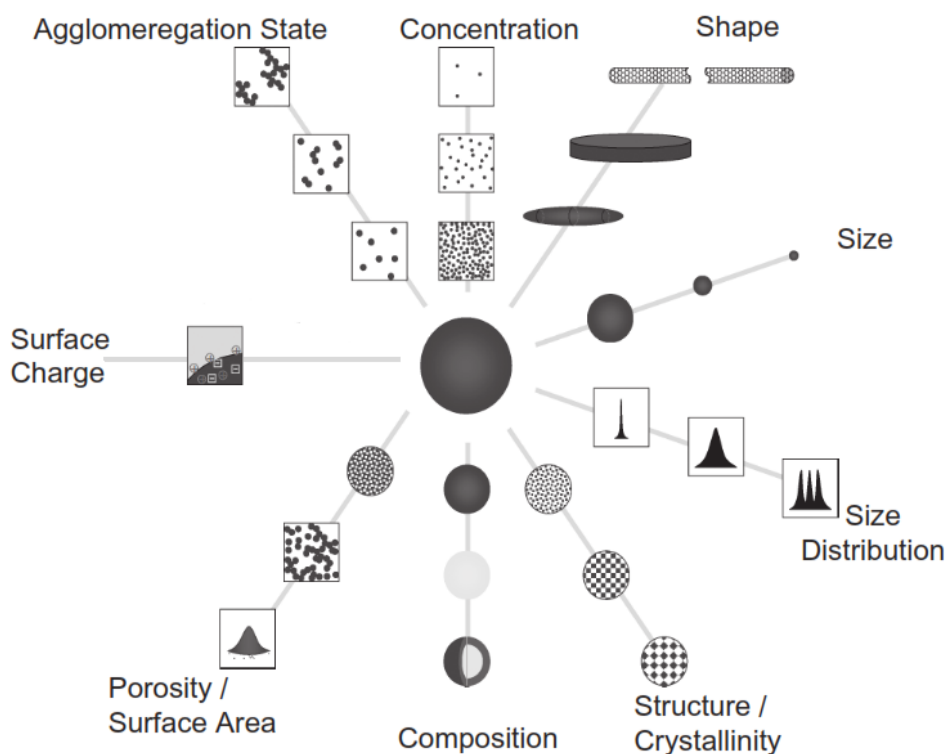


Figure 1. Representation of the main characteristics of nanoparticle, proposed by Lead and Smith (2009).

NMs have a much larger surface area per unit mass compared with bigger particles, and the increase in the surface-to-volume ratio together with the high number of surface atoms determine an increase in the particle surface energy, which may render them more reactive with respect to their corresponding bulk materials (Wohlleben *et al.*, 2015). Among the whole set of NMs intrinsic properties listed in Figure 1, one of the main interested feature is NMs surface chemistry, because it drives the interactions between NMs and its surroundings (e.g. adsorption of ions and biomolecules onto a nano-object's surface). Thus, the study of this specific characteristic could be very useful in elucidating the physico-chemical relationship at the nano-bio interface. Surface area can be expressed as the mass specific surface area ( $\text{m}^2/\text{g}$ ) or as the volume specific surface area ( $\text{m}^2/\text{cm}^3$ ), where the total quantity of the area has been normalized to either the sample's mass or volume (ISO/TR 13014:2012). The high reactivity of the nano-sized materials indeed determines the possibility to create aggregates and agglomerates. In general, the surface area of nano-objects, as well as their agglomerates and aggregates, can be described as 'the quantity of accessible surface of a sample when exposed to either gaseous or liquid adsorbate phase' (Wohlleben *et al.*, 2015).

According to ISO/TS 27687:2008, 'aggregates are strongly bonded or fused particles for which the resulting external surface area may be significantly smaller than the sum of calculated surface areas of the individual components' (Wohlleben *et al.*, 2015). A number of factors can affect the strength

of attraction among NPs in an aggregate and therefore the potential for disaggregation. They can be more easily disaggregated indeed when their surface coatings include organic macromolecules, because of the weaker attractions between NPs in the aggregate. The presence of these macromolecules is controlled by many parameters as the solution composition, pH, ionic strength, time, and flow conditions (Robinson and Lawson, 2016).

The formation of agglomerates occurs when particles or aggregates are bonded together with weak forces (i.e. van der Waals forces). The possibility to form an aggregate or an agglomerate is mainly dependent on the probability of NP collisions and the surface energy possessed by the particles when the interaction occurs (Robinson and Lawson, 2016). This collision can take place among NPs of the same type (homoaggregation) and/or with different particles in the environment (e.g. natural colloids), i.e. heteroaggregation. As a consequence of the collision among particles, whether of the same type or different, the number concentration of NPs in the suspension decreases, with a concomitant increase in their effective size (e.g. hydrodynamic diameter); it is also possible to observe a decrease in the “available” surface area of the materials with a decreasing of the reactivity (Robinson and Lawson, 2016). Although homoaggregation of NPs has been extensively studied (Gallego-Urrea *et al.*, 2014), heteroaggregation is the key phenomenon to be determined under realistic environmental situations, where the expected NPs concentrations are far less than natural colloids (Praetorius *et al.*, 2014). Unfortunately, the investigation of NPs heteroaggregation is still in its infancy because, due to the complexity of the matrix, it comprises the need to develop new approaches with respect to the conventional methods used to study homoaggregation. Therefore, conventional techniques, usually used for assessing homoaggregation of NPs in liquids (e.g. scattering techniques like DLS) cannot be directly applied to investigate NPs heteroaggregation.

Another peculiarity of NMs is their extremely wide diversity in terms of sizes, shapes and compositions (Wohlleben *et al.*, 2015). The particle size and particle size distribution play a crucial role in the characterisation of NMs, because the dimension of nano-objects is extremely important in many areas of science and technology. Both these parameters in fact, have a significant effect on properties like mechanical strength, chemical reactivity, and electrical and thermal properties of nano-objects (Wohlleben *et al.*, 2015).

Many properties of nano-objects, such as dissolution rate, aggregation behaviour, or availability of reactive sites are strongly linked to the shape of the nano-object, which in turn is mainly determined by the symmetry of its constituting crystallites, if any, and by the minimization of the bulk and surface free energy. ENMs of identical composition indeed can be produced in a variety of shapes including spheres, fibers, and plates, and each of these shapes may influence the different physical and chemical properties.

The physico-chemical characterization of a sample should include its chemical composition, crystalline structure and impurities, if any. The chemical composition refers to the entities composing the material and, together with the crystallinity of the ENM, it gives specific properties to the nano-object. Chemical composition of the outermost layers of a nanomaterial highly defines its energy and reactivity, as well as surface charge, while impurities delivered at any stage of NM production can affect the evaluation of its biological toxicity (Wohlleben *et al.*, 2015).

The impossibility to exactly predict nanomaterial fate and transformation in complex biological and environmental media is often directly connected with the lack of understanding of the dynamics at the surface of an ENM. Once discharged into complex environment matrices, uncoated or coated ENMs could undergo transformations either on the surface or bulk and/or interactions that naturally occur with macromolecules, including proteins and polysaccharides (Mudunkotuwa and Grassian, 2015; Robinson and Lawson, 2016). Upon uptake by biological organisms, ENMs may be transformed through their interaction with bio macromolecules that can act as a coating, transforming their outer surface (Robinson and Lawson, 2016). A representation of the main chemical and physical transformations occurring on NPs surface are represented in Figure 2.

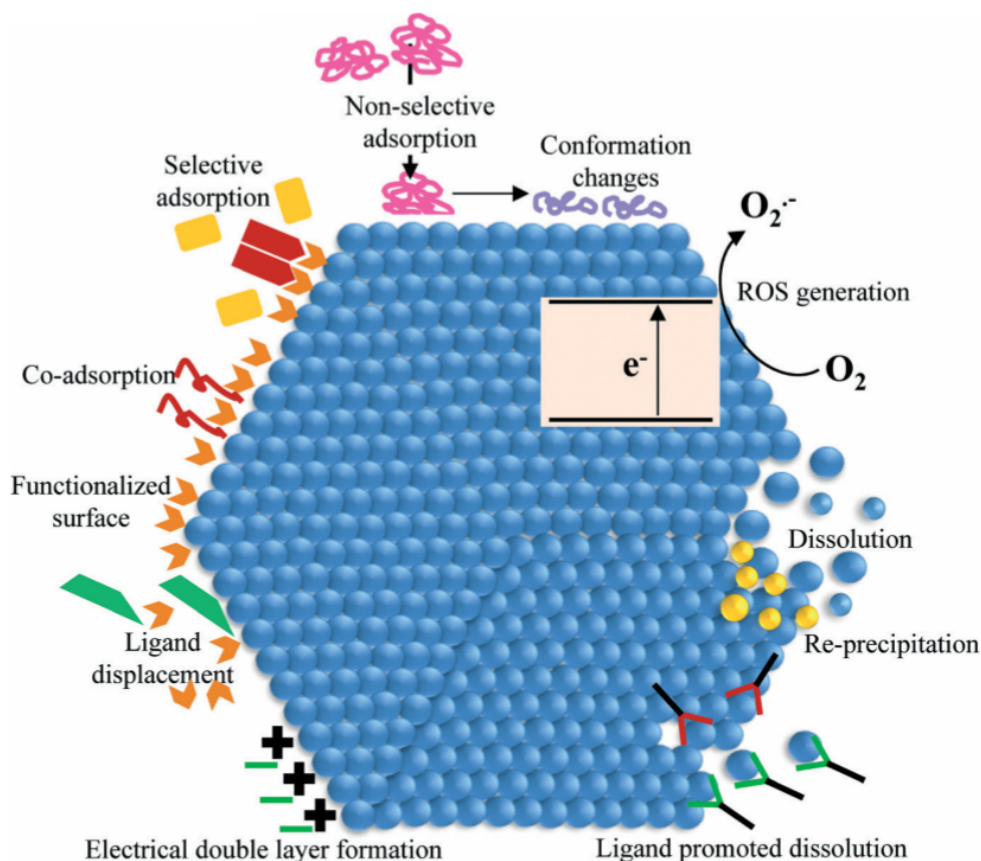


Figure 2. Representation of physicochemical transformations occurring on the surface of nanoparticles, revised by (Mudunkotuwa and Grassian, 2015).

It is therefore important to consider nanoparticles as dynamic entities that undergo transformations that depend on pH, ionic strength and composition of the solution. These processes include surface adsorption, ligand displacement, dissolution, re-precipitation, co-adsorption and reaction chemistry. One of the property controlling surface modifications is the surface charge; ENMs positively charged for example present higher affinity with particles negatively charged creating electrostatic interactions. This property is very much dependent on the pH variations and the ionic strength of the medium, resulting in completely different cellular uptake, toxicity and immune responses. For this reason, it is possible to functionalise these NPs for creating stable suspensions by adding precise functional groups (Mudunkotuwa and Grassian, 2015).

An example of non-selective adsorption is the effect of  $\alpha$ -Fe<sub>2</sub>O<sub>3</sub> NPs on bacteria. The function of antimicrobial peptide can be impaired by adsorption onto NP surfaces, causing an antimicrobial peptide function impairment (Borcherding *et al.*, 2014). Surface ligand adsorption can also cause the dissolution of NMs and the generation of ions, and even smaller NPs with enhanced mobility and uptake properties (Mudunkotuwa and Grassian, 2015).

Some molecules can be co-adsorbed on the surface of the NM, conferring multiple functionalities upon a particular NM system. This can result in terms of toxicity studies in uncontrolled uptake and distribution within a given biological system. Many studies in the literature have provided evidence of altered aggregation behaviour in the presence of natural organic matter (NOM), which is a key indicator of changing surface properties in its presence. NOM adsorption in many of these cases has been shown to promote aggregation but at the same time reduce the uptake and toxicity to test species such as soil organisms (Mudunkotuwa and Grassian, 2015).

Another important characteristic of a NP that occurs when it is in a biological medium containing different components, is determined by the different affinities of each component towards the NP surface. Depending on the initial surface ligand affinity, indeed the NP surfaces may or may not undergo further changes, and surface ligands with relatively low affinity can be easily displaced by those with higher affinity (Mudunkotuwa and Grassian, 2015).

Properties like the small particle size, chemical composition, and the presence of a large reactive surface area can catalyse the formation of reactive oxygen species (ROS), which are chemically reactive molecules containing oxygen (Nel *et al.*, 2006). Examples of ROS include peroxides, superoxides, hydroxyl radical and singlet oxygen. ROS are normally produced in every organism cell at low or moderate concentration by the mitochondrial and cytoplasmic oxidation systems for maintaining all the normal physiological processes. However, at higher concentrations of ROS, inner proteins and lipid can be denatured, and structural alteration of DNA can occur in the cells causing mutations and alterations in gene expression (Feng *et al.*, 2015).

Other important parameters for the characterisation of NPs are solubility and dispersibility. According to ISO 7579:2009, solubility is the maximum mass of a nanomaterial that is soluble in a given volume of a particular solvent under specified conditions. A nano-object is expected to exhibit greater solubility and faster dissolution than a bigger material of the same composition, although, because of the small particle size, it can be difficult to distinguish when a NM is dispersed or dissolved. It is crucial to recognize that dispersibility is described as the degree to which a solid material is uniformly distributed in another material (a dispersing medium), and the resulting dispersion remains stable. In general, the main difference between solubility and dispersibility is that in solubility solid molecules have to be strongly disassociated by the process, while there is no significant disassociation involved in a phase that has been dispersed into another (Wohlleben *et al.*, 2015).

## 1.2 Engineered nanomaterials in conservation science

Regardless of their nature, artefacts are irremediably exposed to several degradation agents: physical erosion, chemical degradation, temperature, relative humidity, light, and microorganisms, all accounting for the natural aging of art materials. Moreover, anthropogenic activities increase the concentrations of SO<sub>x</sub>, NO<sub>x</sub>, and VOC (volatile organic compound) gases in the atmosphere that can lead to the corrosion of artistic substrates, contributing to the degradation of works of art. Depending on the type of artistic substrate, different tasks are necessary for conservation purposes (Baglioni and Chelazzi, 2013). In this context, ENMs are emerging as successful materials for artworks preservation because of their capability in enhancing performance and technical sustainability of art materials (Baglioni and Chelazzi, 2013). For example, the incorporation of relatively low percentages of NPs in paints or coatings, can lead to dramatic improvements in mechanical properties, thermal stability and adhesion (Boumaza *et al.*, 2016). Therefore, all major paint and coating companies are investing on research and development to formulate new performing paints capable to improve many chemical and mechanical properties (Khanna, 2008). Because of the complexity of artistic and historical substrates, conservation science has explored different routes, developing several approaches for solving conservation issues. For instance, new resins that are more stable than natural ones with similar optical properties, have been applied as varnishes for the restoration of paintings (Shchukin *et al.*, 2006).

In the field of stone conservation, Ca(OH)<sub>2</sub> (calcium hydroxide) is one of the most promising products for stone's consolidation because it is easily converted into calcium carbonate (CaCO<sub>3</sub>) as result of

carbonation, when exposed to atmospheric CO<sub>2</sub> under moist conditions (Baglioni and Chelazzi, 2013).

Another example is provided by coatings incorporating nano SiO<sub>2</sub> and used to improve abrasion, increase the resistance and add hydrophobic properties to the stone surface (Al-Kattan *et al.*, 2015). Both hydrophilic and hydrophobic silica are used in solvent-borne coatings to improve the anti-settling additives for pigments (Zuin *et al.*, 2014).

The addition of Ag-NPs in paints for outdoor applications on building facades, instead, determines an antimicrobial effect derived from the activity of silver (Kaegi *et al.*, 2010), while photoactive titanium dioxide (TiO<sub>2</sub>) ENPs are used to optimize the mechanical properties of the products and to give the paint self-cleaning properties through photocatalytic and hydrophilic properties (Zuin *et al.*, 2014).

Zirconia nanoparticles have revealed outstanding properties such as the high strength and fracture toughness, excellent wear resistance, high hardness, chemical resistance, corrosion resistance performance, that can be used to reinforce coatings for metal substrates (Mirabedini *et al.*, 2012).

Moreover, additional new nano-enabled products are currently under development by private companies as well as research institutes in the frame of national and international research projects (e.g. European projects NANORESTART and NanoCathedral). Therefore, as it is done for other market sectors in which nanotechnology plays an important role, risks concerning human health and the environment that could emerge from exposure to NPs for restoration should be estimated through an appropriate safety assessment, a systematic procedure described in Chapter 3.

Indeed, despite the increasing development and application of new nanomaterials and nanotechnologies in restoration, research concerning a “green” (i.e. safer) approach to the conservation of cultural heritage is still needed, which should consider the entire life-cycle of these products (Balliana *et al.*, 2016).

### 1.3 Safety assessment

From a regulatory point of view, in Europe the CLP (European Commission, 2008) and the REACH (European Commission, 2006) regulations represent the references for the safety assessment and management of chemicals when they occur as substances or in mixtures and therefore can also be used for nano-enabled products for restoration.

The CLP (Classification, Labelling and Packaging) is a European Union regulation which conform the EU system of classification, labelling and packaging of chemical substances and mixtures to the

Globally Harmonised System (GHS). The purpose of CLP regulation (EC No 1272/2008) is to ensure a high level of protection of health, especially for workers, and the environment, and the free movement of substances and mixtures in the European area. CLP requires to classify, label and package the hazardous chemicals of substances and mixtures appropriately before placing them on the market. In this context, classification of hazards is the starting point for hazard communication and it is a process involving identification of the physical (indicated PH, e.g. explosives or flammable liquids), health (indicated H, e.g. skin corrosion, toxic for reproduction) and environmental (indicated ENV, hazardous to the aquatic environment) hazards of a substance or a mixture, followed by the comparison of those hazards (including degree of hazard) with defined thresholds. Under CLP, a manufacturer, importer or downstream user applies the following three steps to arrive at a self-classification of a substance or a mixture (ECHA, 2017):

- identification and examination of relevant available information regarding the potential hazards of a substance or mixture;
- comparison of the information (data) with the classification criteria; and
- decision on whether the substance or mixture must be classified as hazardous in relation to the hazard classes or differentiations provided in CLP Annex I, and the degree of hazard, where appropriate.

REACH (Registration, Evaluation, Authorisation of Chemicals) is a EU regulation adopted to improve the protection of human health and the environment from the risks of chemicals.

Under REACH (EC No. 1907/2006) companies are responsible for collecting information on the properties and uses of the substances, and to communicate to ECHA (European Chemicals Agency) through a registration dossier containing the hazard information, an assessment of the risks, and how these risks should be controlled. ECHA and the Member States evaluate the information submitted by companies in order to clarify if a given substance constitutes a risk to human health or the environment.

For substances produced/imported in amounts higher than 10 tonnes/year, REACH requires the Chemical Safety Assessment (CSA) along their life-cycle. A CSA should include ‘all available data and information on the identity, physicochemical and (eco) toxicological properties, uses, emissions, exposures, environmental fate and behaviour of a substance’ (ECHA, 2007a, 2007b, 2007c) (Hristozov *et al.*, 2012).

It therefore requires a risk assessment (RA) that is ‘a process intended to calculate or estimate the risk to a given target organism, system or (sub) population, including the identification of attendant uncertainties, following exposure to a particular agent, taking into account the inherent characteristics of the agent of concern as well as the characteristics of the specific target system’ (OECD, 2003).

Results obtained are then collected in a chemical safety report, in which hazard and exposure data are considered together to assess the risk of a substance under REACH regulation.

The exposure assessment generally starts with the description of one or more initial exposure scenarios (ES), addressing how a chemical is used by workers and/ or consumers in one or several stages of its lifecycle, from synthesis to disposal (Hristozov *et al.*, 2012). Exposure is likely highest for workers, although product specific evaluations should consider consumer uses, wear, disposal, and potential for environmental release and fate for products containing nanomaterials (Tsuji *et al.*, 2006). REACH distinguishes between "initial" and "final" ES. The "initial" ES address how a substance is used throughout the supply chain at the time of the assessment, while the "final" scenarios include the recommended operational conditions (OC) and risk management measures (RMM) under which the risks arising from the uses of the compound are fully controlled (ECHA, 2007c). Then, the exposure has to be estimated for the different routes under the conditions of use described in the initial ES.

According to the REACH Guidelines (ECHA, 2007b), the classification and labelling of the hazard of a substance have to be addressed, threshold levels (e.g., DNEL, PNEC) for human health and/or the environment should be derived and it should be even determined if the compound can be classified as persistent, bioaccumulative and toxic.

In the risk characterisation, the final step of the CSA, the derived exposure estimates are compared to these threshold levels in order to obtain risk characterisation ratios (RCRs). More, specifically, the results of exposure and hazard assessments are combined to derive conclusions on the safety of the formulations in each life cycle stage, including the identification of any hot-spot (Gottardo *et al.*, 2017). Risks to human health (for workers) or environmental compartments can be estimated through qualitative or semi-quantitative, or quantitative methodologies, depending on the typologies of hazard and exposure information and data available from previous step (Hristozov *et al.*, 2016).

The paradigm for risk assessment of chemicals included in REACH is considered applicable to NMs if properly adapted to address the complexity associated with their identity, biological and environmental interactions (OECD and European Commission, 2012) (EFSA, 2010). Indeed, the application of a RA for NPs in the last years has been studied by many governmental and international organisations, industry associations and research institutes, concluding that multiple deficiencies of toxicity and exposure data makes it impossible to perform sound risk assessment of ENMs (Hristozov *et al.*, 2012). In fact, limited availability for ENM about release, exposure, toxicological and characterisation data is encountered at all the steps of risk assessment (Dhawan *et al.*, 2017). This has led to a significant increase in the research activities in Europe and in the United States, intended to

filling these data gaps and thus facilitating the estimation of the hazards and risks from ENMs in order to create a robust RA.

## 1.4 Safety assessment in NANORESTART project

Despite an increasing attention in recent years to “green restoration” of cultural heritage through developing safer and “greener” technologies (Balliana *et al.*, 2016), very few works performed actual assessment of health and environmental risks by means of experimental or modelling techniques (Ferrari *et al.*, 2015; Tedesco *et al.*, 2015; Turk *et al.*, 2017) and an overarching framework for assessing the sustainability of the nano-enabled products used in the restoration of cultural heritage is currently lacking.

For this reason, in the frame of the NANORESTART (NANOmaterials for the REStoration of works of ART) EU project a stepwise Safe by Design (SbD) framework for the sustainability assessment of nano-based products for restoration was proposed, taking into account the current EU legislative context (i.e. CLP and REACH regulations) as well as the specific features of the innovation process in the cultural heritage restoration field, which demands a high interaction between the product developers/formulators and the restorers ( Baglioni *et al.*, 2015). This framework was developed with the aim of assisting formulators in the early steps of development and refinement of these new products. In addition to support efficient innovation pathways, the framework is expected to facilitate communication with conservators for selection and use of safer and more sustainable nano-based products in different conservation contexts.

Such a framework explicitly incorporates the SbD concept (Movia *et al.*, 2014) and includes the following five steps: step 0) drawing the state of the art assessment; step 1) developing initial formulations; step 2) screening hazard assessment; step 3) advanced hazard assessment; step 4) safety assessment and finally, step 5) sustainability assessment.

While all these steps have been implemented in the NANORESTART project, this thesis work focused only on step 3 (by performing colloidal characterisation and by defining a suitable method for leaching testing, to support the advanced hazard assessment, as explained in Chapter 1.6 and 1.7), and 4 (by structuring the safety assessment, as explained in Chapter 2.3). A brief description of all the steps will follow.

Step 0 of the SbD approach is a detailed assessment of restoration and conservation products already on the market with specific properties and functionalities, in order to generate new product ideas, considering technical (e.g. compatibility with artistic materials), environmental (e.g. toxicity of

ingredients), social (e.g. ethical criteria such as reversibility of treatment), and economic (e.g. cost of the final product) criteria.

According to the results of the previous step, in Step 1 formulators propose a set of innovative formulations for a specific functionality, taking into account the final goal of developing safer products compared to the existing ones.

In the Step 2, the environmental performance of innovative formulations proposed in Step 1 is checked by a screening hazard assessment. For this purpose, the EU CLP self-classification approach for mixtures is applied in order to derive the health (H) and environmental (ENV) hazards potentially associated with the innovative products. Accordingly, formulators can adjust the initial formulation in order to reduce its hazard or decide to discard it in case an adjustment to the composition would negatively impact its technical performance.

In the Step 3, an advanced hazard assessment is performed in which computational as well as experimental approaches could be adopted, according to an Integrated Testing Strategy. An Integrated (or Intelligent) Testing Strategy (ITS) is a hierarchical, resource-effective testing scheme consisting of a set of decision nodes, allowing for taking different routes for information gathering and inference for decision-making about a chemical's hazard or risk (van Leeuwen and Vermeire, 2007).

In the NANORESTART ITS, three tiers are foreseen. In the first tier, a set of ecotoxicological tests are proposed according to the CLP regulation, including acute tests with crustaceans (48-h), algae (72-h) and Microtox® test. Only formulations with a  $EC_{50} < 1$  mg/l for at least one species are classified as acutely toxic (Acute I). If this criterion is not met for any species, the toxicological testing should move to tier 2 which focuses on the long term (chronic) effects. *D. magna* reproduction test is proposed in this step for characterizing long term (21 days) effects on survival, time to first brood and number of offspring produced per female exposed to chemicals and mixtures. Aim of the chronic test with *D. magna* is the identification of the NOEC (No Observed Effect Concentration), namely the maximum tested concentration providing a response (in this case offspring production and survival) not significantly different from the control. According to CLP regulation, a NOEC in the range 0.1-1 mg/l classifies a formulation as “Chronic 3”, if in the range 0.01-0.1 mg/l classifies it as “Chronic 2”, whilst a  $NOEC \leq 0.01$  mg/l classifies it as “Chronic 1”, the most hazardous class for long-term effects. The third and last tier is aimed at the exploration of possible effects that cannot be detected by applying acute and chronic toxicity test, such as cytotoxicity, DNA-damage and mutagenicity. To this end, the set of bioassays has been expanded with the addition of the umu- and SOS-Chromotest systems (ISO 13829:2000), two short-term test systems based on the detection of chemically-induced DNA lesions that could lead to DNA mutations or SOS response (bacterial error prone repair system) to bacterial strains that have been genetically engineered.

Finally, to support exposure assessment, colloidal characterisation as well as leaching testing are performed to get more information regarding the behaviour and possible exposure to the nano-enabled products (as will be described in details in chapters 2.1 and 2.2).

In the Step 4, the results of exposure and hazard assessments performed in Step 2 and 3 are combined in the safety assessment to derive conclusions on the safety of the formulations in each life cycle stage and identify any hot-spot.

In this work, in order to assess the overall safety of the innovative formulations, the results of hazard and exposure assessment are expressed according to five and four classes, respectively (Figure 3). By combining each of them in the control banding matrix, safety is assessed by using a simple colour code, from the greenest top left corner (i.e. excellent level of safety) to the reddest bottom right corner (i.e. bad level of safety).

RMM/ no RMM applied		HAZARD				
		0	1-2	3-4	5-6	>6
EXPOSURE	negligible					
	low					
	medium					
	high					

Figure 3. Safety assessment matrix

The five hazard classes correspond to the number of H and ENV hazards was assigned to a specific formulation according to the results obtained by the application of the CLP self-classification approach. When formulation's toxicity and ecotoxicity are also experimentally tested, these results can be used to adjust hazard classification in the matrix (e.g. by not counting "hazard to the aquatic environment" if such environmental hazard is not confirmed by experimental tests performed on the formulation).

Considering the application phase (i.e. when the formulation is applied by conservator to the work of art), since the hazardousness is mainly driven by volatile components (classified for e.g. eye irritation, respiratory tract irritation, acute toxicity), while nanomaterials represent only a very small percentage in the mixture composition, it was decided to define the four exposure classes according to the concentration (%w/w) of hazardous volatile components in the formulation. More specifically, exposure is classified as follows: *negligible* when the concentration of hazardous volatile components is lower than 1% or when all recommended Risk Management Measures (RMM; e.g. gloves, goggles,

suitable ventilation) are applied; *low* when the concentration of hazardous volatile components is between 1% and 10% and recommended RMM are not applied; *medium* when the concentration is between 11% and 50% (with no RMM); and finally, *high* when the concentration is higher than 50% (with no RMM).

For the post-application phase, a different approach should be used, based on the identification (and possible quantification) of environmental releases of NPs or other chemicals from the product applied to the work of art and exposed to environmental conditions. To this end suitable leaching tests must be performed (as explained in Chapter 2.2).

## 1.5 Case study

The ENM-based formulations proposed within the NANORESTART project can be classified in 5 different product families: 1) cleaning systems, 2) surface consolidation systems, 3) coatings for the protection of metal surfaces, 4) coatings for the protection of plastic surfaces and 5) sensing and diagnostic systems for detection of degradation products. In this study only the first three families were investigated, with the aim to understand their environmental behaviour (as explained in Chapter 1.4), and thus support both the integrated testing strategy (ITS) and the safety assessment of such innovative products.

### 1.5.1. Cleaning formulations

Cleaning of a work of art involves the removal of any undesired material from artistic or historical surfaces without damaging the original artefact by means of different processes such as mechanical stress, swelling, leaching of components, discoloration (Baglioni *et al.*, 2015).

Cleaning mainly consists of the selective removal of dirt, grime (greasy material, dust, etc.), and natural or synthetic polymers of coated movable and immovable works of art from the surface.

In the past, the application of natural varnishes has been largely performed and has been traditionally adopted by easel painting artists for enhancing the visual properties of artworks. In addition to improving the appearance, the use of such materials was adopted in order to provide hydrophobic properties and surface protection in a vast number of different artistic substrates (Baglioni *et al.*, 2013).

Art surfaces, particularly those made of highly viscous paints such as acrylic paints, are exceptionally difficult to clean and they readily attract dirt and dust particles. Particulate matter indeed can be incorporated into the paint layer over time, causing a difficulty of removal with conventional solvents without significantly affecting the authentic paint layer but altering important surface characteristics (Ormsby and Learner, 2014).

An important feature of innovative cleaning formulations is that aqueous amphiphilic systems allow a significant decrease in the amount of organic solvents involved in a typical cleaning procedure, therefore depressing the system's toxicity and environmental impact. In addition to that, regardless of the type of micro emulsion or micellar solution applied, the use of a confining system to trap a micellar solution or micro emulsion is always encouraged in order to have fine control of the cleaning action (Baglioni *et al.*, 2013).

In the NANORESTART project, the cleaning of modern and contemporary works of art has been addressed by developing either micellar system, oil-in-water (o/w), water-in-oil (w/o) and oil-in-oil (o/o) systems. Out of them, most promising o/w systems were selected with the aim to decrease the solvent content of the cleaning formulations and the amount of surfactants used, while maintaining effective removal of unwanted materials. Oil-in water (o/w) micro-emulsions are based on an organic solvent dispersed into nano-sized surfactant micelles surrounded by a continuous water phase (Figure 4). These systems are highly effective in the removal of surface dirt and detrimental coatings from the surface of artefacts without dropping residual parts, as resulted by testing them on paintings, wall paintings, paper and metals.

The three investigated formulations: AM5, G1 and G1-Ncap are water-based systems with small content of "green" and low-toxicity solvents, such as diethyl carbonate, propylene carbonate, methyl ethyl ketone, ethyl acetate, and 2-butanol. AM5 contains both ionic (BioSoft N91-6) and non-ionic surfactants. G1 contains the same ionic surfactant as AM5 but in lower content. Finally, G1-Ncap is similar to G1 but contains a reagent for polymer synthesis (Ncap) instead of the ionic surfactant.

Ethanol and xylene/toluene (50/50) were indicated by products' developers as suitable conventional products for comparison purposes.

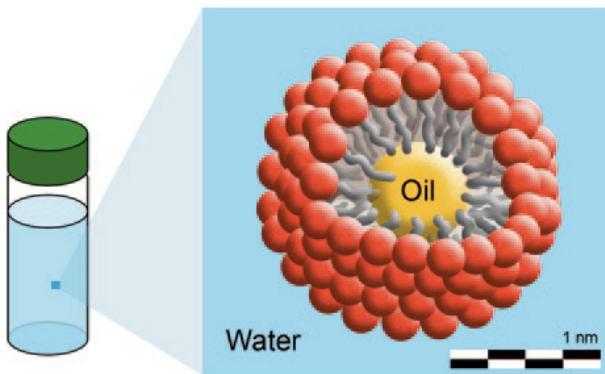


Figure 4. An oil-in-water (o/w) microemulsion, where organic solvents are dispersed into nano-sized surfactant micelles surrounded by a continuous water phase, revised of Baglioni, Chelazzi and Giorgi (2015).

### 1.5.2. Surface consolidations systems

Another class of works of art subjected to degradation are cellulose-, parchment-, and leather-based artefacts, which are threatened mainly by hydrolysis and oxidation reactions (acidity plays a fundamental role in the catalysis of these reactions) that lead to the loss of paper/parchment mechanical resistance and to the deacidification of canvas. Because of their adhesive properties, synthetic polymers have been used to adhere in detached or damaged parts in the external layers of works of art. For instance, acrylate, vinyl, silicone, and epoxy polymers are widely used for the consolidation and protection of stone and wall paintings. However, the use of synthetic adhesives results in the strong alteration of physicochemical properties of the original substrates in the long term, such as an increase in porosity, water vapour permeability, and surface wettability, generating enhanced degradation that can proceed even up to the loss of the artefacts (Baglioni *et al.*, 2013).

In this context, the use of nanoparticles as consolidants in the restoration of artworks was explored, because the effectiveness of the treatment is highly increased when the size of the consolidants is reduced to the nanoscale, and dispersions of nanoparticles in solvents exhibit good penetration and consolidating power (Baglioni *et al.*, 2015). These inorganic NMs systems aim at arresting the degradation process and providing some mechanical reinforcement at the yarn/thread/fiber level. For instance, alkaline earth metal hydroxides can be used for a twofold task in the field of cultural heritage conservation. In wall painting consolidation, nanoparticles replace the original pigment's binder lost during the degradation process, reconsolidating the painting in a fully compatible way. In addition to that, calcium and magnesium hydroxides have proven to be excellent compounds for the deacidification of cellulosic works of art (Baglioni *et al.*, 2013). Nanocellulose applied on the canvas instead can strengthen the canvas by acting as reinforcing agent (Cataldi *et al.*, 2014).

The formulations developed in NANORESTART for increasing the surface strengthening of cellulose-based artworks are SILICA/PEI, SILICA/PEI/CMC, CNF, CSGI 1, CSGI 2 and NRA-CE04. SILICA/PEI is a water-based formulation containing polyelectrolytes, providing compatibility improvement and mechanical strengthening, and alkaline silica nanoparticles added both as a filler and as a deacidification agent. SILICA/PEI/CMC instead has more or less the same composition of the previous formulation, but with an additional anionic polyelectrolyte: carboxymethyl cellulose (CMC). CNF is water-based and contains a small amount of cellulose nanofibrils. CSGI 1 and CSGI 2 have been formulated for cellulose-based surfaces in order to obtain a composite for consolidating fibers using alkaline nanoparticles (calcium carbonate) instead of silica particles. The particles of both products are stabilized in water/ethanol mixture by adding a polyelectrolyte; in addition, CSGI 2 contains also CMC that increases coating colour viscosity and impedes latex migration to the surface during drying. Finally, NRA-CE04 is also a formulation aimed to increase the surface strengthening of cellulose-based artworks but it is formed by isopropyl alcohol and isobutanol with nanoparticles of  $\text{Ca}(\text{OH})_2$  and cellulose microcrystalline.

Paraloid B-72 was indicated by products' developers as suitable conventional products for comparison purposes.

### *1.5.3. Coatings for the protection of metal substrates*

Concerning the protection of metal substrates, anticorrosive coatings are used to avoid the formation of alteration products and reactive compounds. The corrosion process induced by these species can modify the entire object surface either uniformly or locally in the form of spots. In Cu-based alloys for example, an irreversible and nearly inexorable corrosion process, known as “bronze disease”, occurs when chlorides (in the presence of water and oxygen from the environment) come into contact with the metal surface (Scott, 1990).

The most widespread approach for corrosion protection of metallic artefacts is the application of protective polymer coatings, which act as an effective physical barrier against corrosive species present in the environment. A real breakthrough in the conservation of metal works of art would be the realization of protective systems, which can be also able to *actively* respond to corrosive phenomena. In this sense, direct incorporation of corrosion inhibitors into coating formulations, able to confer an active protection when the coating barrier properties fail, could represent a viable solution to the problem.

Another promising strategy is represented by the encapsulation of the inhibitors within inert host nanostructures, generally referred as nano-carriers. These nano-structures guarantee the storage of the inhibitors while the coating is able to maintain the metallic substrate protected by simple barrier effect (Shchukin *et al.*, 2006; Xu *et al.*, 2015). Addition of inorganic or organic inhibitors to the coating decreases the corrosion rate when the protective barrier layer gets damaged and thus allows to attain active, self-healing properties. The embedded nanoparticles should additionally serve as nano-containers encapsulating the active inhibiting agent, preventing its direct interaction with the matrix and controlling its release (Borisova *et al.*, 2011), as represent in figure 5.

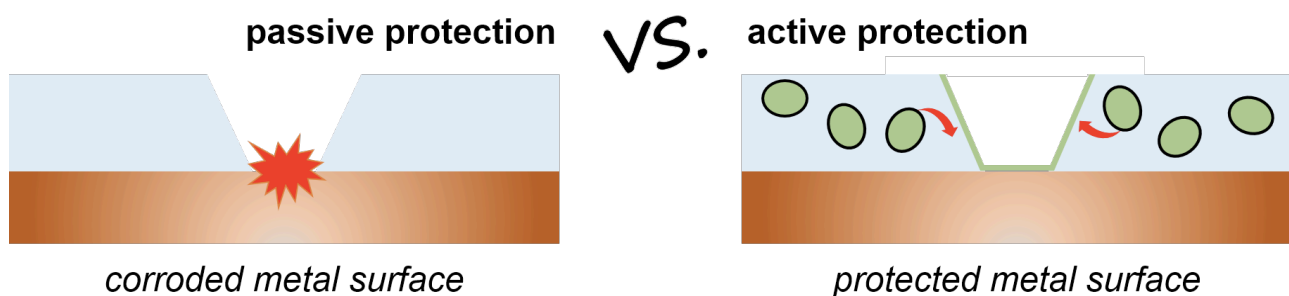


Figure 5. Sketch of the working mechanism of passive (left) and active (right) protective coatings. In the right-hand scheme, the red arrows indicate the diffusion of the anticorrosion compounds towards the exposed metal surface. Images adapted from (CNR-DSCTM, 2017, Deliverable 4.1).

Besides the corrosion protection, the coating has to be optically transparent in order to preserve the appearance of the artefact, and it has to be easily removable without compromising the integrity of the underlying metallic surface.

Two scenarios have been taken into account for the development of active coatings for metals substrates in NANORESTART project, namely indoor and outdoor environment.

Active coatings for indoor application are represented by five water/ethanol-based formulations (F1 to F5). F1 and F2 have similar composition, as they both contain nanocarrier, benzotriazole (F2 with a slightly higher content than F1) and nano-CaCO<sub>3</sub>. F3 and F4 instead differ from the previous two formulations for the absence of nano-CaCO<sub>3</sub> and a lower content of nanocarrier. A small difference between these formulations is that F4 contains HAVOH, an ingredient affecting the stability which is absent in F3. Concerning F5, it does not contain any NPs.

The active coatings for outdoor application SCEv1 and SCEv3 (the latter being the SCE-based final formulation) instead are based on a mixture of isopropyl alcohol and heptane, including modified cellulose, benzotriazole, and Ca(OH)<sub>2</sub> nanoparticles. SCEv3 differ from SCEv1 only for the slightly higher amount of nano-calcium hydroxide.

As far as passive coatings are concerned, U2 BYC 333 was developed and it is composed of polyurethane with hydrophilic isocyanate in butyl acetate solvent, trisilanol-isooctyl-POSS, a UV absorber and a light stabilizer.

INCRALAC and SOTER 201 LC were indicated by products' developers as suitable conventional products for indoor and outdoor applications, for comparison purposes.

## 1.6. Colloidal characterisation of ENMs

ENM features such as particle size, shape, surface charge and agglomeration state, may cause adverse effects on human health and the environment, driving their toxicological behaviour. Therefore, ENMs colloidal characterization is a fundamental step, both considering their early life stages (i.e. development, manufacturing, and commercialization), but also investigating their behaviour under different physical and chemical conditions and their mobility through several environmental compartments. In this study, the colloidal characterization of the new ENM-based formulations was performed according to their physico-chemical properties.

In general, a colloid is defined as a mixture in which one substance of microscopically dispersed insoluble particles is suspended throughout another substance, that does not settle or would take a very long time to settle considerably. Differently from a solution, whose solute and solvent constitute only one phase, a colloid has a dispersed phase (the suspended particles) and a continuous phase (the medium of suspension). The particles of the dispersed-phase usually show diameters in the range of 1 and 1000 nm (Robinson and Lawson, 2016), and they can be subjected to different forces. In detail, the main forces playing an important role in the interaction of colloid nanoparticles are: i) electrostatic interactions, which are linked to the electrical charge carried by the colloidal particles; ii) van der Waals forces, due to interaction between permanent or induced dipoles; iii) steric forces between polymer-covered surfaces or modulation of interparticle forces by not-adsorbed polymers contained in the solution; iv) excluded volume repulsion: normally occurring between hard particles which cannot overlap; v) entropic forces which make evolve the system toward a state maximized entropy, according to the second law of thermodynamics. The sum of interaction forces between particles is responsible of the agglomeration phenomena normally occurring to NPs once dispersed in a medium. Thus, the stability of a colloidal system is defined by the particles which remain suspended in the medium at equilibrium. If the attractive forces (i.e. van der Waals forces) prevail over the repulsive one (i.e. electrostatic forces) the particles tend to agglomerate. For this reason, electrostatic and steric stabilization are the two-main pathway employed for stabilizing NPs from agglomeration. Among

the different techniques used to monitor the dispersion state of a product, Light Scattering techniques are the most widely used.

### *1.6.1. Dynamic Light Scattering*

Dynamic Light Scattering (DLS) is particularly useful technique for determining the size distributions of nanoparticles in suspension or polymers in solution (Pecora, 2000), giving information on their state of aggregation/agglomeration.

In particular, this non-invasive technique measures the intensity of the light scattered by particles inside a fluid, which is caused by the Brownian motion of the particles (Babick, 2016). These motions are random movement of particles due to the radiation by the solvent molecules that surrounded them. Sample is thus crossed by the incident light wave, representing in a rapidly oscillating electric field. The alternating field near the particle induces all of the electrons to oscillate at the same frequency, which produce in turn, a new oscillating electric field that radiates in all directions. Different properties as molecular weight, size, shape, and the refractive indices of the particle and the surrounding solvent determine a different intensity of scattered light by a single particle. Briefly, dispersed NPs scattered incident light proportional to the 6<sup>th</sup> power of their radii. When the particles size is  $< \lambda/10$ , where  $\lambda$  is the wavelength of the incident light, the scattered light carries the same energy of the incident light (elastic scattering) and it is not angle-dependent (Rayleigh scattering). From the other side, when the particles size is  $> \lambda/10$ , the Rayleigh scattering is replaced by the anisotropic Mie Scattering, leading to an inelastic scattering of the light (unequal in energy with respect to the incident light) and angle-dependent. In this case, the scattered light is most intense towards the direction of the incident light. A schematic showing the differences between Rayleigh and Mie Scattering is reported in Figure 6.

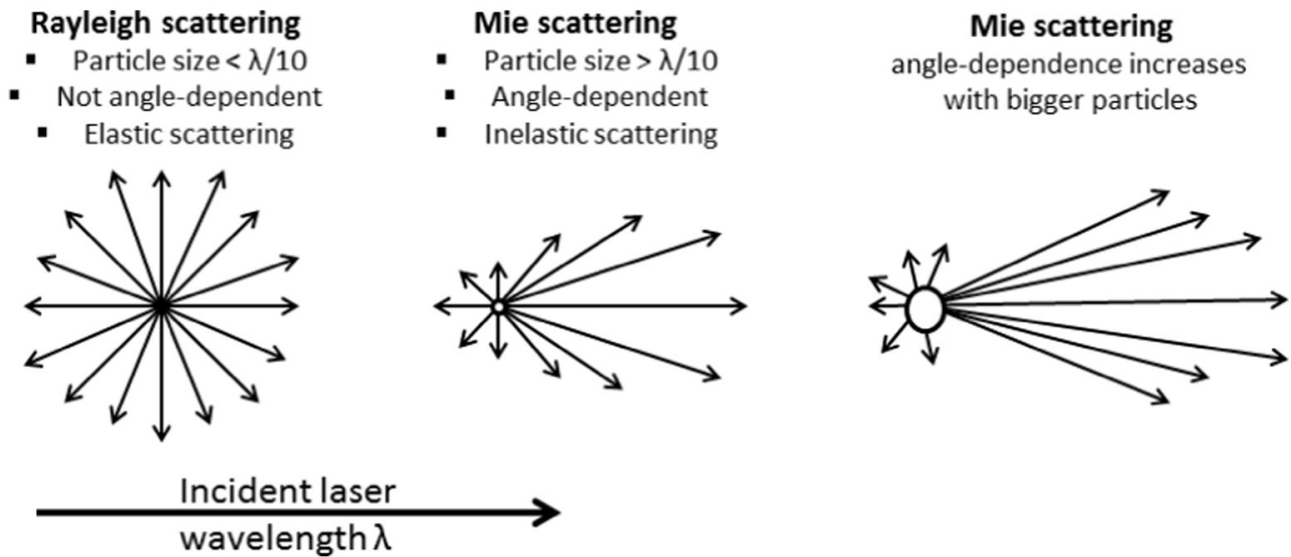


Figure 6. Schematic of Rayleigh and Mie scattering taken from Bhattacharjee (2016)

The fluctuations of the scattered intensity of light are then analysed by a correlator, which uses some algorithms to compare several signals coming from a detector, placed after the sample.

The size of the particles is then calculated by the Stokes-Einstein equation as follow (equation 4):

$$d(h) = \frac{k \cdot T}{3\pi\eta D} \quad 4)$$

where  $d(h)$  = hydrodynamic diameter,  $k$  = Boltzmann's constant,  $T$  = absolute temperature,  $D$  = translational diffusion coefficient, and  $\eta$  = viscosity.

This equation highlight that the hydrodynamic diameter measured by DLS is referred to how a particle diffuse within a fluid. This value refers to a sphere that has the same translational diffusion coefficient ( $D$ ) as the real particle. Thus,  $D$  will depend not only on the size of the particle but also on any surface structure, type and concentration of ions in the medium.

In general, a typical DLS is formed by six components: 1) a monochromatic light beam that put in the light source in the sample 2) a cuvette which contain the sample 3) a detector for estimating the scattered light, positioning at  $90^\circ$  from the surface beam 4) an attenuator to adjust the laser intensity over time 5) a correlator to digitalize the scattering intensity signal from the detector and 6) a computer to analyse data collected. DLS could be employed both as reference technique for primary but also secondary characterization of nanomaterials or colloidal dispersions.

In this study, DLS was performed by means of the multi-angle Nicomp ZLS Z3000 (Particle Sizing System, Port Richey, FL, USA). A picture is reported in Figure 7. More specifically, the

hydrodynamic diameter was measured with an optical fiber set at 90° scattering angle ( $W=25$  mW and  $\lambda=639$  nm) over at least 6 min at room temperature. The formulations were bath sonicated for 5 minutes before the analysis. Refraction index of 1.333 and viscosity value of 0.993 cP were used for water based formulations, 1.36 and 2cP respectively for water/ethanol 50:50 mixtures while 1.385 and 0.96 cP for isopropyl alcohol dispersions respectively.



Figure 7. Nicomp ZLS Z3000 Particle Sizing System

### 1.6.2. Centrifugal Separation Analysis

The analytical centrifuge is a technique usually used to investigate demixing phenomena of a sample in a liquid over time, like sedimentation, flotation and coalescence. Centrifugal Separation Analysis (CSA) was employed in this work to assess the dispersion stability of the new formulations in terms of sedimentation velocity. This method was already successfully applied to calculate the sedimentation kinetics of TiO<sub>2</sub> NPs and multi-walled carbon nanotubes (Sayes *et al.*, 2013; Brunelli *et al.*, 2016) as well as to gather information on the sedimentation velocity distribution of CuO NPs in both environmental and biological media (Ortelli *et al.*, 2017). In detail, sedimentation velocity was determined through CSA, by using the Multiwavelength Dispersion Analyzer LUMiSizer® 651 (Figure 8a). The transmission profiles obtained by CSA represent the transmittance values over the length of the cuvette containing the sample. In detail, parallel light  $I_0$  illuminates the entire sample cell and the transmitted light  $I$  is detected by thousands of sensors arranged linearly across the whole sample from the top to the bottom with a micro-scale resolution (Figure 8b). The resulting transmission profile shows the intensity of the light transmitted as a function of the radial coordinates, an example is reported in figure 9. The radial position indicates the distance from the rotor's centre.

For this reason, the highest position value (in nm) corresponds with the bottom of the cuvette. The sedimentation rate and the shifting (called front tracking) of the sample from the beginning to the bottom of the cuvette over time, can be evaluated by calculating the area below the profile obtained by the monochromatic light beam that irradiates the sample (see Figure 8b).

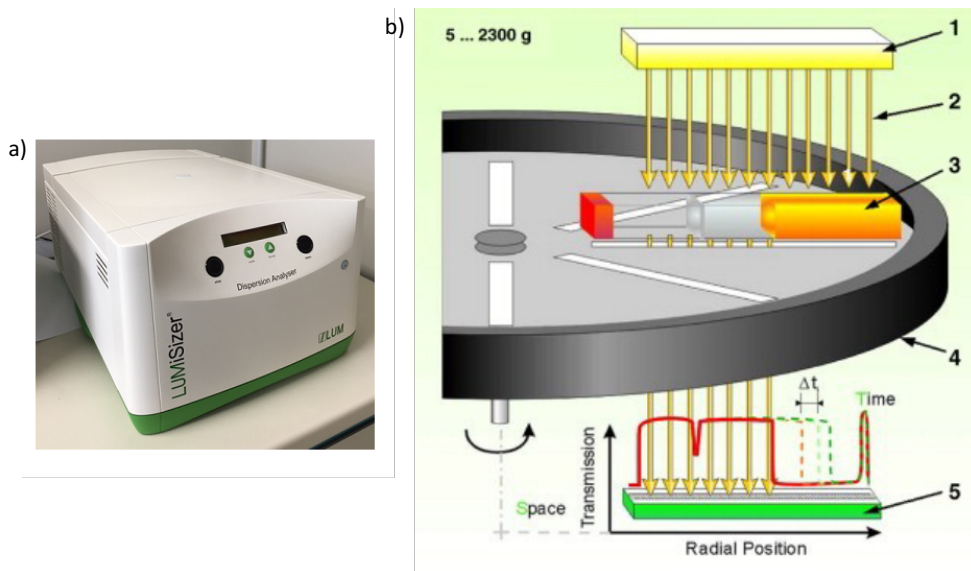


Figure 8. a) CSA instrument and b) Scheme of CSA. The light source (1) sends out parallel NIR-light (2), which passes through the sample cells (3) lying on the rotor (4). The distribution of local transmission is recorded over the entire sample length by the CCD-Line detector (5) adapted from Lerche and Sobisch (2007).

In Figure 9, the transmission profiles vary along the blue arrow, which indicate the variation over time, from the first a) to the last profile b). Information concern the kinetics of the separation/sedimentation process was provided calculating the sedimentation rates of solid material from the variation of the transmission profiles (Brunelli *et al.*, 2016). Particles migration due to centrifugal force results in a variation of the local particle concentration and, correspondingly, local and temporal variations of transmission occur (Lerche, 2002).

During the process of centrifugation, all the particles in the sample move towards the bottom of the cuvette, which results in the formation of a ‘sediment’, and in a decrease of particle concentration in the direction from the sediment to the ‘meniscus’ (Babick, 2016).

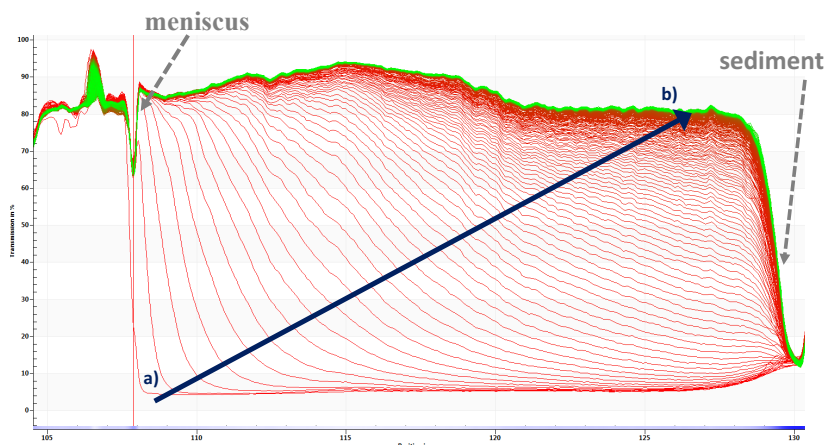


Figure 9: transmission profiles of a sample, where the x axis represents the position on the cuvette [mm] and y axis the variation of transmission values [%] from the start a) to the end b).

In this study, the separation of different components in dispersion was achieved at 3000 Rotation Per Minute (RPM), which corresponds to a Relative Centrifugal Force (RCF) of 1207 at 120 mm far from the rotor of the centrifuge. Sedimentation velocity data were calculated from the transmittance values obtained setting the wavelength of the transmitted light at 470 nm and collecting the transmittance (%) over time at three different positions (115, 120 and 125 mm far from the rotor) over the length of the cuvette. The runtime of each analysis (ranging from 40 to 70 min) was chosen according to the lowest time needed to reach the plateau, i.e. the maximum transmittance values, indicating the complete sedimentation of NPs. The linear dependency between RCF and sedimentation velocity allowed to extrapolate sedimentation velocity data at gravity by dividing these values, calculated by the instrument, for the RCF applied. The RCF is calculated as follow:

$$\text{RCF} = 1.1179 \cdot 10^{-3} \cdot \text{RPM}^2 \cdot R \quad 1)$$

where RPM [ $\text{min}^{-1}$ ] was selected before starting the analysis and R [m] is the radius, calculated from the centre of the rotor to the point at which the transmittance values were considered.

For both CSA and DLS techniques, samples were analysed as received or after dilution with the ecotoxicological medium (M4) with a ratio of 1:2, 1:5 and 1:10 in volume, depending on the characteristics of the formulation investigated and the detection limits of the instrument. Unfortunately, because of the instrumental limits it was not possible to work at the same concentrations used for ecotoxicological tests (ranging between 0.1 and 1000 mg/l). However, the results obtained are helpful to understand the behaviour of the formulations containing nano-based ingredients, once dispersed in the ecotoxicological medium. Sedimentation velocity and

hydrodynamic diameter were measured in duplicate and results are expressed as median for CSA and average for DLS.

## 1.7. Bibliographic research about leaching testing

The increased number of new engineered nanomaterials (ENM) and ENM-based formulations provided to conservators on one side has enhanced the performances and technical sustainability of art materials (Baglioni and Chelazzi, 2013), but on the other side has led concerning about the potential risks which can emerge from the release of these materials into the environment. Possible release scenarios of NPs need to be considered for all their life cycle, as 1) the release during their production, 2) release from the manufacturing processes of products containing ENM, 3) release into the environment during the use, recycling and disposal of ENM in products and 4) the indirect release from several technical processes (e. g. nano-paints production, ENM as food additive, medical uses) to different environmental compartments (water, soil, air, groundwater) (Gottschalk and Nowack, 2011).

For most ENM, no techniques are available to specifically monitor their release and to quantify their concentration, especially in the environment at trace levels. Nanomaterials that actually reach the environment indeed may be completely different from the materials originally produced by industry because of aging processes that may cause transformations (Zhang *et al.*, 2017). It is therefore very crucial to collect information on the amount and characteristics of the materials that are released under real-world conditions using standard methods (e.g. ISO and ASTM standards).

As defined by the International Organization for Standardization (ISO) and by the International Electrotechnical Commission (IEC), a standard is ‘a document, established by consensus and approved by a recognized body, that provides, for common and repeated use, rules, guidelines or characteristics for activities or their results, aimed at the achievement of the optimum degree of order in a given context’ (ISO/IEC Guide 2, 1996). In general, standards provide guidance on the design, use or performance of materials, products, processes, services, systems or persons, by technical specifications or other precise criteria which ensure that they are fit for their intended purpose.

In order to identify the best experimental conditions to develop laboratory test methods, a deep literature research was performed. Scientific papers published from 2000 to 2017 were searched, looking for standardized methods to investigate the release of nanoparticles in the environment. Results allowed to identify the most suitable method to be applied in this thesis work to study the

environmental releases occurring in the post application phase (in outdoor conditions) from active and passive coatings for protection of metal substrates, as reported in Chapter 2.2.

## 2. Results and discussion

### 2.1. Colloidal characterization

A description of the results obtained by DLS and CSA techniques is reported in this chapter for each of the three families of products described in Chapter 1.5. As explained below, DLS was not performed on those formulations presenting CSA transmission profiles similar to the profiles of pure water, indicating that no nano-ingredients were present. Not even the formulations containing different solvents were analysed by DLS since it was not possible to choose the correct values of refraction index and viscosity, parameters which are needed for the analysis.

#### 2.1.1. Cleaning formulations

The three selected cleaning fluids (i.e. AM5, G1 and G1-Ncap), presented in Chapter 1.5.1, were characterized.

Since none of them contains nano-ingredients, their CSA transmission profiles resulted to be the same of pure water (Figure 10). For this reason, DLS analysis as well as colloidal characterization in the ecotoxicological medium (M4) were not performed.

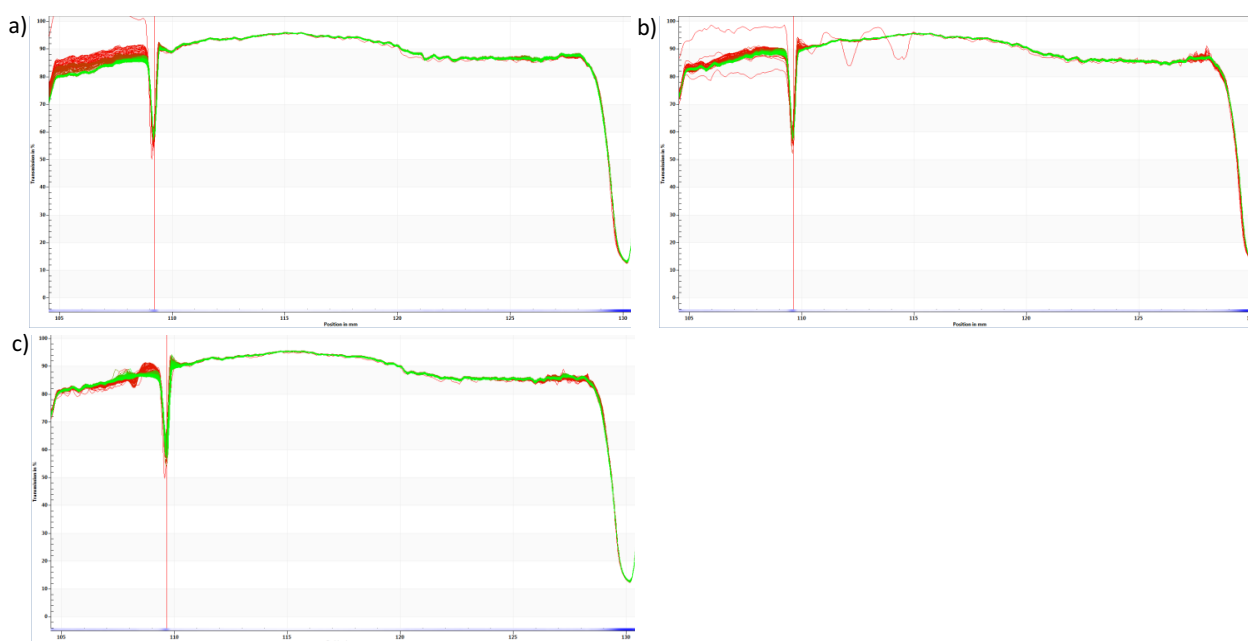


Figure 10. Transmission profiles of a) G1 b) AM5 and c) G1-Ncap formulation

Two ingredients of the formulations (i.e. Biosoft, a surfactant included in AM5 and G1, and Ncap, a substance of unknown composition included in G1-Ncap) were also investigated by CSA (Figure 11). Biosoft showed a transmission profile similar to that of pure water, while Ncap showed the presence of nano-based ingredients in the formulation. Since in G1-Ncap, containing Ncap ingredient, no signals were detected, this indicated a low concentration of such ingredient in the final formulation. DLS analysis of Ncap was not performed because the diffraction index of the mixture was unknown.

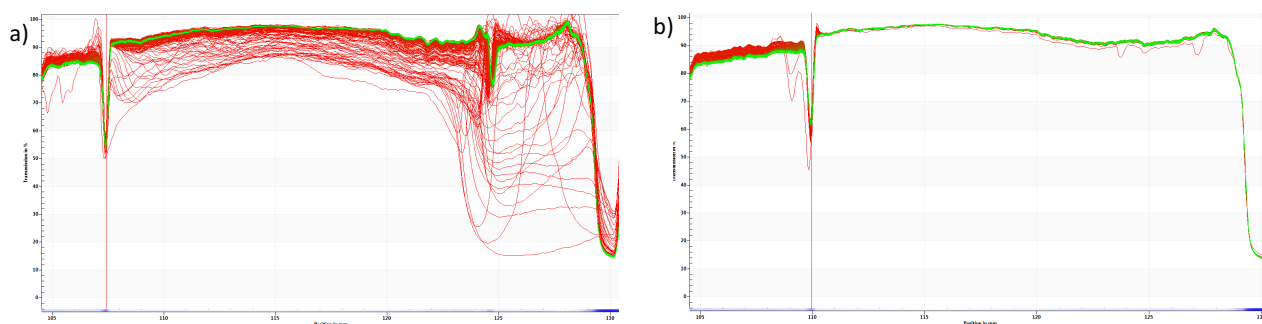


Figure 11. Transmission profiles of a) Ncap and b) Biosoft ingredients.

### 2.1.2. Surface consolidation systems

The six selected formulations (i.e. Silica/PEI, Silica/PEI/CMC, CNF, NRA-CE04, CSGI 1, CSGI 2) presented in Chapter 1.5.2, were characterized.

As result, the transmission profiles of Silica/PEI and Silica/PEI/CMC displayed by CSA (Figure 12a and 12b) resulted to be the typical profiles of stable dispersions containing silica NPs. Sedimentation velocity was not calculated by CSA for these stable formulations because of the already high initial transmittance value. Concerning CNF, the transmission profiles displayed in Figure 12c showed that a sedimentation process occurred only on the top of the cuvette, indicating the highly compactness of the formulation (initial transmission of 20%).

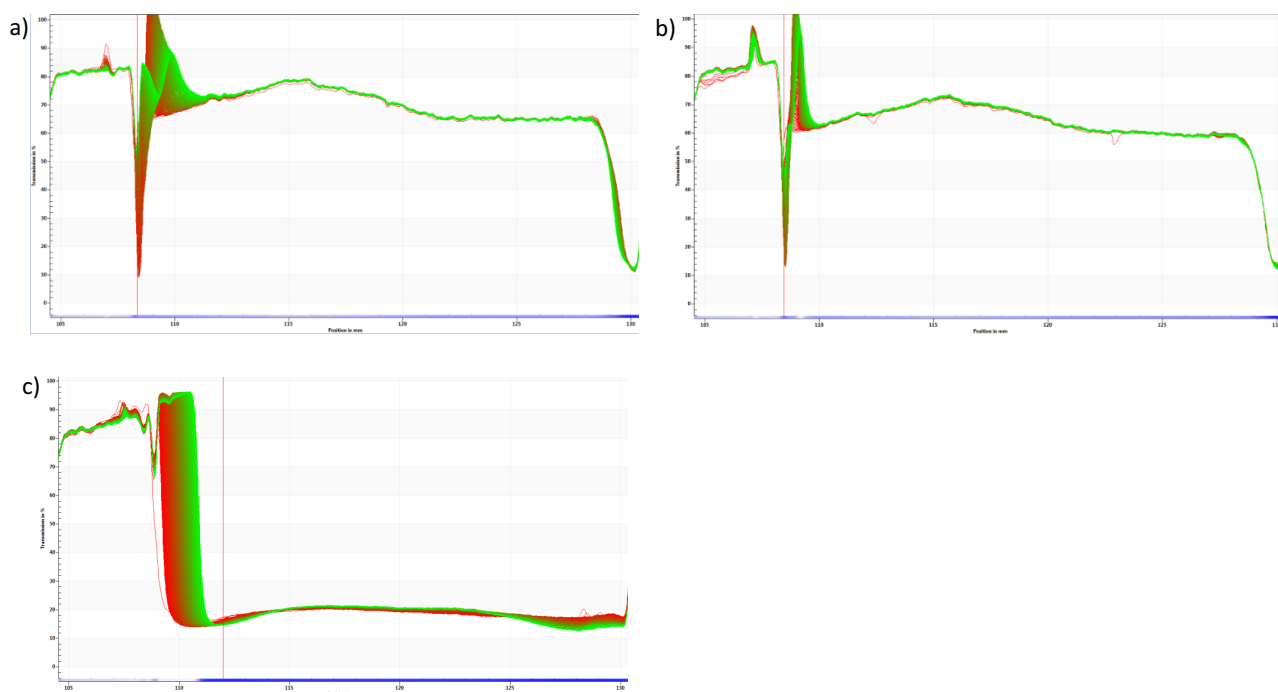


Figure 12. Transmission profiles of a) SILICA/PEI b) SILICA/PEI/CMC and c) CNF formulation

The sample was then diluted in the ecotoxicological medium (M4) and the obtained transmission profiles are reported in Figures 13. Both dilutions with the medium (1:5 and 1:10 in volume) led to profiles which are typical for cellulose based-materials. In this case, the relative sedimentation velocities were estimated as  $0.11 \pm 0.01 \mu\text{m/s}$  for 1:5 dilution and  $0.70 \pm 0.01 \mu\text{m/s}$  for 1:10, mainly suggesting a decrease of the colloidal stability for more diluted samples.

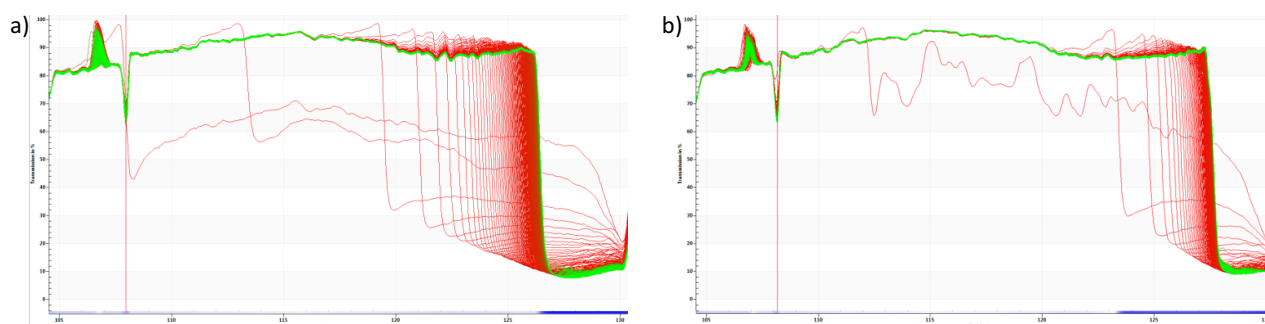


Figure 13. Transmission profiles of a) CNF diluted 1:5 and b) CNF diluted 1:10.

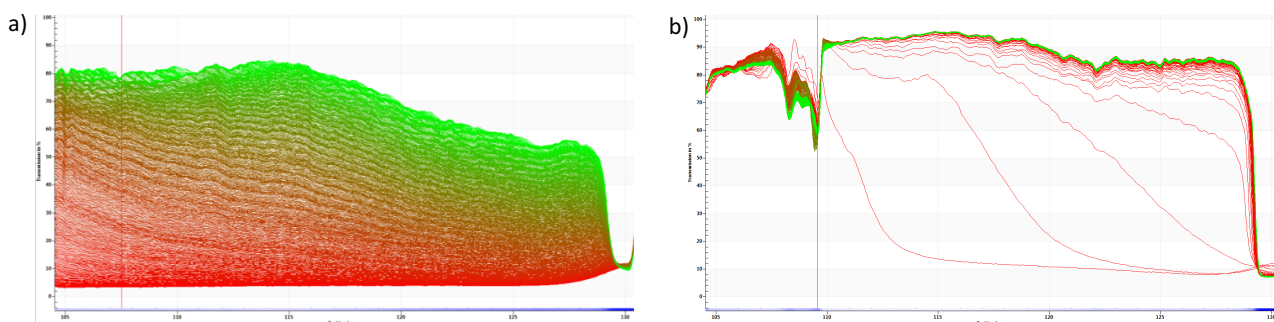
The hydrodynamic diameter of the three formulations (Silica/PEI, Silica/PEI/CMC and CNF) was also investigated by DLS technique, leading to  $37 \pm 7.4 \text{ nm}$ ,  $193 \pm 33 \text{ nm}$  for Silica/PEI and Silica/PEI/CMC respectively. For 1:5 diluted samples (in M4 medium) similar results were obtained (i.e.,  $48 \pm 8 \text{ nm}$  for Silica/PEI and  $180 \pm 18 \text{ nm}$  for Silica/PEI/CMC). For CNF formulation, the pure

sample was not analysed by DLS, because of its high concentration, but a diameter of  $5100 \pm 6200$  nm was obtained after 1:5 dilutions with M4, suggesting that nanoparticles were still in high concentration or in the agglomeration state.

NRA-CE04 formulation was initially analysed by CSA and DLS techniques as received, without performing any sample dilution (Figure 14a). NRA-CE04, which contains 1% of  $\text{Ca}(\text{OH})_2$  NPs and cellulose microcrystalline (<1%), showed a highly dense set of transmission profiles (Figure 14a) by CSA with a calculated sedimentation velocity of  $0.01 \pm 0.01$   $\mu\text{m/s}$ . The sample was then analysed by DLS technique and the obtained hydrodynamic diameter was of  $516 \pm 105$  nm. The size distribution observed for NRA-CE04 was likely due to the presence of the cellulose microcrystalline.

The formulation was then diluted with M4, the medium used in the ecotoxicological tests. According to the instrument detection limits, NRA-CE04 was diluted 1:2 in volume with M4 and the sedimentation velocity at gravity resulted  $0.86 \pm 0.01$   $\mu\text{m/s}$ . However, very few profiles were observed after dilution (Figure 14b) with respect to the initial formulation (Figure 14a), likely indicating that a dissolution process of  $\text{Ca}(\text{OH})_2$  NPs could also occur in M4. Further dilutions in M4 media, 1:5 and 1:10 in volume, were also performed (Figure 14c and 14d).

It has to be highlighted that the hydrodynamic diameter of NRA-CE04 dispersed in M4 reached the micron size at 1:2 dilution while at 1:5 and 1:10 dilutions, values of  $1368 \pm 276$  nm and  $5200 \pm 888$  nm were obtained. Diluting this alcoholic formulation in an aqueous medium is highly affecting the colloidal stability of the nano-based dispersion.



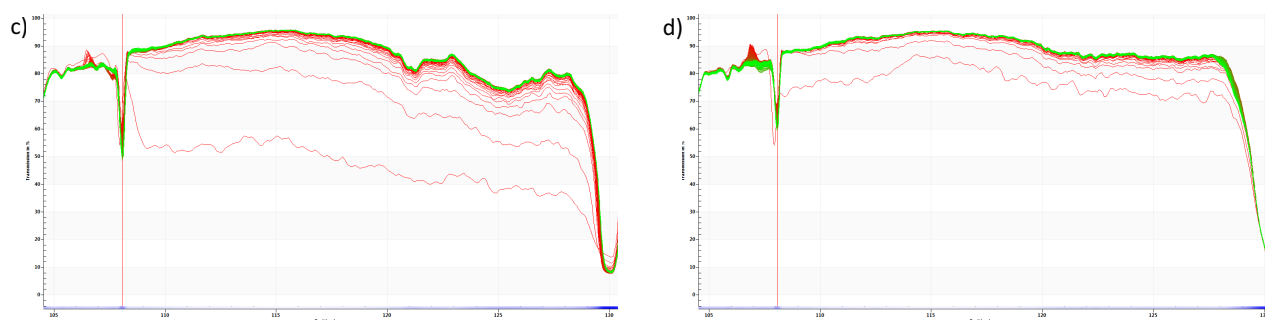


Figure 14. Transmission profiles of a) NRA-CE04, b) NRA-CE04 diluted 1:2, c) NRA-CE04 diluted 1:5, d) NRA-CE04 diluted 1:10.

As observed by transmission profiles of CSGI 1 and CSGI 2 in Figure 15a and 15b, both dispersions were very concentrated for CSA analysis in terms of nano-based components and no sedimentation velocity could be calculated for undiluted samples. Both samples were then diluted with M4 medium with a dilution of 1:5 and 1:10 in volume. For each dilution rate, the profiles of CSGI 2 (Figure 15d and 15f) resulted denser than the profiles of CSGI 1 (Figures 15c and 15e). This effect can probably be attributed to the presence of CMC in CSGI 2 formulation, which is the only ingredient that differs from the composition of CSGI 1. The sedimentation velocity at gravity for 1:5 dilutions resulted  $0.14 \pm 0.01 \mu\text{m/s}$  for CSGI 1 and  $0.12 \pm 0.01 \mu\text{m/s}$  for CSGI 2, indicating a slight increase of colloidal stability for CSGI 2 formulation. This difference was increased by diluting the samples 1:10 in M4 medium, with sedimentation velocities of  $0.28 \pm 0.01 \mu\text{m/s}$  for CSGI 1 and  $0.18 \pm 0.01 \mu\text{m/s}$  for CSGI 2, which represent a higher colloidal stability of CSGI 2 than CSGI 1.

As far as DLS measurements is concerned, CSGI 1 and CSGI 2 showed a hydrodynamic diameter of  $59 \pm 11 \text{ nm}$  and  $1831 \pm 1132 \text{ nm}$ , respectively. An increase of the hydrodynamic diameters was observed for CSGI 1 diluted in M4 medium (Table 1) suggesting the increase of agglomeration process, while similar values were obtained for diluted CSGI 2.

Formulation	$d_{Z\text{-ave}} \pm \text{st } d_v \text{ (nm)}$		
	pure	1:5 in M4	1:10 in M4
CSGI 1	$59 \pm 11$	$522 \pm 100$	$1000 \pm 217$
CSGI 2	$1831 \pm 1132$	$1584 \pm 307$	$2099 \pm 473$

Table 1. Hydrodynamic diameters ( $d_{Z\text{-ave}}$ ) of formulations CSGI 1 and CSGI 2 as received and diluted in M4.

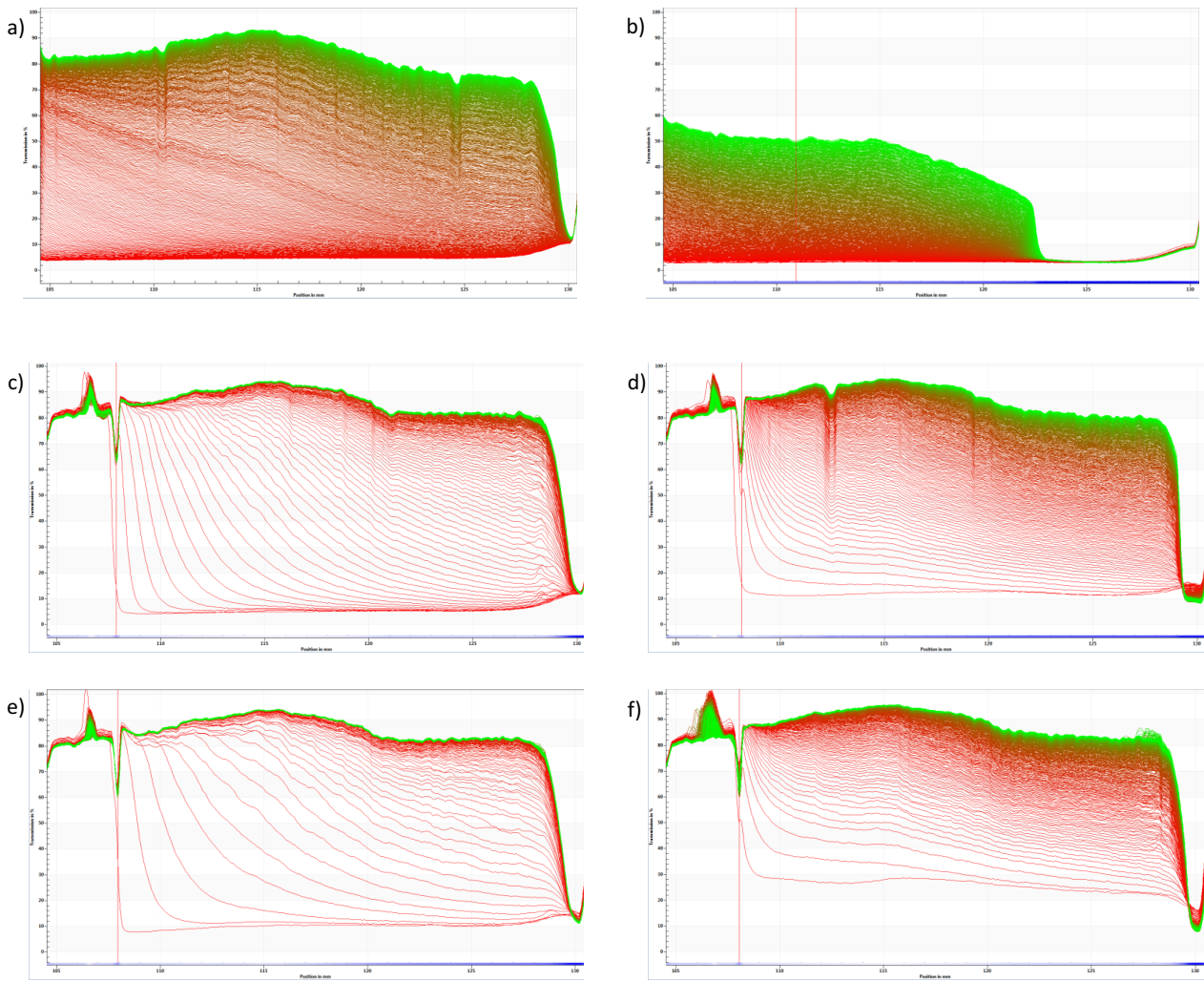


Figure 15. Transmission profiles of a) CSGI 1, b) CSGI 2, c) CSGI 1 diluted 1:5, d) CSGI 2 diluted 1:5, e) CSGI 1 diluted 1:10, f) CSGI 2 diluted 1:10.

Finally, the transmission profiles of the conventional product Paraloid B-72 showed that it does not include colloids (Figure 16), because of its high transmittance values (90%) and similar profiles of pure water.

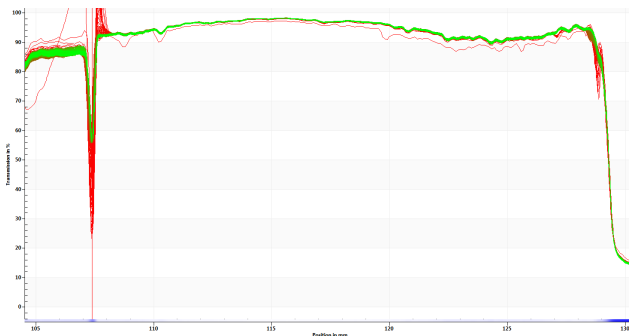


Figure 16. Transmission profile of Paraloid B-72

### 2.1.3. Coatings for the protection of metal substrates

The seven selected active coatings (i.e. formulations from F1 to F5, and SCEv1 and v3) and their conventional INCRALAC (88% in toluene), as well as the selected passive coating U2 BYC 333 and its conventional SOTER 201 LC, presented in Chapter 1.5.3, were characterized.

The colloidal characterization of the different formulations was performed by CSA and DLS techniques. According to CSA results obtained by Formulations 1-5 (Figure 17), the observed signals represent the nano-based ingredients, which were used in the first four formulations out of five. The five formulations were initially analysed as received (Figure 17a, b, c, d, e), without performing any sample dilution. Similar transmission profiles were obtained for F1 and F2 which contained both 0.06 % w/w of nanocarrier and 0.02 % w/w of NRA-CC04. In fact, the same sedimentation velocity value at gravity was determined for both formulations ( $0.05 \mu\text{m/s}$ ).

The single ingredient NRA-CC04, which contained 2% of  $\text{Ca}(\text{CO}_3)_2$  NPs, was also analysed by CSA and provided a sedimentation velocity value of  $0.53 \pm 0.01 \mu\text{m/s}$ . The corresponding transmission profiles are reported in Figure 17f.

A different behaviour was observed for F3 and F4, containing only 0.03 % w/w of nanocarrier, which presented similar profiles, but initial transmission values higher than those obtained for F1 and F2. Sedimentation velocity resulted in  $0.01 \mu\text{m/s}$  and  $0.04 \mu\text{m/s}$  for F3 and F4, respectively. Since, in general, highest sedimentation velocities correspond to less stable dispersions, most probably the presence of HAVOH in F3 is affecting the stability of the dispersion.

F5, in which nano-based ingredients are not present, showed a transmission profile similar to the profile of pure water (Figure 17e).

The relative stability ranking obtained considering the sedimentation velocities calculated at gravity is the following:  $F1, F2 < F4 < F3$ . The obtained values are reported in Table 2.

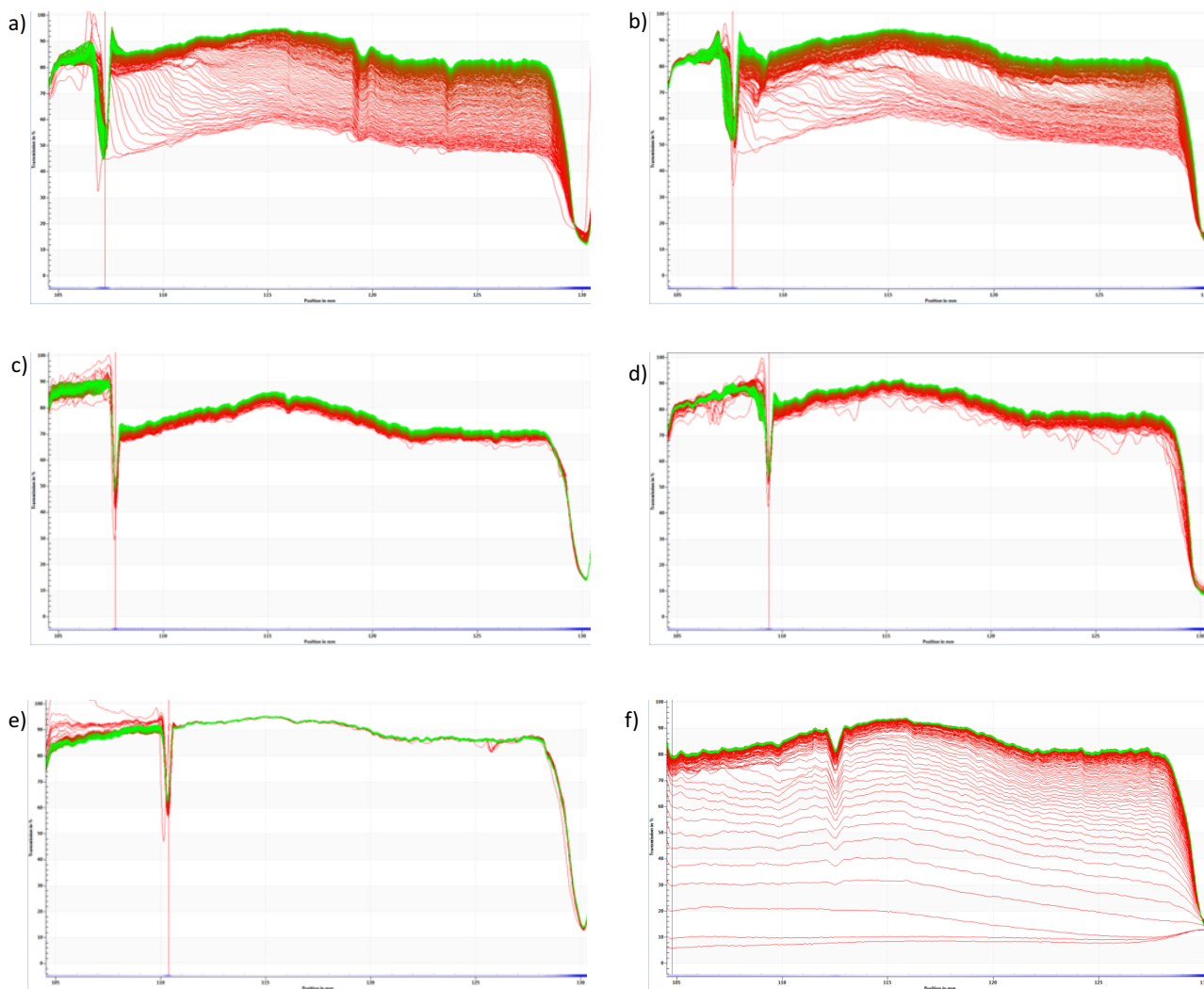


Figure 17. Transmission profiles of a) Formulation 1, b) Formulation 2, c) Formulation 3, d) Formulation 4, e) Formulation 5 and f) NRA-CC04.

The different behaviour observed by CSA analysis reflected the content of nanoparticles in the 5 different formulations. F5, which did not contained nano-based ingredients showed transmission profiles similar to pure water, F3 and F4 which had only the nanocarrier (0.03%w/w) as nano-based ingredient, showed more marked profiles, while F1 and F2, which contained a % of nanocarrier bigger than F3 and F4 (0.06%w/w) and also  $\text{CaCO}_3$  NPs (0.02%w/w), showed in the transmission profiles two different populations of NPs, probably representing the two different type of NPs present in the formulation.

After dilution, nanoparticles of  $\text{CaCO}_3$  seems to partially dissolved in water, while the nanocarrier is still stable, as represented in Figure 18a and 18b.

<b>Formulation</b>	<b>Sed. Vel (<math>\mu\text{m/s}</math>)</b>	<b><math>d_{Z\text{-ave}} \pm \text{st dv}</math> (nm)</b>
1	$0.05 \pm 0.01$	$1772 \pm 294$
2	$0.05 \pm 0.01$	$1514 \pm 250$
3	$0.01 \pm 0.01$	$1800 \pm 376$
4	$0.04 \pm 0.01$	$2583 \pm 522$
5	-	-

Table 2. Sedimentation velocity (Sed. Vel.) and hydrodynamic diameter ( $d_{Z\text{-ave}}$ ) of undiluted formulations from 1 to 5.

F1 and F2 were then diluted 1:2 (in volume) with the medium used for ecotoxicological tests (M4) and their transmission profiles are reported in Figure 18. Under these conditions, sedimentation velocities of  $0.02 \pm 0.01 \mu\text{m/s}$  and  $0.03 \pm 0.01 \mu\text{m/s}$  were obtained for F1 and F2 respectively. For these diluted samples, hydrodynamic diameters of  $681 \pm 112 \text{ nm}$  and  $550 \pm 82 \text{ nm}$  were obtained. F3 and F4 were not diluted in the medium because the initial transmission profiles were already high (>65%) for the undiluted formulations and the instrument detection limits would not allow to analyse diluted samples. As far as NRA-CC04 ingredient, it was also diluted 1:2 in volume with M4. As expected by the transmission profile of the undiluted formulation (Figure 17f), only few profiles were obtained in M4 (Figure 18c). This result showed the effect of the dilution process because solubility of  $\text{Ca}(\text{CO}_3)_2$  NPs in water is very low. The sedimentation velocity calculated under these conditions was  $0.95 \pm 0.01 \mu\text{m/s}$ .

NRA-CC04 was also diluted 1:5 in volume with M4 (Figure 18d), giving a sedimentation velocity at gravity of  $0.90 \pm 0.01 \mu\text{m/s}$ . This indicated that dilution with M4 medium is not significantly altering the colloidal stability of this dispersion and confirmed that no solubilization of the nano-based component occurs.

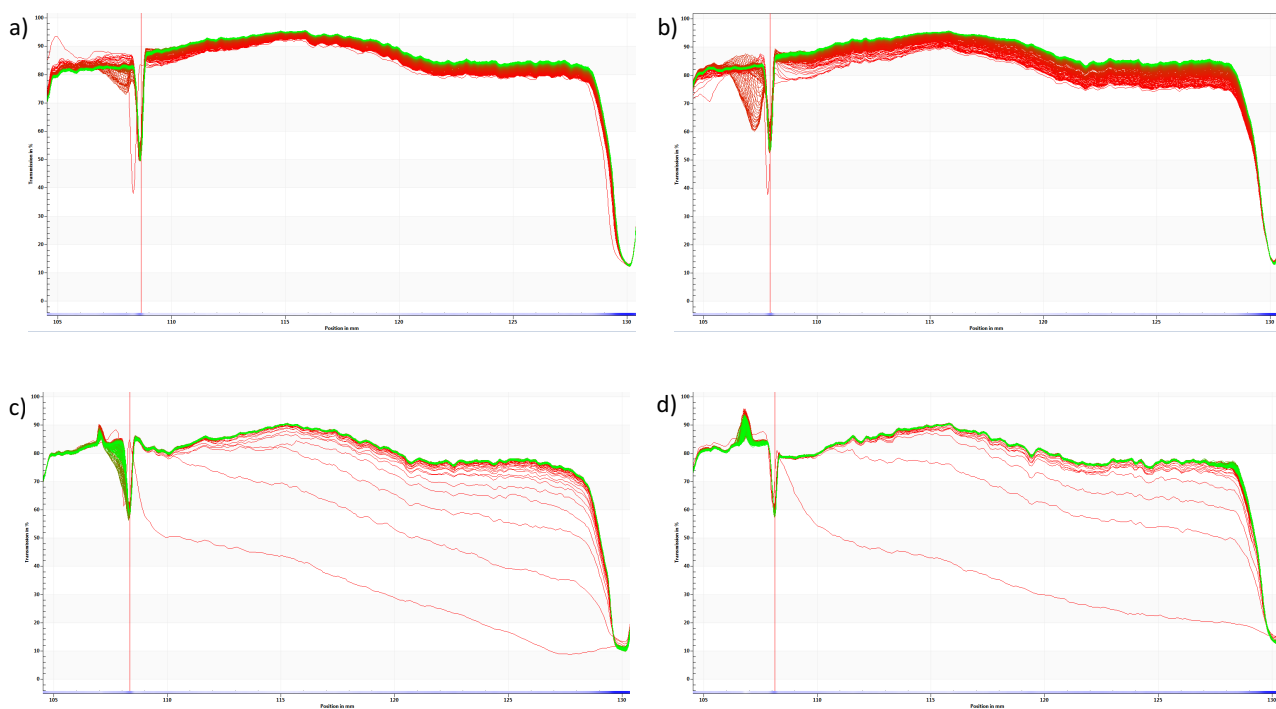


Figure 18. Transmission profiles of a) Formulation 1 diluted 1:2, b) Formulation 2 diluted 1:2, c) NRA-CC04 diluted 1:2 and d) NRA-CC04 diluted 1:5.

As reported in Figure 19, the transmission profiles of SCE v1 and SCE v3 obtained by CSA were similar to pure water's profile. This indicated that the content of  $\text{Ca}(\text{OH})_2$  NPs in these formulations (in SCE v1 is 0.02 %w/w, in SCE v3 is 0.03%w/w) was probably dissolved or its concentration was too low to be revealed by Lumisizer.

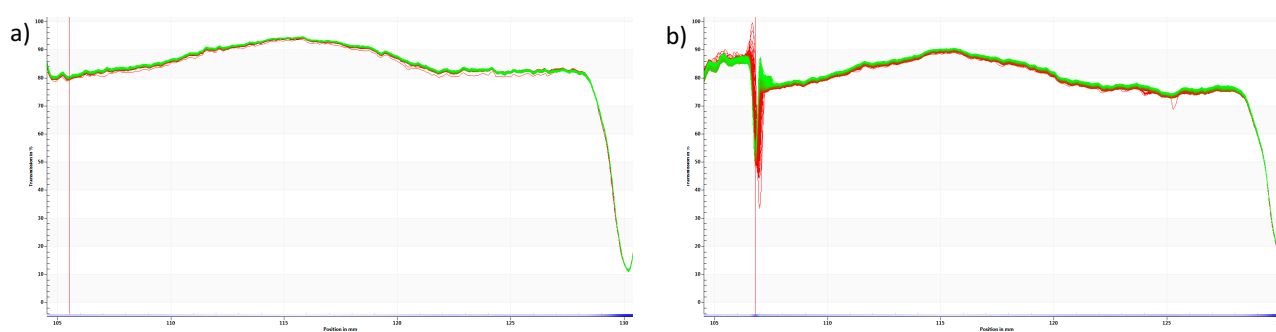


Figure 19. Transmission profile of a) SCE v1 and b) SCEv3.

The conventional product identified for active coatings was INCRALAC, and its transmission profiles showed the transmission profile of another conventional product of which it is made (Paraloid B44), since the other ingredients are solvents (Figure 20). These profiles indicated the high instability of this product, which presented a sedimentation velocity of  $0.06 \pm 0.01 \mu\text{m/s}$ . This conventional

product was not analysed by DLS because of its high contents of different solvents, which make impossible to find appropriate values of viscosity and refraction index.

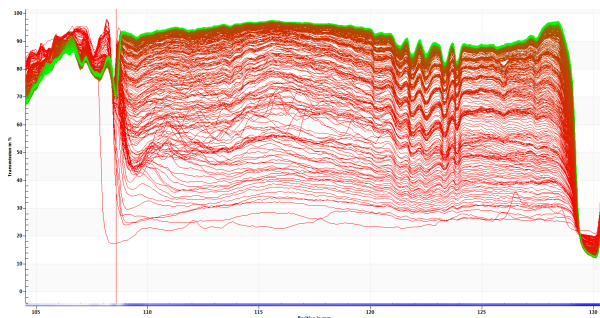


Figure 20. Transmission profile of INCRALAC

As far as passive coatings are concerned, U2 BYC 333 and the protective conventional product SOTER 201 LC were analysed by CSA (Figure 21a and 21b respectively). Both the transmission profiles obtained are similar to the profiles of water. For this reason, these products were not analysed by DLS.

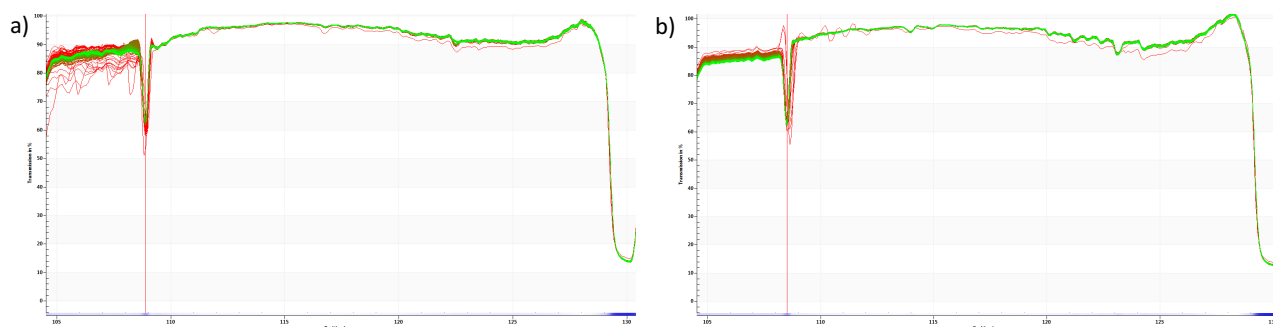


Figure 21. Transmission profile of a) U2 BYC 333 and b) SOTER 201 LC

## 2.2. Leaching tests

The selected formulations were also characterized in the post-application phase, where attention was paid to possible materials' (chemicals or nano-based ingredients) releases which can occur from the treated surfaces under specific environmental conditions. To develop this part of the thesis, 1) a detailed bibliographic search of suitable methods for studying environmental releases, and 2) experimental leaching tests using the best experimental conditions found by the bibliographic search, were performed.

### *2.2.1 Bibliographic search*

The bibliographic research was performed by firstly identifying the most common standard methods present in the literature for investigating both the performances of treated materials (i.e. the adhesion of the coating to the substrate, its mechanical resistance, flexibility, etc.) and releases because of the application of artificial weathering. The results of the properties tested in the standard methods selected are represented in Table 3. The materials investigated have been divided into two main groups: 1) materials treated with coatings (general organic coatings as well as paints and varnishes) and 2) plastics and rubber. Afterwards, all the papers of interest including the aforementioned standard methods in their experimental design were investigated, considering also the papers in which a modification of these standards was performed.

Table 3. Standard methods to evaluate performances and release from coatings or plastic and rubber (in rows) divided by the investigated properties (in columns)

	<b>Adhesion</b>	<b>Resistance to abrasion</b>	<b>Resistance to a falling weight</b>	<b>Flexibility (A)/ Hardness (B)</b>	<b>Wettability (A)/ Permeability (B)</b>	<b>Artificial weathering (A)/ release (B)</b>	<b>Thickness</b>	<b>Gloss</b>	<b>Tensile and flexural properties</b>	<b>Description of performance requirements</b>
<b>Coatings, paints and varnishes</b>	ASTM D3359-17 ASTM D4541-17 ASTM D7234-12 ASTM D3363-05 (2011)	ASTM D4060-14 DIN68861-2:2013-02 ASTM D6037-13e1 ASTM D968-17 ISO 7784-2:2016 ASTM G195-13a ISO 2409:2013	ISO 6272-1:2011 ASTM D7136 / D7136M -15	ASTM D522/D522M-17 (A) ISO 1522:2015 (B)	DIN 5560-1:2012-12 (A) ISO 2812:2017 (B)	ISO 16474:2013 (A) ASTM B117-16 (A) EN 1062-11:2002 (A) EN 16105:2011 (B)	ISO 2808:2010	ASTM D523-14 ISO 2813:2014	ISO 20340:2011 ASTM G154-16	
<b>Plastics and rubber</b>		ISO 5470-1:2016	ASTM D5420-16 ISO 179-2:2013	ASTM D2240-15 (B)				ASTM D638-14 ISO 14125:1998 ISO 527-4:1997		

### *2.2.1.1. Coatings, paints and varnishes*

#### ***Adhesion***

Among the different standards concerning coatings adhesion on rigid substrates (i.e. metal, concrete or wood) **ASTM D4541-17** (replacing the standard of 2002) describes a standard test method for pull-off strength of coatings using portable adhesion testers. Pull-off strength of coatings from concrete is also described in Test Method **ASTM D7234-12**. This test offers two test protocols. Protocol 1 describes a test to investigate the resistance of a material to fracture, and it consists in the application of the greatest perpendicular force in tension that a surface area can bear before a plug of material is detached. Protocol 2 (pass/fail test) determines if the coated surface remains intact at a defined load criterion. Fracture will occur along the weakest plane within the system comprised of the test fixture, glue, coating system, and substrate, and will be exposed by the fracture surface. The adhesion between organic coating and different type of substrate were also performed with **ASTM D 3363-05** (2011), the standard test method for film hardness by Pencil Test. The pencil hardness measurements have been used to determine the cure of coatings, testing the film hardness of an organic coating on a substrate in terms of drawing leads or pencil leads of known hardness. Coatings industry used this test method for many years to determine the hardness of clear and pigmented organic coating films. The strength of the bonds between the coating and the substrate is investigated by the standard test method Test **ASTM D3359-17**, for rating adhesion by Tape. The aim of this test is to evaluate adhesion of an organic coating to different non-metallic substrates (e.g. wood and plaster) or surface treatments. The standard requires that the free end of the tape can be removed rapidly at as close to a 180° angle as possible. When the peel angle and rate vary, the force required to remove the tape can change dramatically due to the rheological properties of the backing and adhesive. The result of this type of method do not give an absolute value for the force required for bond rupture, but serves only as an indicator that some minimum value for bond strength was met or exceeded.

#### ***Abrasion***

As described in **ASTM G195-13a**, ‘the resistance of material surfaces to abrasion may be affected by factors including test conditions, type of abrasant, pressure between the specimen and abrasant, mounting or tension of the specimen, and type, kind, or amount of finishing materials’. The resistance of material surfaces to abrasion, as measured on a testing machine in the laboratory, is generally only one of the several factors contributing to wear performance as experienced in the actual use of the material. For this reason, the application of standard method is necessary to minimise the effect of such factors. The quantification of abrasion resistance of material surfaces is

defined in this standard, using the rotary platform abraser. Other similar tests concerning the simulation of abrasion are also conducted with the application of abrading wheels, as described in **ISO 7784-2:2016**, which consists in the determination of resistance to abrasion using the rotating abrasive rubber wheel method. It replaced the ISO 7784-2006, for which two loaded, freely rotatable but eccentrically arranged abrasive rubber wheels affect the coating of the rotating test specimen. These test methods were applied in different technical data sheets by the paint industries in order to give a quantitative value of the performance of their products (e.g. Intertec Plastics Technology Laboratories, BYK Additives and Instruments, SpecCoat, Chillabs, Co-ax, La Croix optics). Another similar test to investigate the resistance to abrasion is conducted with the application of the Taber Abraser, as described in **ASTM D4060-14**. This standard was introduced in around 1930 to perform accelerated wear testing (Micom Laboratories). This test method has been useful in evaluating the abrasion resistance of coatings applied to a plane rigid surface, such as a metal panel, and it allows to simulate the typical handling with high reproducibility (Vorbau et al. 2009). The Taber Abraser consists of two abrasion wheels which are moved by the rotation of the sample and the abrasion is caused by the friction at the contact line between the sample surface and the abrasion wheels. The measurement of the released particle mass mainly depends on the type of substrate and coating, and the material of the wheels. This is not only used to determine the abrasion resistance of coated samples but, in general, to assess the protective properties of different types of coating (Rossi, Deflorian and Risatti, 2006). Abrasive wheels are also adopted in **ASTM D60373-13e1**, in order to provide a way to estimate the ability of high gloss coatings to resist mar damage. High gloss coatings (e.g. applied on automobiles and boats) indeed are subject to different conditions that can mar their surface as wiping, weathering exposure. This standard is divided in two tests methods, where both methods may be used to evaluate the dry abrasion mar resistance of planar, rigid surfaces covered by coatings. In detail, test method A uses a device that contains a rotating specimen holder and two abrasive wheels, while test method B uses a reciprocating specimen holder and a single wheel that has been fitted with abrasive paper. The determination of resistance of organic coatings to abrasion has been also described in **ASTM D968-17**, which is evaluated by the effect of an abrasive falling onto coatings applied to a plane rigid surface, such as a metal or glass panel. Silica sand or silicon carbide falling on a treated surface which is inclined 45° to the trajectory of the falling sand. In this standard method there is a detail description of the apparatus required with some sketches and design details for the abrasion test apparatus. Another test method concerning resistance is reported in **ISO 2409:2013** (updating the 2007 version). This standard describes a cutting tool used with automatic cross-cut apparatus for creating the specified V-shape throughout the total coating thickness, for assessing the resistance of paint coatings to separation from substrates when a right-angle lattice pattern is cut into the coating, penetrating through the substrate. The cross-cut test can be used in manual or in motor-driven apparatus. The method is not suitable for coatings

of total thickness greater than 250 micrometres or for textured coatings. It is possible to use this ISO standard either as a pass/fail test or, where circumstances are appropriate, as a six-step classification test. Concerning abrasion, we can also find the standard **DIN 68861-2:198**: Furniture surfaces- Part 2: Behaviour at abrasion. This document specifies a classification for test results determined in accordance with **DIN EN 15185** as it is not contained in the denominated European test standard. It serves for the uniform description of the behaviour of furniture surfaces at abrasion for application in product standards with requirements for the usability requirements of furniture surfaces or for informative marking of products.

### ***Resistance to a falling weight***

The effect of a falling weight on a surface treated with paint or varnish, is instead tested by **ISO 6272-1:2011**, which replaced ISO 6272-1:2002 and which was confirmed in 2017. This is another method for evaluating the resistance of a coating, in particular of a dry film of paint, varnish or related product to cracking or peeling from a substrate when it is subjected to a deformation caused by a falling weight, with a 20-mm-diameter spherical indenter, dropped under standard conditions. It can be applied like a pass/fail test or as a classification test, to determine the minimum mass and/or drop height for which the coating cracks or peels from its substrate by gradually increasing the drop height and/or the mass. The damage resistance of a fiber-reinforced polymer matrix composite is evaluated by a drop weight impact event in standard **ASTM D7136/D7136M-15**. Susceptibility to damage from concentrated out-of-plane impact forces is evaluated in this standard, in order to provide knowledge of the damage resistance properties of a laminated composite plate. The effects of stacking sequence, fiber surface treatment, variations in fiber volume fraction, on the damage resistance of a particular composite laminate to a concentrated drop-weight impact force is useful in polymer industry in regard to the anticipated damage resistance capability of composite structures of similar material, thickness or stacking sequence.

### ***Flexibility and Hardness***

As far as the flexibility of organic coatings, **ASTM D 522/D522M-17** is a description of different standard test methods for mandrel bend test of attached organic coatings. These tests cover the determination of the resistance to cracking (flexibility) of attached organic coatings on substrates of sheet metal or rubber-type materials and they have been useful in rating attached flexible coatings for their ability to resist cracking when elongated. On the contrary, for measuring the hardness of paints or varnishes, the standard **ISO 1522:2006** (revised and confirmed in 2015) can be useful because it specifies two methods of carrying out a pendulum damping test on a coating of paint, varnish or other, related, product. It is applicable to single coatings and to multi-coat systems. The pendulum hardness test is based on the principle that the amplitude of the pendulum's oscillation

will decrease more quickly when supported on a softer surface. The hardness of any given coating is given by the number of oscillations made by the pendulum within the specified limits of amplitude determined by accurately positioned photo sensors. The instrument consists of a pendulum which is free to swing on two balls resting on a coated test panel.

### ***Wettability and Permeability***

Wettability is another of the main parameters considered. A German Standard that permit to determine this property is **DIN 55660-2:2011-12**. This standard specifies a test method for measuring the contact angle for determining the surface free energy of a solid surface. At least three drops, each of at least two test liquids, are dispensed onto a flat test specimen surface. The contact angle is measured for every drop. Using a suitable model divided up into polar and dispersive fractions, the free surface energy of the solid is calculated from the averaged contact angles of each fluid, their surface tensions and their polar and dispersive fractions. On the other side, permeability is investigated in the **ISO 2812:2007**, in which there is a description about all the steps for the determination of the resistance of an individual-layer or multi-layer system of coating materials to the effects of water by partial or full immersion and the assessment of the damage to the substrate. The first part of this protocol contains all the information concerning the immersion method with different kinds of liquid, and the second part is specific for the immersion in water. This standard is currently under revision and will be replaced by ISO/DIS 2812.

### ***Artificial weathering and releases***

Other important standard methods that have been applied for studying the release of chemical or nanoparticles from materials are protocols which simulate the damage of weathering on coatings. An example is the standard **EN 1062-11:2002** which contains four methods for the conditioning of test specimens which have been prepared for testing the resistance to weather conditions of coatings for exterior masonry and concrete. Standard **ISO 16474:2013** (replaced ISO 11507:2007) also give a general guidance for developing the appropriate methods of exposure. The first part of this standard provides information about performances required for the application of artificial accelerated weathering or artificial accelerated irradiation devices. The second part of this ISO specifies methods for exposing specimens to xenon-arc light under controlled conditions in the presence of moisture to reproduce the weathering effects that occur when materials are exposed in actual end-use environments to daylight or to daylight filtered through window glass. The third part instead contains the method of exposure to laboratory light sources and the descriptions of general performance requirements for devices used for exposing paints and varnishes to laboratory light sources.

Prediction of performance in natural environments has also been performed by **ASTM B117-16** which simulates a corrosive environment in order to produce relative corrosion resistance information for specimens of metals and coated metals exposed in a given test chamber. In this standard, the description of the salt spray (fog) test is illustrated, including the apparatus, procedure, and all the conditions required.

The only standard method found that describes the leaching behaviour of substances from coatings into water over defined time intervals is **BS EN 16105:2011**. Under specific laboratory conditions required by this standard, it is possible to identify all the substances that can be leached from coatings, particularly by driving rain, and transferred into the environment, in intermittent contact with water. Coatings indeed are exposed under natural weather conditions to intermittent cycles of wetting (rainfall, thaw, condensate) and drying. As describes in ISO procedure, it is necessary that coating shall have a homogeneous planar surface, which shall be inert and coatings shall adhere well to it during the entire period of immersion in water. The water from each immersion cycle is analysed for determining the concentration of released target substances.

### ***Thickness***

Another important parameter is the thickness of coatings applied to a substrate, which is described in the **ISO 2808:2007**, which was confirmed in 2010. In this standard the methods for determining wet-film thickness, dry-film thickness and the film thickness of uncured powder layers are described. This standard will be replaced by ISO/NP 2808.

### ***Gloss***

An important parameter considered in restoration of work of arts is the gloss. Gloss indeed is associated with the capacity of a surface to reflect more light in directions close to the specular than in others. **ISO 2813:2014** (replaced ISO 2813:1994) specifies a method for determining the gloss of coatings using the three geometries of 20°, 60° or 85°. The 60° geometry is applicable to all paint films, but for very high gloss and near-matt films 20° or 85° may be more suitable. The 20° geometry is intended to give improved differentiation between high-gloss paint films, the 85° geometry is intended to give improved differentiation between low-gloss paint films. The method is suitable for the gloss measurement of non-textured coatings on plane, opaque substrates.

Also the standard **ASTM D523-14** represent a suitable protocol to measure the gloss of coatings, but this is a test method which compare the specular reflectance from the specimen to that from a black glass standard, measuring gloss rating. Since specular reflectance depends also on the surface refractive index of the specimen, the measured gloss ratings change as the surface refractive index changes. This standard covers the measurement of the specular gloss of 60, 20, and 85° as the previous standard ISO.

### ***Description of performance requirements***

Many other ISO found contain descriptions and protocols concerning the performance requirements to test paints or coatings in general. For instance, **ISO 20340:2011**(replaced ISO 20340:2009) describes performance requirements for protective paint systems for offshore and related structures (i.e. those exposed to the offshore environment, as well as those immersed in sea or brackish water). This standard will be replaced by ISO/FDIS12944-9 and it contains the test methods to be used to determine the composition of the separate components of the protective paint system, the laboratory performance test methods for the assessment of the likely durability of the protective paint system and the criteria to be used to evaluate the results of performance tests. Another standard which describe the standard practice for operating UV light exposure is also defined by **ASTM G154-16**. This practice gives general procedures for using fluorescent UV lamp weathering devices for simulate a wide range of exposure conditions. Exposure may simulate the effects of sunlight through window glass through the application of procedures for obtaining, measuring, and controlling conditions of exposure. Other performance requirements were found in the description of individual standard, depending on the aim of the protocol.

#### ***2.2.1.2. Plastics and rubber***

##### ***Abrasion***

Resistance to abrasion is also performed in plastic industry by the application of **ISO 5470-1:2016** (replaced ISO 5470-1:1999). This standard indeed contains the determination of abrasion resistance of rubber- or plastics- coated fabrics with the Taber abrader. This protocol is similar to the standard applied for paints and varnishes (ISO 7784-2:2016), which uses the rotating abrasive rubber wheel method in order to simulate the effect of human contact or to perform the resistance to abrasion.

##### ***Resistance to a falling weight***

As plastics are viscoelastic, they may be sensitive to changes in velocity of weights falling on their surfaces. Thus, **ASTM D5420-04** (replaced by ASTM D5420-16) is a test method that describes the determination of the relative ranking of materials according to the energy required to crack or break flat, rigid plastic specimens considering specified conditions of impact of a striker impacted by a falling weight. This protocol also called Gardner Impact, contained similar characteristics of ISO 6272-1:2011, which performs the resistance to a falling weight on paints and varnishes.

Another similar test which determines the strength of plastics under defined conditions of Charpy impact is **ISO 179-3:2010**. In this standard there are many different protocol for test configurations, according to the type of materials, the type of test specimen and the type of notch, under the impact conditions defined and for estimating the brittleness or toughness of specimens within the limitations inherent in the test conditions. It is also useful for the determination of comparative data from similar types of material.

### ***Flexibility and Hardness***

The hardness of plastics or rubber can be analysed by **ASTM D2240-15e1** (replaced ASTM D2240), that is the standard test method for rubber property for measuring hardness based on the penetration of a specific type of indenter (a hard tip whose mechanical properties are known) when forced into the material under specified conditions. The indentation hardness is inversely related to the penetration and is dependent on the elastic modulus and viscoelastic behaviour of the material. As explained in this standard, measurements obtained with a specific type of durometer (rubber hardness measurement devices) can differ to those obtained with another type of durometer. Therefore, it is necessary to consider the geometry of the indenter and the applied force before starting the analysis.

### ***Tensile and flexural properties***

**ASTM D 638-14** is a standard test method for tensile properties of plastics, designed to obtain qualitative data for the control and specification of plastic materials. However, because of the high degree of sensitivity exhibited by many plastics to rate of straining and environmental conditions, data obtained by this test method cannot be considered valid for applications involving load-time scales or environments widely different from those of this test method. It is necessary to have a tensile testing machine for measuring the elastic strength of unreinforced and reinforced plastics. Similar to this test method is the **ISO 14125:1998**. It gives information about the determination of flexural properties of fibre-reinforced plastic composites. In 2001 this standard was extended with a Corrigenda, and in 2011 with an Amendment. Another standard that contain the description of tensile properties of plastics is **ISO 527-4:1997**. It was confirmed in 2014 and in the 4<sup>th</sup> part of this standard describes the test conditions for isotropic and orthotropic fibre-reinforced plastic composites.

All the standard method reported so far, have been developed for investigating the performances of both coatings (surfaces with organic coating, paints or varnishes) and plastic/rubber. As it can be seen in table 1, there is only a technical standard evaluating the release of substances from coatings (BS EN 16105:2011) used in the treatment of rigid substrates. Although it is true that most of these

standards have been applied in the literature to investigate materials performances, most of them have been adapted in order to investigate the possible releases which can occur from the materials under specific conditions. Moreover, for release tests there are also many papers in which no standards are applied. As far as only few studies concerning material releases from substrates are present in the literature, papers containing performances studies were also considered in this study since they can be adapted for developing useful leaching tests. In this context, the literature research performed was schematized in Table 4. In the table, the relevant papers selected have been reported in chronological order. For each paper, it was identified the material investigated and the substrate where the material was applied for the test (if present), the identification name of the standard methods applied, the simulated weathering conditions (in the case of studies of material release into the environment), the analytical techniques employed and in blue, the specific instrumentation described in the standards.

References were divided between studies of material releases from coatings (in green cells) and studies that analyse the performances of coatings (in blue cells). Standard methods applied in the different works (or their adaptation) are represented in black colour, while standards which are only cited within the paper are marked in red colour. Standards withdrawn (in orange) and standards not specific for this research (in purple) were not considered. It is also necessary to specify that important standards were not applied in many studies and they were only cited by the authors (in red). The latter were reported because they can be useful for specific applications.

Table 4. Schematics of the studies present in the literature concerning material performances (blue cells) and material releases (green cells). Orange colour indicate a standard which has been removed, purple colour indicated standards not useful for this research and standards in red indicated that they have been cited by the study but not necessary applied. The techniques marked in blue are specific for standard methods.

Reference	Substrate/materials	Standard test	Simulated conditions	Techniques
Fahrenheitz <i>et al.</i> 2002	aluminium panels/ nano CeCl <sub>3</sub>	ASTM B117		SEM, EDS, XPS
Rossi <i>et al.</i> 2006	panels of carbon steel/ organic coatings	ASTM D 4060-95		EIS, TMP-ESEM, Taber abrader
Hsu and Chein 2007	wood, polymer, tile panels/ nano TiO <sub>2</sub>	no standard	sunlight, wind, human contacting	SMPS, simulation box

<b>Soucek et al. 2007</b>	aluminium panels/ silicone resin	ASTM D 4541-02, ASTM D 5420-04, ASTM D4060-95, ASTM D3363-00, ASTM D 522-93a		NMR, FTIR, contact angles, Taber abrader, Pencil hardness, conical mandrel bend, pull-off adhesion
<b>Kaegi et al. 2008</b>	fiber cement panels, real façade / nano TiO <sub>2</sub>	no standard	rain water	TEM, SEM, ICP- OES, ICP-MS, EDX, centrifugation
<b>Vorbau et al. 2008</b>	fiberboard plate, fiber cement plate, steel panels/ nano ZnO	DIN 53754:1977, DIN 68861-2:1981, ISO 5470-1:1999, ASTM D 4060- 95:2007	wind	SMPS, CPC, ESP, SEM, TEM, EDX, Taber abrader
<b>Guiot et al. 2009</b>	cotton fabric sample/ nano SiO <sub>2</sub>	ASTM C1353/C1353M-15a		CPC, SMPS, Taber Abrader
<b>Kaegi et al. 2010</b>	facade panels/ nano TiO <sub>2</sub> , nano Ag	no standard	rain water	ICP-MS, TEM, EDX, centrifugation
<b>García-Pacios et al. 2011</b>	stainless steel plates/ PUD	ASTM D2240, ISO 2409:2007, ISO 2808:2007, ISO 1522:2006, ISO 2813:1994, ASTM D1925-70, ISO 4210: 1979		TEM, DSC, TGA, ATR-IR spectroscopy, laser confocal microscopy, cross- cutter adhesion, thickness, Persoz hardness, gloss, yellowness index, chemical resistance against ethanol
<b>Menini et al. 2011</b>	Al <sub>2</sub> O <sub>3</sub> underlayer/ PTFE	ASTM D3359-02 ASTM B489, 2004		SEM, tape test
<b>Scrinzi et al. 2011</b>	steel panels/ nano SiO <sub>2</sub>	ASTM D6037, ASTM D4060, ASTM D968, ASTM G154, ASTM B117, ASTM D 523-14		FTIR, TEM, weathering chamber, Taber abraser test, falling abrasive test, differential

				scanning calorimeter
<b>Wood et al. 2011</b>	no substrate/ epoxy composites	ISO 527-4:1997, ISO 14125:1998, ISO 179-2:1999		SEM, optical microscope, Pendulum impact system
<b>Mirabedini et al. 2012</b>	PFTE sheets/ nano ZrO <sub>2</sub> , nano clay	ASTM D 638, ASTM B117		TEM, SEM, DSC, DMTA, XRD, salt spray test
<b>Olabarrieta et al. 2012</b>	no substrate/ nano TiO <sub>2</sub>	JIS R 1703-2:2007, ASTM D3359-17, ASTM D 3363-05 (2011)	water	SEM, AFM, EDX, X- ray, ICP-OES, tape test, pencil test
<b>Saber et al. 2012</b>	no substrate/ nano TiO <sub>2</sub>	no standard	wind	SEM, DLS, FMPS, EDS
<b>Schlagenhauf et al. 2012</b>	Si and Al wheels/ CNTs	ISO 7784-2:2006, ISO 9352:1995, ISO 5470-1:1999, ASTM G195-08	wind	FMPS, APS, TEM, SEM, EDX, Taber abrader
<b>Schoknecht et al. 2013</b>	extruded polystyrene (XPS) panels/ general coating	EN 15824, EN 1062-1, EN 998-1, EN 15824, EN 16105:2011, EN 1484		HPLC and UV detector, immersion method
<b>Al-Kattan et al. 2013</b>	fiber cement panels/ nano TiO <sub>2</sub>	ISO 16474-1:2013, EOTA ETAG 004	rain water, sunlight	SEM, EDX, TEM, ICP-OES, ICP-MS, weathering chamber
<b>Stepien et al. 2013</b>	paperboard/ nano TiO <sub>2</sub> , nano SiO <sub>2</sub>	no standard		FESEM, AFM, RMS, Taber abrader, contact angle goniometer
<b>Zuin et al. 2014</b>	fibre cement panels/ nano: TiO <sub>2</sub> , Ag, SiO <sub>2</sub>	ISO 7784-2:2006, ISO 2812-2:2007, ISO 16474-1:2013	rain water, sunlight	DLS, TEM, EDX, XRF, ICP-OES, weathering

				chamber, Taber abrader
<b>Künniger et al. 2014</b>	wood panels/ nano Ag	no standard	rain water	LC-MS/MS, ICP-MS, TEM, EDX, NTA, DGT
<b>Al-Kattan et al. 2015</b>	fiber cement panels/ nano SiO <sub>2</sub>	ISO 16474-1:2013, EOTA ETAG 004	tap water, sunlight	DLS, XRF, STEM, EDX, ICP-OES, weathering chamber
<b>Fiorentino et al. 2015</b>	wood panels/ nano SiO <sub>2</sub> , nano TiO <sub>2</sub>	ISO 16474-3:2013, ISO 7784-2:2006	sunlight	TEM, HR-SEM, DSC, EDS, Taber Abrader + ELPI, weathering chamber
<b>Luangtriratana et al. 2015 a</b>	no substrate/ glass fiber (GRE)	ISO 2409:2013, ISO 2812-2:2007		IR-ATR, cone calorimeter, tape pull test, water soak test
<b>Luangtriratana et al. 2015</b>	no substrate/ yttria doped zirconia, Si glass, alumina tintannate, nanoclay, nano Si	ISO 2812-2:2007, ISO 2409:2007, ASTM D3359, ASTM: D7136, ISO 14125:1998		SEM, water soak test, tape pull test, cone calorimeter, impact drop weight test, flexural performance
<b>Momber et al. 2016</b>	steel panels	ISO 20340:2009, ISO 4287:1997, DIN 55660-2:2011, DIN 55660-1:2011, ISO 12949:2001, ISO 19906:2010, ISO 6272-1:2011, ISO 7784-2:2006		SEM, weathering chamber, abrasion tests, wettability tests, Taber abrader
<b>Shandiya et al. 2015</b>	brick, concrete panels/ nano TiO <sub>2</sub>	ISO 16474-1:2012, ASTM D4060:2007, ASTM D 6037:1996, ASTM D1044:2008	rain water, sunlight and wind	EDS, TEM, CPC, SMPS, APS, MPS, ICP-MS, weathering chamber, Taber abrader
<b>Sung et al. 2014</b>	no substrate/ nano SiO <sub>2</sub>	NIST protocol	sunlight	ICP-OES, ATR-FTIR, XPS, UV-

				Vis, AFM, LSCM, SPHERE UV chamber
<b>Boumaza <i>et al.</i> 2016</b>	steel panels/ nano: ZrO <sub>2</sub> , ZnO, SiO <sub>2</sub> , Fe <sub>2</sub> O <sub>3</sub>	no standard		FTIR-ATR, nanoindentation
<b>Kandola <i>et al.</i> 2016</b>	no substrate/ epoxy composites	ISO 2812-2:2013, ISO 2409:2007, ASTM D3359-17		cone calorimeter, SEM
<b>Xu <i>et al.</i> 2017</b>	no substrate/ nano TiO <sub>2</sub>	no standard		TEM, XRD, SEM, contact angle analyser, <a href="#">weathering chamber</a>
<b>Zhang <i>et al.</i> 2017</b>	fiber cement panels/ nano: SiO <sub>2</sub> , Ag, TiO <sub>2</sub>	ISO 16474-1:2013, ISO 2812-2:2007, EN 1062-11:2002	rain water, acid rain water, sunlight	ICP-MS, SEM, TEM, DLS, <a href="#">weathering chamber</a>

Since the aim of this study was to identify the best experimental conditions to perform leaching test on the new formulation provided by NANORESTART partners, after the application step, we primarily focused on the papers concerning release tests. A brief description of these works will follow below, according to the different test methods/properties (reported in Table 3) chosen by the authors.

A novel method was proposed by Vorbau *et al.* (2009) for the quantification of NPs release from surface coatings into air. Abrasion process (using Taber test) that simulates typical handling (cleaning, walking and sliding) was combined with a Scanning Mobility Particle Sizer (SMPS), and Condensation Particle Counter (CPC) in order to measure the aerosol concentration and the number size distribution. Tests were performed on polyurethane coatings embedded with ZnO nanoparticles and an electrostatic precipitator (ESP) was used for depositing the released particles for further analysis, as and Scanning Electron Microscopy (SEM), Transmission Electron Microscopy (TEM), Energy Dispersion X-ray Spectroscopy (EDX or EDS). From the results obtained, no free ZnO could be collected and the differences between surface coatings with and without NPs after the Taber test were minimal. A similar test was performed by Schlagenhauf *et al.* (2012) to investigate the releases from a sanding process and for studying the abrasion resistance of epoxy-coatings containing carbon-nanotubes (CNTs) in different contents. Authors used Taber Abraser coupled with a Fast Mobility Particle Sizer (FMPS) and an Aerodynamic Particle Sizer (APS) for the identification of the concentration of released CNTs. Analysis of the abraded coatings using SEM,

TEM and EDX showed that free-standing CNTs were released into the environment, even if aerosol instruments (FMPS, APS) were not able to quantify the filler release because of the low content of NPs. Taber Abraser was also modified by Shandilya *et al.* (2015) for simulate the emission into air of TiO<sub>2</sub> nanoparticles embedded in coating matrix. It was used a vitrified clay-carborundum abrasant wheels placed in a nano-secured work post that can permit to obtain the particle size distribution and the particle number concentration using aerosol measurement techniques as CPC, SMPS, APS and Mobility Particle Sizer (MPS) techniques. An artificial weathering was also performed in coated and uncoated brick samples using a weathering chamber that simulate natural sunlight and rainfall. The releases of TiO<sub>2</sub> were quantified by Inductively Coupled Plasma Mass Spectrometry (ICP-MS). Despite the deterioration by weathering that created cracks on the surface, nanocoated sample resulted strong enough to resist leaching of NPs.

Particle size distribution of NPs released from paints was also taken into account by Saber *et al.*, (2012) whose collected dust samples from coating embedded with nano TiO<sub>2</sub> and nano SiO<sub>2</sub> by ESP and the dust was analysed by FMPS and APS. They affirmed that minimal differences from the dust generated by paints with NPs and the conventional products were observed.

Fiorentino *et al.* (2015) instead investigated the release of NPs from paints containing TiO<sub>2</sub> and SiO<sub>2</sub> before and after several types of aging (mechanical, light, moisture). Mechanical aging was simulated on coated panels using a Taber Abraser, and particle number concentration and particle size distribution were determined by electric low-pressure impactor (ELPI). SEM-EDS was used for determining the morphology and size of the collected NPs. Treated panels were exposed to UV lamps and humidity in an accelerated weathering machine in order to simulate the outdoor aging. The results obtained, revealed that the addition of SiO<sub>2</sub> in paints reduced by a factor of 2 the total number of aerosolised NPs during abrasion.

Research conducted by Al-Kattan *et al.* (2013) on the release of paint with and without nano-TiO<sub>2</sub> from fiber cement treated panels was also considered. The simulation of the weathering by sunlight and rain in climate chambers were conducted using standardised conditions of UV irradiation. Studies on the effect of weathering were also discussed by Al-Kattan *et al.* (2015), to simulate the outdoor weathering of different kind of paints (i.e. paints containing pristine nano-SiO<sub>2</sub>, paints with added nano-SiO<sub>2</sub>, dried milled paints and aged milled paints). They also used the weathering chamber to simulate natural weathering by sunlight and rain, based on a European norm. Before starting the artificial weathering experiments, they used XRF for understanding which materials may be released from paints and Dynamic Light Scattering (DLS) for measuring their size distribution. Both these studies investigated the content of powder in the different paint, scraping off paints by a plastic spatula and then exposing it to UV light in the accelerated weathering machine, in order to obtain powder of aged paints. Analytical techniques as Inductively Coupled Plasma Optical Emission spectroscopy (ICP-OES) and ICP-MS were then used, for having a

quantitative measure of the release from rainfall water derived from the weathering chamber and the content of powered and aged paints, while the effects of weathering on the surface of painted panels were characterised by SEM, TEM and EDX. Results by Al-Kattan *et al.* (2013) revealed that even if resulted images show that the polymer matrix was partially destroyed after weathering, TiO<sub>2</sub> NPs remain attached to the surface. Al-Kattan *et al.* (2015) instead revealed that the majority of the released Si was present in the dissolved form and only a small percent was in the nano-particulate form, and the particulate Si was contained in the paint matrix.

Experimental technique for the quantification of the release of nano SiO<sub>2</sub> from coatings altered by UV exposure were also studied by Sung *et al.* (2014). Authors exposed nano-based coatings to precise UV light, temperature and humidity conditions according to the National Institute of Standards and Technology (NIST) in the SPHERE UV chamber. Measurement of NPs released collected from the weathering chamber were analysed using an ICP-OES technique. Chemical degradation of the surface of paints due to the UV exposure was measured by Atomic Force Microscope (AFM) and Fourier Transform Infrared spectroscopy (FTIR), X-ray Photoelectron Spectroscopy (XPS), UV-Vis. Results revealed that both the amount of SiO<sub>2</sub> NPs and the chemical degradation increased with UV dose. The effect of UV light, wind and the human contacting were analysed by Hsu & Chein (2007), which studied the TiO<sub>2</sub> nanoparticles emission from different substrates, as wood, polymer and tile. The simulation box contained UV light/fluorescent lamps, a fan and a rubber knife were connected to a SMPS which measure the particle size distribution and number concentration during tests. After the simulated experiment of the three different panels, tile coated was found to have the highest particle emission and the particle released from wood and polymer substrates decrease significantly with the increase of weathering.

The alteration of paints exposed to weathering conditions was also studied by Kaegi *et al.* (2008), whose collected façade runoff from nano-TiO<sub>2</sub> paints applied on a building painted 2 years before, on an experimental building area painted with the same product. Rain water from a greater urban catchment was also sampled in order to characterise residential and business buildings runoff. Samples of water were then analysed by ICP-MS and ICP-OES after centrifugation and they were then investigated by TEM, EDX, ESEM, HR-SEM. Number densities of synthetic NPs in the runoff were calculated by combining results from microscopic analysis and bulk chemicals. The runoff volume of individual rain events was also determined by Kaegi *et al.* (2010) whose provide direct evidence of release of Ag-NPs from exterior paints to the aquatic environment, collecting façade runoff water from all rain events over a period of one year. Therefore, ICP-MS and microscopic analysis (TEM, EDX) were conducted, and the results revealed that more than 30% of the Ag-NP were released to the environment and these nanoparticles were likely transformed to considerably less toxic forms such as Ag<sub>2</sub>S.

In order to derive information regarding emission into water of substances applied on facades, Schoknecht *et al.* (2013) have been developed an interlaboratory comparison with 8 participants for validating the test method EN16105:2011 for the evaluation of release of substances from coatings. Panels of extruded polystyrene were coated with different coatings and exposed in intermittent contact with water for 1 hour, to simulate the alternation of rain events and dry seasons. Analysis of released substances were conducted by applying high-performance liquid chromatography (HPLC) combined with UV detection, liquid chromatography-mass spectrometry(LC/MS) and LC/MS/MS. Results revealed that the procedure described in the standard method is suitable to investigate the potential released substances with good reproducibility. Authors also affirmed that an adaptation of the analytical methods to circumvent interference with co-eluted substances is necessary.

Loss of Ag-NPs contained in paints in one year of exposition of environmental weathering were also monitored by Künniger *et al.* (2014). In this study, LC-MS/MS, ICP-MS, TEM, EDX, Nanoparticle tracking analysis (NTA) and diffusive gradients in thin films (DGT) were employed to quantify the effect of weathering, mechanical abrasion and deterioration by microorganisms, and the results indicate that the nanoparticles of Ag are likely transformed to Ag clusters, reducing the Ag toxicity.

Accelerated aging of photocatalytic coatings under a water flow was simulated by Olabarrieta *et al.* (2012), creating an experimental protocol in order to study the loss of photocatalytic activity, to identify the degradation of mechanical properties and to quantify the release of TiO<sub>2</sub> nanoparticles in different coatings. It was tested a commercial product as a reference material for photocatalytic coatings and a experimentally prepared coating containing 50 wt.% of TiO<sub>2</sub> NPs embedded in a siliceous matrix. The accelerated aging procedure was designed specifically for this study, which simulate the effect of water and UV light. After investigating the adhesion and the hardness of these coatings, SEM, X-ray diffraction, EDX and ICP-OES results showed a deactivation of the active sites upon prolonged immersion and a release of NPs by the interaction among TiO<sub>2</sub>, NaCl and UV light.

The most promising works for our scope, are those of Zuin *et al.* 2014 and Zhang *et al.* 2017, both investigating the release of titanium dioxide (TiO<sub>2</sub>), silica (SiO<sub>2</sub>) and silver (Ag) ENPs embedded in paints applied on fiber cement panels. Standard methods were considered for both these studies, in order to provide release data, simulating the exposure to ambient weather conditions.

Zuin *et al.* (2014) used a spectrophotometer to determine colorimetric variations on coated panels before and after the implementation of short wave UV for 500 h in the accelerated weathering machine according to ISO 11507:2007 revised by ISO 16474-1:2013, for reproducing the damaging effects of sunlight. Abrasion was also carried out on coated panels by adopting a Taber Rotary Platform Abrader under dry condition, applying 500 cycles/rotation with a rotating abrasive rubber

wheel, according to ISO 7784-2:2006. The procedure for the determination of the resistance to liquids, and more specifically the water immersion method described in ISO 2812-2:2007, was opportunely adapted in this case study, to provide data of the release of ENPs from the different paints. Leaching analysis were started directly after finishing UV exposure and after the application of the Taber abrader, and they consist on the immersion of  $\frac{3}{4}$  of the length of the panels and with a surface/volume ratio  $S/V=2$  in order to submerge the maximum of the surface of the panel; they collected leaching liquids after 4, 8, 24, 120 hours which were then analysed by ICP-OES. After the water immersion test, they add a small amount of acetic acid as leaching solution in order to simulate acid rain effect on coated panels. The particle released from coated panels was also observed by TEM, EDX and XRF, providing images of the surface degradation. The results confirmed that release of  $\text{SiO}_2$  is related to the duration of the immersion cycles, while  $\text{TiO}_2$  NPs has a low release into water and Ag NPs measured was under detection limit of ICP-OES ( $0.1\mu\text{g/l}$ ).

Zhang *et al.* (2017) also applied the protocol described in ISO 16474-1:2013 for the identification of possible releases from the exposure of coatings to artificial weathering, and the samples were analysed after 100, 150, 200, 250, 300, 350, 400 and 500h for the leaching tests. Water immersion method was also employed by applying ISO 2812-2:2007 and following the same experimental conditions reported by Zuin *et al.* 2014. NPs releases were investigated after 500h of weathering. The effect of pH on the releases was also investigated by varying the pH from 3 to 10. Authors studied the particle size distribution by the means of DLS, the release of NPs by ICP-MS, while SEM and TEM were used to identify the distribution of the nanoparticles in the matrix before starting the analysis. ISO 1062-11:2002 was taken into account as method for conditioning the samples before testing the coating materials. The results obtained, explained that the duration of weathering test and rainfall are more important in controlling the release of NPs than the variation of pH.

### 2.2.2. *Experimental leaching test*

According to the results obtained from the bibliographic search, leaching tests for the products' post-application phase (i.e. when the treated work of art is exposed to indoor or outdoor conditions) were performed in collaboration with the groups of Dr. Marino Lavorgna (CNR-IPCB of Naples) and Dr. Gabriella Di Carlo (CNR-ISMN of Roma).

The interest was focused on multilayer coating systems used for the protection of bronze works of art, especially for outdoor environments. In fact, after discussing with products' developers in NANORESTART, it was agreed that for the other categories of products releases of formulations' components (including nanomaterials) were negligible or not significant.

In detail, the two active formulations F3 and F4, and the passive coating U2 BYC 333 (represented in diagrams as U2) were selected for this study. Since it was not possible to analyse nano-based ingredient releases because of the detection limits of the conventional instruments used for nanoparticles characterization, it was decided to follow the release of benzotriazole (BTA) which is an ingredient of the active coatings, and it can be detected also at very low concentrations by UV-Vis spectroscopy. BTA is used as anticorrosive compound for metal substrates (Finšgar and Milošev, 2010; Finšgar and Merl, 2014) and it is usually encapsulated into nanocarriers to avoid interactions with the coating matrix which can lead to the degradation of the barrier layer or inactivation of the inhibitor. The role of nanocarriers is to release the inhibitor in response to local changes of pH, since the initiation of corrosion activity leads to local changes of pH near the surface defects (damages produced by degradation). For this reason, it is expected an increase of releases of BTA at acidic pH levels (Kamburova *et al.*, 2014). It has to be underline that in the framework of safety assessment, investigating the release of BTA from treated coatings is of great interest since this inhibitor is classified as harmful to aquatic life with long-lasting effects (H 412) by CLP self-classification.

The procedure followed by the groups of Naples was extrapolated from the bibliographic research previously reported. In particular, the procedure described by Zuin *et al.* 2014 was adapted according to the experimental requirements.

An active layer and a passive over layer were applied on the surface of a first bronze panel and then full immersed in 20 ml of MilliQ water and a second panel in 20 ml of MilliQ water acidified to pH 5 with acetic acid (0.1 M CH<sub>3</sub>COOH) respectively. The acidification was performed to simulate acid rain effect, according to the procedure reported by Zuin and colleagues, but also to investigate the increased release of BTA from nanocarrier in these conditions. The volume of 20 ml was selected considering the detection limits of UV-Vis analysis for BTA and the maximum amount of BTA that could be released in the leaching medium from the active coating. Leaching behaviour was investigated collecting aliquots of 400 µl after 4, 8, 24, 120 and 156h. All leachates were analysed directly after sampling by UV-Vis spectroscopy for the investigation of the inhibitor release from coated disks.

The concentration of BTA released from F3 and F4 was estimated by using the linear fit of BTA alone (Figure 22a) performed in MilliQ water, considering the absorbance of BTA at 278 nm. Then, it was calculated the maximum amount of BTA that could be release from F3 and F4 in the leaching medium in order to understand the range of possible releases and indicated as 'F3 max' (Figure 22b) and 'F4 max' (Figure 23b).

The active coatings alone were previously investigated by UV-Vis in order to understand their behaviour during several days of total immersion in water. As expected, from these preliminary tests it emerges that F3 and F4 layers completely dissolve in solution (both neutral and acidified)

after 24 hours. Passive coating alone was also investigated by following the same experimental procedure described for active ones, since it contained BTA derivatives among the ingredients which can interfere with the signals of BTA. Indeed, these ingredients exhibit an intense absorbance in the 200-400 nm range, thus masking the BTA absorption bands even after short-time immersion, especially under acid conditions (Figure 22c).

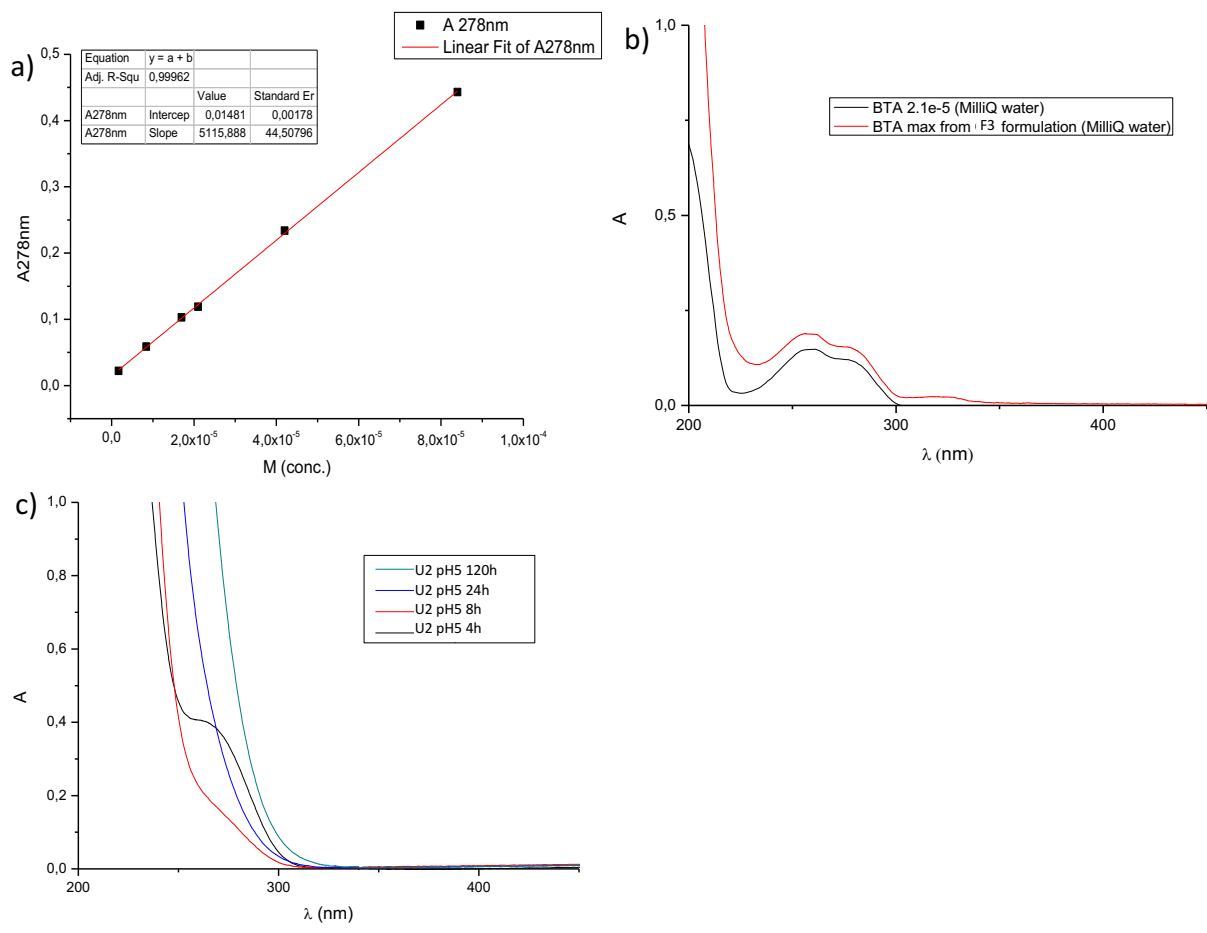


Figure 22. a) Linear fit of BTA absorption at 278 nm in MilliQ water, b) UV-Vis spectra of BTA in MilliQ water (black line) and maximum BTA which can be released by F3 in MilliQ water (red line), c) UV-Vis spectra of the leaching solutions of U2 BYC 333 passive coating deposited on the reference alloy after different time of immersion in MilliQ acidified water.

Based on previous results, leaching tests were performed by immersing in MilliQ water the reference alloy disks covered by the selected multi-layered coatings, consisting of active layer and passive overlayer.

The results are reported in Figure 23, where UV-Vis spectra show that BTA is partially released from active coatings F3 and F4 covered by the passive coating U2 BYC 333 in MilliQ water (Figure 23a and 23b) and acidified MilliQ water (Figure 23c and 23d). In these spectra, as expected, it is possible to notice that the passive overlayer avoid the total active film dissolution, preventing BTA release from multi-layered coatings in neutral conditions; indeed, the signal corresponding to the maximum amount of BTA which can be released from F3 and F4 is always higher than the signals observed for the multi-layer system. More specifically, considering the multi-layer system U2 BYC 333 and F4, the BTA released after immersion in neutral water for 4 h was less than 50% (Figure

23b). This value was also comparable to the one obtained after 8h of immersion. On the contrary, for multi-layered coatings consisting of U2 BYC 333 and F3, the inhibitor release was negligible even after 8 h of immersion, since no significant absorption band was observed at 278 nm in the UV-Vis spectra of the leaching solutions (Figure 23a).

In the case of immersion tests in acidified MilliQ water, it was not possible to quantify the release of BTA by UV-Vis spectroscopy, as clearly evidenced in Figure 23c and 23d because of the interferences of ingredients contained in U2 BYC 333 passive coating. Therefore, these results show that, in neutral conditions, the hydrophobicity and the barrier properties of the passive layer are effective in reducing and/or slowing down the release of the inhibitor embedded in the active layer. However, although the BTA released in this experiment is low (estimated as  $<0.1\text{ mg/l}$ ), this amount could be relevant for the environment, depending from the extent of the treated artworks surface.

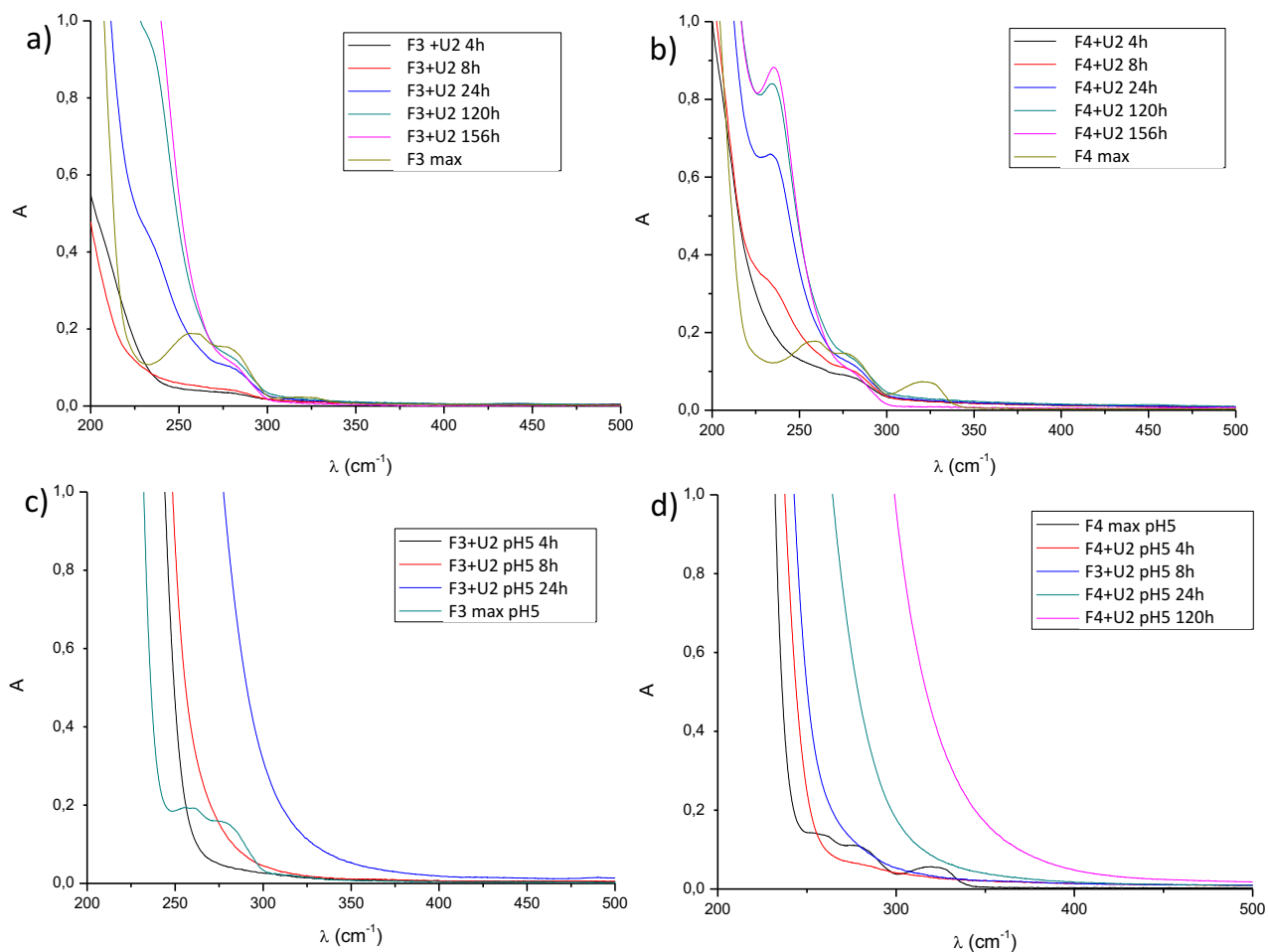


Figure 23. UV-Vis spectra of the leaching solutions after 4, 8, 24, 120 and 156 h of immersion of F3 and F4 max and multi-layered coatings made with F3 active coating and U2 passive coating a) in MilliQ water and b) in acidified water, and made with F4 and U2 c) in MilliQ water and d) in acidified water.

## 2.3. Safety assessment

In this chapter, the results of the safety assessment performed for application and post-application phases of the selected innovative nano-enabled products presented in Chapter 1.5, are reported. As explained in Chapter 1.4, they are derived by combining the information collected in Step 2 (CLP self-classification) and Step 3 (ITS, colloidal characterization as well as leaching testing; the latter two described in Chapters 1.6 and 1.7, respectively) of the SbD framework.

### 2.3.1. Cleaning formulations

Three cleaning fluids (i.e. AM5, G1 and G1-Ncap) were selected to perform safety assessment according to the methodology presented in Chapter 1.4, and were compared to Ethanol and Xylene/Toluene (50/50), indicated as suitable conventional products by relevant partners.

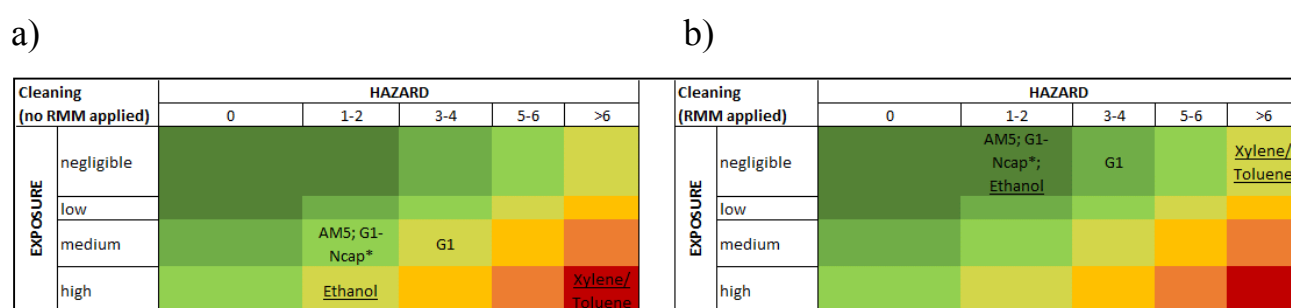
The screening hazard assessment (i.e. CLP self-classification) was performed on both cleaning formulations and conventional products, showing that the mixture of xylene/toluene (50/50) is classified for eight H hazards, followed by G1 classified for three H hazards, AM5 and G1-Ncap classified for two H hazards each, and Ethanol classified for one H hazard. However, it must be noted that the classification of 5% of G1-Ncap is unknown due to the presence of the ingredient Ncap, which was newly synthesized in the project. Therefore, the advanced hazard assessment was performed to better understand whether AM5 should be preferred to G1-Ncap or vice versa.

According to the proposed ITS, acute ecotoxicological tests were performed showing no acute toxicity for the three tested formulations (i.e. the CLP threshold  $EC_{50} > 1$  mg/l was satisfied by all of them). Looking in detail at the results provided by the experts in ecotoxicology, AM5 resulted to be more toxic towards the 3 test species than G1, which in turn was more toxic (by one order of magnitude) than G1-Ncap. Moreover, the conventional ingredient BioSoft resulted clearly more toxic than the greenest equivalent Ncap, with a difference of an order of magnitude. This finding is in agreement with the data observed for the formulation G1 and represents a further evidence that the effects exerted by G1 (and AM5) are strictly linked to the toxicity of BioSoft, as well as G1-Ncap toxicity is linked to Ncap.

By combining the results of the screening hazard assessment and the acute ecotoxicological testing, G1-Ncap resulted to be the most promising product to be forwarded to the second tier of ecotoxicological analyses (i.e. chronic toxicity). Experimental results obtained on chronic test with *D. magna* (i.e. 60% mortality) allowed to classify G1-Ncap as “Chronic 3” (i.e.  $0.1 \text{ mg/l} < \text{NOEC} < 1 \text{ mg/l}$ ). Since chronic ecotoxicological data on relevant ingredients (i.e. 2-butanol, methyl ethyl

ketone, ethyl acetate, propylene carbonate) are not available in the literature, it was not possible to understand which of them are playing a major role in the whole formulation's toxicity.

Finally, the overall safety of the innovative cleaning formulations was assessed for the application phase, by applying the methodology described in Chapter 1.4. Results are depicted in Figure 24a and b, highlighting that the safety ranking for cleaning formulations is AM5; G1-Ncap > G1. In the worst-case scenario (i.e. no RMM applied, Figure 5a), G1 can be considered equal to ethanol in terms of safety but much better compared to a mixture of xylene and toluene (50/50), the latter showing the lowest safety in the matrix. Looking at the more realistic case (i.e. recommended RMM applied, Figure 24b), it can be concluded that all the proposed innovative systems have an excellent to very good environmental performance.



\* Hazard for aquatic environment was not assigned according to CLP self-classification; however chronic toxicity was assessed with *D.magna* test and classified the formulation at least as Chronic 3.

Figure 24. Safety assessment of cleaning formulations and (underlined) conventional cleaning products: a) with no RMM applied and b) with recommended RMM applied from the greenest top left corner (i.e. excellent level of safety) to the reddest bottom right corner (i.e. bad level of safety).

However, the light chronic toxicity for aquatic environment showed by G1-Ncap indicates that attention must be paid in case of relevant exposure to the aquatic environment and suggests the need to extend this analysis to the other formulations (at least to the conventional ones for comparison purposes).

Safety assessment for the post-application phase was not performed since, according to product's developers, no residues of cleaning formulations are left on the artefact surface after treatment.

### 2.3.2. Surface consolidation systems

Six formulations (i.e. Silica/PEI, Silica/PEI/CMC, CNF, NRA-CE04, CSGI 1, CSGI 2) were studied and they were compared to Paraloid B-72, indicated as an example of suitable conventional product by relevant partners.

In the screening hazard assessment step, formulations were classified as follows: NRA-CE04 for two H hazards, CSGI 1 and CSGI 2 for one H hazard each, while Silica/PEI, Silica/PEI/CMC, CNF

and the conventional Paraloid B-72 were not classified. However, it should be noted that for CSGI 1 and CSGI 2, the classification is partly unknown (for 2% each) due to the presence of ingredients newly synthesized in the project.

According to the first tier of the proposed ITS, none of the tested consolidants resulted acutely toxic (i.e. the CLP threshold  $EC_{50} > 1$  mg/l was satisfied by all of them). Looking in detail at the results provided by the experts in ecotoxicology, Silica/PEI/CMC, CNF, CSGI 1, CSGI 2 and NRA-CE04 showed a negligible acute effect while Silica/PEI exhibited a significant ability to impair algal development, even if the effects were not so marked to be classified as acutely toxic. Since the main difference in the composition of Silica/PEI and Silica/PEI/CMC concerns the percentage (w/w) of the polyelectrolyte (0.7% in Silica/PEI; 0.01% in Silica/PEI/CMC), it cannot be excluded that the lower toxicity observed towards *P. subcapitata* could be due to the lower amount of polyelectrolyte used in the composition of Silica/PEI/CMC. This hypothesis is reinforced if we consider that the used polyelectrolyte is the only ingredient classified as hazardous for the aquatic environment (Cat 2) among those used for the development of the formulations for surface strengthening and consolidation.

Finally, the conventional Paraloid B-72 showed significant effects towards the green algae *Pseudokirchneriella subcapitata*.

By combining the results of the screening hazard assessment and the acute ecotoxicological testing, as well as technical considerations provided by products' developers, the most promising formulations forwarded to the ITS' second tier were CNF, Silica/PEI/CMC, CSGI 1 and CSGI 2. The *D. magna* reproduction test applied on these four formulations resulted into a "Chronic 2" classification.

Finally, as depicted in Figure 25a and 25b, the safety ranking for surface consolidation systems in the application phase is Silica/PEI; Silica/PEI/CMC; CNF > CSGI 1; CSGI 2 > NRA-CE04 .

In the worst-case scenario (i.e. no RMM applied, Figure 25a), Silica/PEI, Silica/PEI/CMC and CNF can be considered equal to Paraloid B-72 in terms of safety. Looking at the more realistic case (i.e. recommended RMM applied, Figure 25b), it can be concluded that all the proposed innovative systems have an excellent to very good environmental performance.

a)

b)

Consolidation (no RMM applied)		HAZARD				
		0	1-2	3-4	5-6	>6
EXPOSURE	negligible	Silica/PEI; Silica/PEI/CMC*; CNF*; Paraloid B-72				
	low					
	medium		CSGI 1*; CSGI 2*			
	high		NRA-CE04			

Consolidation (RMM applied)		HAZARD				
		0	1-2	3-4	5-6	>6
EXPOSURE	negligible	Silica/PEI; Silica/PEI/CMC*; CNF*; Paraloid B-72	CSGI 1*; CSGI 2*; NRA-CE04			
	low					
	medium					
	high					

\* Hazard for aquatic environment was not assigned according to CLP self-classification; however chronic toxicity was assessed with D.magna test and classified the formulation as Chronic 2.

Figure 25. Safety assessment of strengthening formulations and (underlined) conventional strengthening products: a) with no RMM applied and b) with recommended RMM applied from the greenest top left corner (i.e. excellent level of safety) to the reddest bottom right corner (i.e. bad level of safety).

However, the chronic toxicity for aquatic environment showed by CNF, Silica/PEI/CMC, CSGI 1 and CSGI 2 indicates that attention must be paid in case of relevant exposure to the aquatic environment and suggests the need to extend this analysis to other formulations (at least to the conventional one for comparison purposes).

Safety assessment for the post-application phase was not performed since, according to product's developers, after treatment the product is bounded to the substrate and cannot be distinguished from it.

### 2.3.3. Coatings for the protection of metal substrates

As far as active coatings are concerned, seven formulations (i.e. F1 to F5, SCEv1 and SCEv3) were investigated and compared to INCRALAC (diluted to reach 88% toluene), indicated as suitable conventional product by relevant partners. Among the developed passive coatings, only U2 BYC 333 was investigated and compared to the conventional SOTER 201 LC.

The screening hazard assessment (Step 2 of the framework) resulted as follows: the conventional SOTER is classified for six H hazards and one ENV hazard, followed by SCEv1 and SCEv3 (four H hazards and two ENV hazards each), the passive coating U2 BYC 333 and the conventional INCRALAC (four H hazards each), and F1 to F5 (one H hazard each). However, it should be noted that for F5 and SCEv1 and SCEv3 the classification is partly unknown (for 0.06%, 0.70%, and 1.09% respectively) due to the presence of ingredients newly synthesized in the project.

According to the first tier of the proposed ITS, none of the tested formulations resulted acutely toxic (i.e. the CLP threshold  $EC_{50} > 1$  mg/l was satisfied by all of them), and the differences among the formulations' toxicity were minimal. Looking in detail at the results provided by the experts in ecotoxicology, as far as active coatings are concerned, with the Daphnia test, only SCE v1 (SCEv3 was not tested being very similar to SCEv1) showed an appreciable effect after 24-h and 48-h of exposure, nevertheless the observed toxicity did not allow for an "Acute I" classification despite the significant  $EC_{50}$  calculated after 48-h. F1 and F2 showed an appreciable effect only after 48-h of exposure, while for the other 3 products the effects were minimal also at the highest tested concentration (1000 mg/l). A similar trend was observed with the bacteria: in this case, SCEv1 resulted toxic toward *Vibrio fischeri* at all the tested intervals (5, 10 and 15 minutes), F1 provided

an EC<sub>50</sub> after 15 and 30 minutes, while for all the other formulations the effects were low also at the highest tested concentration.

As for the algal growth inhibition test, only F4 did not exert any appreciable effect on the growth rate of *P. subcapitata*, while for all the other mixtures it was possible to calculate an EC<sub>50</sub>. The different effects observed among F4 (non toxic) and the other formulations (especially F1 and F2, toxic towards at least 2 bioindicators), cannot be related either to the ethanol concentration, since it is very similar for all the 5 products, or to the ingredient NRA-CC04 (developed in the project), since it resulted not toxic towards daphnids and bacteria, even if it inhibited significantly algal growth. Finally, as compared to the conventional product INCRALAC, all the formulations resulted less toxic but SCE v1, which showed an higher toxicity towards *D. magna* and provided comparable results with Microtox® Test.

As far as passive coatings are concerned, due to the reaction observed once the formulation U2 BYC 333 was diluted with the testing media (formation of clumps and white patina), it was possible to perform with success only the test with *D. magna* and the results highlighted a significant effect on water fleas survival, but not so strong to generate an “Acute I” classification. In addition, the conventional product SOTER (i.e. only the liquid fraction of the biphasic mixture) showed no effect towards water fleas and green algae, but was significantly toxic toward the bacteria, even if also in this case the magnitude of the effects was not enough to generate an acute classification.

The most promising formulations forwarded to the ITS second tier (i.e. chronic testing) were F3 and F4. For both the formulations, the estimated NOEC was < 0.1 mg/l and therefore they were classified as "Chronic 2" according to CLP thresholds.

Finally, as depicted in Figure 26a and 26b, the safety ranking for active coatings in the application phase is F1; F2; F3; F4; F5 > SCE v1; SCE v3. In the worst-case scenario (i.e. no RMM applied, Figure 26a), SCEv1 and SCEv3 can be considered equal to INCRALAC in terms of safety. Looking at the more realistic case (i.e. recommended RMM applied, Figure 26b), it can be concluded that all the proposed innovative active systems have an excellent to very good environmental performance.

a)

b)

Active coatings (no RMM applied)		HAZARD				
		0	1-2	3-4	5-6	>6
EXPOSURE	negligible	Green	Green	Green	Yellow	Orange
	low	Green	Green	Yellow	Orange	Red
	medium	Green	F1; F2; F3*; F4*; F5	Yellow	Orange	Red
	high	Green	Yellow	SCE v1***; SCE v3***; INCRALAC	Orange	Red

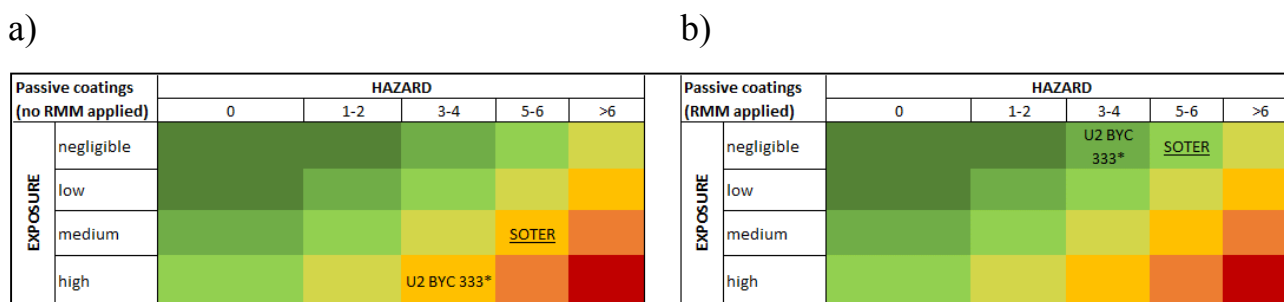
Active coatings (RMM applied)		HAZARD				
		0	1-2	3-4	5-6	>6
EXPOSURE	negligible	Green	F1; F2; F3*; F4*; F5	SCE v1***; SCE v3***; INCRALAC	Yellow	Orange
	low	Green	Green	Yellow	Orange	Red
	medium	Green	Green	Yellow	Orange	Red
	high	Green	Green	Yellow	Orange	Red

\* Hazard for aquatic environment was not assigned according to CLP self-classification; however chronic toxicity was assessed with *D. magna* test and classified the formulation as Chronic 2. \*\* Hazard for aquatic environment - CAT1(A) and CAT 1 - should be added according to CLP; however acute toxicity was not confirmed by experimental tests on SCE v1.

Figure 26. Safety assessment of active coatings and (underlined) conventional coatings: a) with no RMM applied and b) with recommended RMM applied from the greenest top left corner (i.e. excellent level of safety) to the reddest bottom right corner (i.e. bad level of safety).

However, the chronic toxicity for aquatic environment showed by F3 and F4 indicates that attention must be paid in case of relevant exposure to the aquatic environment and suggests the need to extend this analysis to other formulations (at least to the conventional one for comparison purposes).

As far as passive coatings are concerned, Figure 27a and 27b shows the safety classification for the application phase for U2 BYK 333 compared to the conventional SOTER. In the worst-case scenario (i.e. no RMM applied in Figure 27a), U2 BYK 333 can be considered equal to SOTER in terms of safety while in the more realistic case (i.e. recommended RMM applied in Figure 27b), it performs better than the conventional product, their safety being classified as very good and good, respectively.



\* Hazard for aquatic environment - CAT1(A) and CAT 1 - should be added according to CLP; however acute toxicity was not confirmed by experimental tests on the (very similar) previous version of the formulation (U2).

Figure 27. Safety assessment of passive coatings and (underlined) conventional coatings: a) with no RMM applied and b) with recommended RMM applied from the greenest top left corner (i.e. excellent level of safety) to the reddest bottom right corner (i.e. bad level of safety).

As far as safety assessment for the post-application phase is concerned, leaching tests were performed on multi-layered (i.e. an active layer and passive overlayer) coatings for bronze surfaces, as reported in Chapter 2.2. Obtained results allowed to identify a partial release of BTA, which was not possible to be exactly quantified because of interference substances in the passive coatings. An estimation of the maximum amount of release of BTA was performed (<0.1mg/l) and the comparison of EC<sub>50</sub> found literature reveal differences of three order of magnitude, highlighting no effect considering acute test.

However, due to the lack of information regarding the chronic effect of BTA in literature, it can be useful to perform chronic ecotoxicological tests.

### 3. Conclusions

In this study, the development of innovative nano-enabled formulations for the conservation and restoration of modern and contemporary artworks, was supported according to a Safe-by-Design (SbD) approach.

More specifically, to address the first objective of the thesis' work, the colloidal characterization of the selected innovative formulations was performed by means of Dynamic Light Scattering (DLS) and Centrifugal Separation Analysis (CSA) techniques. The stability of the dispersions, in terms of agglomeration and dissolution of specific nanoparticles after proper dilutions of samples, was assessed. Important information through the comparison of different formulations with different stability but similar compositions were obtained, as the identification of i) the samples which do not contained nanoparticles or ii) the ingredients which increase the stability of a formulation.

It has to be underline that the detection limits of the employed techniques did not allow to characterize the formulations at the concentrations relevant for ecotoxicological testing (i.e. from 0.1 mg/l to 1000 mg/l), and that there is a lack of precise information regarding the possible correlation between the stability (revealed by CSA and DLS) and the toxicity (revealed with ecotoxicological tests) of the formulations. However, the results obtained so far are useful to elucidate fate and behaviour of nano-components and therefore to support the experimental design needed for ecotoxicological testing.

The second thesis' objective was met by conducting a literature review and identifying a suitable experimental procedure for the quantification of possible product's releases into the environment from treated artworks. Only few papers concerning nanoparticles releases from works of art were found while more results were obtained for treated buildings façades. Among the different procedures, immersion test was selected as the most suitable method considering: the type of material investigated (coating of bronze artworks), the environment (outdoor) and the released substance to follow (chemical or nano-based ingredient).

In this context, the identification of BTA was carried out during the time of immersion in water of the panel covered by multi-layer coatings, while its precise quantification was not possible to perform. In the passive coating indeed, there were some BTA derivate which interfere with the BTA signal, which cannot permit to derive the concentration of BTA released. Even if it was not possible to exactly predict this release, from this study emerge the importance of testing innovative formulation by keeping experimental setting close to reality.

Finally, preliminary conclusions on the chemical safety of innovative products' in the application and post-application phases could be derived in semi-quantitative and qualitative terms, respectively. Obtained results allowed to raise additional questions that could be investigated and

answered in the future, once more precise information on production volumes and uses of such products will be available.

# References

Al-Kattan, A., Wichser, A., Vonbank, R., Brunner, S., Ulrich, A., Zuin, S., Arroyo, Y., Golanski, L., Nowack, B. (2013) 'Release of TiO<sub>2</sub> from paints containing pigment-TiO<sub>2</sub> or nano-TiO<sub>2</sub> by weathering', *Environmental Science: Processes & Impacts*, 15 (12), pp. 2155–2358.

Al-Kattan, A., Wichser, A., Vonbank, R., Brunner, S., Ulrich, A., Zuin, S., Nowack, B. (2015) 'Characterization of materials released into water from paint containing nano-SiO<sub>2</sub>', *Chemosphere*. Elsevier Ltd, 119, pp. 1314–1321.

ASTM D4541-17, 'Standard Test Method for Pull-Off Strength of Coatings Using Portable Adhesion Testers'. American Society for Testing and Materials. Philadelphia, USA, 2017.

ASTM D7234-12, 'Standard Test Method for Pull-Off Adhesion Strength of Coatings on Concrete Using Portable Pull-Off Adhesion Testers'. American Society for Testing and Materials. Philadelphia, USA, 2017.

ASTM D3363-05 (2011), 'Standard Test Method for Film Hardness by Pencil Test'. American Society for Testing and Materials. Philadelphia, USA, 2017.

ASTM G195-13a, 'Standard Guide for Conducting Wear Tests Using a Rotary Platform Abraser'. American Society for Testing and Materials. Philadelphia, USA, 2017.

ASTM D7136 / D7136M-15, 'Standard Test Method for Measuring the Damage Resistance of a Fiber-Reinforced Polymer Matrix Composite to a Drop-Weight Impact Event'. American Society for Testing and Materials. Philadelphia, USA, 2017.

ASTM D5420-16, 'Standard Test Method for Impact Resistance of Flat, Rigid Plastic Specimen by Means of a Striker Impacted by a Falling Weight (Gardner Impact)'. American Society for Testing and Materials. Philadelphia, USA, 2017.

ASTM D522/D522M-17, 'Standard Test Methods for Mandrel Bend Test of Attached Organic Coatings'. American Society for Testing and Materials. Philadelphia, USA, 2017.

ASTM B117-16, 'Standard Practice for Operating Salt Spray (Fog) Apparatus'. American Society for Testing and Materials. Philadelphia, USA, 2017.

ASTM D523-14, 'Standard Test Method for Specular Gloss'. American Society for Testing and Materials. Philadelphia, USA, 2017.

ASTM D638-14, 'Standard Test Method for Tensile Properties of Plastics'. American Society for Testing and Materials. Philadelphia, USA, 2017.

ASTM G154-16, 'Standard Practice for Operating Fluorescent Ultraviolet (UV) Lamp Apparatus for Exposure of Nonmetallic Materials'. American Society for Testing and Materials. Philadelphia, USA, 2017.

ASTM D968-17, 'Standard Test Methods for Abrasion Resistance of Organic Coatings by Falling Abrasive'. American Society for Testing and Materials. Philadelphia, USA, 2017.

ASTM D4060-14, 'Standard Test Method for Abrasion Resistance of Organic Coatings by the Taber Abraser'. American Society for Testing and Materials, Philadelphia, USA, 2010.

ASTM D3359-08 'Standard Test Methods for Measuring Adhesion by Tape Test'. American Society for Testing and Materials. West Conshohocken, PA, USA.

ASTM D 6037-13e1. 'Standard test method for dry abrasion mar resistance of high gloss coatings'. West Conshohocken, PA, USA.

Babick, F. (2016) 'Suspensions of Colloidal Particles and Aggregates'. pp. 1-358. Springer.

Baglioni, P., Chelazzi, D., Giorgi, R., Poggi, G. (2013) 'Colloid and materials science for the

conservation of cultural heritage: Cleaning, consolidation, and deacidification', *Langmuir*. American Chemical Society, 29 (17), pp. 5110–5122.

Baglioni, P. and Chelazzi, D. (2013) 'Nanoscience for the Conservation of Works of Art'. Royal Society of Chemistry.

Baglioni, P., Chelazzi, D., Giorgi, R. (2015) 'Nanotechnologies in the Conservation of Cultural Heritage'. Springer Netherlands.

Balliana, E., Ricci, G., Pesce, C., Zendri, E. (2016) 'Assessing the value of green conservation for cultural heritage: positive critical aspects of already available methodologies.', *International Journal of Conservation Science*, 7(1), pp. 185–202.

Bhattacharjee, S. (2016) 'DLS and zeta potential - What they are and what they are not?', *Journal of Controlled Release*. Elsevier B.V., 235, pp. 337–351.

Borcherding, J., Baltrusaitis, J., Chen, H., Stebounova, L., Wu, C. M., Rubasinghege, G., Mudunkotuwa, I. A., Caraballo, J. C., Zabner, J., Grassian, V. H., Comellas, A. P. (2014) 'Iron oxide nanoparticles induce *Pseudomonas aeruginosa* growth, induce biofilm formation, and inhibit antimicrobial peptide function', *Environmental Science: Nano*, 1 (2), pp. 123-155.

Borisova, D., Möhwald, H. and Shchukin, D. G. (2011) 'Mesoporous silica nanoparticles for active corrosion protection', *ACS Nano*, 5(3), pp. 1939–1946. doi: 10.1021/nn102871v.

Boumaza, M., Khan, R. and Zahrani, S. (2016) 'An experimental investigation of the effects of nanoparticles on the mechanical properties of epoxy coating', *Thin Solid Films*. Elsevier B.V., 620, pp. 160–164. doi: 10.1016/j.tsf.2016.09.035.

Brunelli, A., Zabeo, A., Semenzin, E., Hristozov, D., Marcomini, A. (2016) 'Extrapolated long-term stability of titanium dioxide nanoparticles and multi-walled carbon nanotubes in artificial freshwater', *Journal of Nanoparticle Research*, 18 (5), p. 113.

Cataldi, A., Dorigato, A., Deflorian, F., Berglund, L., Pegoretti, A. (2014) 'Polymer composite with

micro- and nanocellulose for artwork protection and restoration', ECCM16-16<sup>TH</sup> EUROPEAN CONFERENCE ON COMPOSITE MATERIALS, Seville, Spain.

Dhawan, A., Anderson, D. and Shanker, R. (2017) *Nanotoxicology: Experimental and Computational Perspectives*. *Royal Society of Chemistry*.

Deutsches Institut für Normung e. V., DIN 68861-2:2013-02. 'Furniture surfaces. Part 2: Behavior at abrasion'. DIN, Berlin.

Deutsches Institut für Normung e. V., DIN 55660-2:2011-12. 'Paints and varnishes. Wettability. Part 2: Determination of the free surface energy of solid surfaces by measuring the contact angle'. DIN, Berlin.

ECHA (2007a) 'Guidance for the implementation of REACH: guidance on information requirements and chemical safety assessment. Part A: introduction to the guidance document'.

ECHA (2007b) 'Guidance for the implementation of REACH: guidance on information requirements and chemical safety assessment. Part B: hazard assessment'.

ECHA (2007c) 'Guidance for the implementation of REACH: guidance on information requirements and chemical safety assessment. Part D: exposure scenario building'.

ECHA (2017) 'Guidance on the application of the CLP criteria'. Helsinki.

EFSA (2010) 'Opinion on the Potential Risks Arising from Nanoscience and Nanotechnologies on Food and Feed Safety'. Brussels.

Ente Italiano di Normazione, EN 1062-11:2002 'Paints and varnishes. Coating materials and coating systems for exterior masonry and concrete. Methods of conditioning before testing'. UNI, Milano.

Ente Italiano di Normazione, EN 16105:2011. Paints and varnishes. Laboratory method for

determination of release of substances from coatings in intermittent contact with water

European Commission (2006) 'Regulation (EC) No 1907/2006 of the European Parliament and of the Council of 18 December 2006 concerning the Registration, Evaluation, Authorisation and Restriction of Chemicals (REACH), establishing a European Chemicals Agency'.

European Commission (2008) 'Regulation (EC) No 1272/2008 of the European Parliament and of the Council of 16 December 2008 on classification, labelling and packaging of substances and mixtures, amending and repealing Directives 67/548/EEC and 1999/45/EC, and amending Regulation (EC)'.

Fahrenholtz, W. G., O'Keefe, M. J., Zhou, H., Grant, J.T. (2002) 'Characterization of cerium-based conversion coatings for corrosion protection of aluminum alloys', *Surface and Coatings Technology*, 155, pp. 208–213.

Feng, X., Chen, A., Zhang, Y., Wang, J., Shao, L., Wei, L. (2015) 'Central nervous system toxicity of metallic nanoparticles', *International Journal of Nanomedicine*, 10, pp. 4321–4340.

Ferrari, A., Pini M., Neri, P., Bondioli, F. (2015) 'Nano-TiO<sub>2</sub> Coatings for Limestone: Which Sustainability for Cultural Heritage?', *Coatings*, 5(3), pp. 232–245.

Finšgar, M. and Kek Merl, D. (2014) 'An electrochemical, long-term immersion, and XPS study of 2-mercaptobenzothiazole as a copper corrosion inhibitor in chloride solution', *Corrosion Science*, 83, pp. 164–175.

Finšgar, M. and Milošev, I. (2010) 'Inhibition of copper corrosion by 1,2,3-benzotriazole: A review', *Corrosion Science*, 52 (9), pp. 2737–2749.

Fiorentino, B., Golanski, L., Guiot, A., Damlencourt, J. F. Boutry, D. (2015) 'Influence of paints formulations on nanoparticles release during their life cycle', *Journal of Nanoparticle Research*, 17(3).

Gallego-Urrea, J. A., Perez Holmberg, J. and Hassellöv, M. (2014) 'Influence of different types of natural organic matter on titania nanoparticle stability: effects of counter ion concentration and pH', *Environmental Science: Nano*, 1 (2), pp. 181–189.

Gottardo, S., Alessandrelli, M., Atluri, R., Barberio, G., Bergonzo, P., Bleeker, E., Andy, M., Borges, T., Buttol, P., Castelli, S., Chevillard, S., Dekkers, S., Delpivo, C., Fanghella, D. P., Dusinska, M., Einola, J., Ekokoski, E., Fito, C., Gouveia, H., Hoehener, K., Jantunen, P., Laux, P., Lehmann, H. C., Leinonen, R., Mech, A., Micheletti, C., Pesudo, L. Q., Polci, M. L., Walser, T., Wijnhoven, S., Crutzen, H. (2017) 'NANoREG framework for the safety assessment of nanomaterials'.

Gottschalk, F. and Nowack, B. (2011) 'The release of engineered nanomaterials to the environment', *Journal of Environmental Monitoring*, 13, pp. 1145–1155.

Guiot, A., Golanski, L. and Tardif, F. (2009) 'Measurement of nanoparticle removal by abrasion', *Journal of Physics: Conference Series*, 170.

Hassellöv, M., Readman, J. W., Ranville, J. F., Tiede, K. (2008) 'Nanoparticle analysis and characterization methodologies in environmental risk assessment of engineered nanoparticles', *Ecotoxicology*, 17 (5), pp. 344–361.

Hristozov, D., Gottardo, S., Semenzin, E., Oomen, A., Bos, P., Peijnenburg, W., van Tongeren, M., Nowack, B., Hunt, N., Brunelli, A., Scott-Fordsmand, J. J., Tran, L., Marcomini, A. (2016) 'Frameworks and tools for risk assessment of manufactured nanomaterials', *Environment International*. Elsevier Ltd, 95, pp. 36–53.

Hristozov, D., Gottardo, S., Critto, A., Marcomini, A. (2012) 'Risk assessment of engineered nanomaterials: A review of available data and approaches from a regulatory perspective', *Nanotoxicology*, 6(8), pp. 880–898.

Hsu, L. Y. and Chein, H. M. (2007) 'Evaluation of nanoparticle emission for TiO<sub>2</sub> nanopowder coating materials', *Journal of Nanoparticle Research*, 9 (1), pp. 157–163.

International Organization for Standardization (ISO) (2008) 'ISO/TS 27687:2008 Nanotechnologies. Terminology and definitions for nano-objects. Nanoparticle, nanofibre and nanoplate'. ISO, Geneva.

ISO/IEC Guide 2 (1996) 'Standards in our world. Available at: [http://www.iso.org/sites/ConsumersStandards/1\\_standards.html](http://www.iso.org/sites/ConsumersStandards/1_standards.html), ISO/IEC Guide 2:1996, definition 3.2.

International Organisation for Standardisation (ISO) 'ISO 7784-2:2016. Paints and varnishes. Determination of resistance to abrasion. Part 2: Method with abrasive rubber wheels and rotating test specimen. ISO, Geneva.

International Organisation for Standardisation (ISO) 'ISO 2409:2013. Paints and varnishes. Cross-cut test. ISO, Geneva.

International Organisation for Standardisation (ISO) 'ISO 5470-1:2016. Rubber- or plastics-coated fabrics. Determination of abrasion resistance. Part 1: Taber abrader. ISO, Geneva.

International Organisation for Standardisation (ISO) 'ISO 6272-1:2011. Paints and varnishes. Rapid-deformation (impact resistance) tests. Part 1: Falling-weight test, large-area indenter. ISO, Geneva.

International Organisation for Standardisation (ISO) 'ISO 179-2:2013. Plastics. Determination of Charpy impact properties. Part 2: Instrumented impact test. ISO, Geneva.

International Organisation for Standardisation (ISO) 'ISO 1522:2015. Paints and varnishes. Pendulum damping test. ISO, Geneva.

International Organisation for Standardisation (ISO) 'ISO 2812-2:2017. Paints and varnishes. Determination of resistance to liquids. Part 2: Water immersion method. ISO, Geneva.

International Organisation for Standardisation (ISO) 'ISO 16474:2013. Paints and varnishes.

Methods of exposure to laboratory light sources. ISO, Geneva.

International Organisation for Standardisation (ISO) 'ISO 2808:2010. Paints and varnishes. Determination of film thickness.

International Organisation for Standardisation (ISO) 'ISO 2813:2014. Paints and varnishes. Determination of gloss value at 20 degrees, 60 degrees and 85 degrees. ISO, Geneva.

International Organisation for Standardisation (ISO) 'ISO 20340:2011. Paints and varnishes. Performance requirements for protective paint systems for offshore and related structures. ISO, Geneva.

International Organisation for Standardisation (ISO) 'ISO 14125:1998. Fibre-reinforced plastic composites -- Determination of flexural properties. ISO, Geneva.

International Organisation for Standardisation (ISO) 'ISO 527-4:1997. Plastics. Determination of tensile properties. Part 4: Test conditions for isotropic and orthotropic fibre-reinforced plastic composites. ISO, Geneva.

Kaegi, R., Ulrich, A., Sinnet, B., Vonbank, R., Wichser, A., Zuleeg, S., Simmler, H., Brunner, S., Vonmont, H., Burkhardt, M., Boller, M. (2008) 'Synthetic TiO<sub>2</sub> nanoparticle emission from exterior facades into the aquatic environment', *Environmental Pollution*. Elsevier Ltd, 156 (2), pp. 233–239.

Kaegi, R., Sinnet, B., Zuleeg, S., Hagendorfer, H., Mueller, E., Vonbank, R., Boller, M., Burkhardt, M. (2010) 'Release of silver nanoparticles from outdoor facades', *Environmental Pollution*. Elsevier Ltd, 158 (9), pp. 2900–2905.

Kamburova, K., milkova, V., Radeva, Ts. (2014) 'Polyelectrolyte coatings on hematite nanoparticles impregnated with corrosion inhibitor benzotriazole', *Colloids and Surfaces A: Physicochemical Engineered Aspects*, 462, pp. 237-243.

Kandola, B. *et al.* (2016) 'Thermal Protection of Carbon Fiber-Reinforced Composites by Ceramic

Particles', *Coatings*, 6(2), p. 22.

Khanna, S. (2008) 'Nanotechnology in High Performance Paint Coatings', *Asian Journal of Experimental Science*, 21(2), pp. 25–32.

Künniger, T., Gerecke, A. C., Ulrich, A., Huch, A., Vonbank, R., Heeb, M., Wichser, A., Haag, R., Kunz, P., Faller, M. (2014) 'Release and environmental impact of silver nanoparticles and conventional organic biocides from coated wooden façades', *Environmental Pollution*. Elsevier Ltd, 184, pp. 464–471.

Lead, J. R. and Smith, E. (2009) 'Environmental and human health impacts of nanotechnology'. Blackwell Publishing Ltd.

van Leeuwen, C. J. and Vermeire, T. G. (2007) 'Risk Assessment of Chemicals: An Introduction'. Springer Netherlands.

Lerche, D. (2002) 'Dispersion Stability and Particle Characterization by Sedimentation Kinetics in a Centrifugal Field', *Journal of Dispersion Science and Technology*. Taylor & Francis, 23(5), pp. 699–709.

Lerche, D. and Sobisch, T. (2007) 'Consolidation of concentrated dispersions of nano-and microparticles determined by analytical centrifugation', *Powder Technology*, 174, pp. 46–49.

Luangtriratana, P., Kandola, B. K. and Ebdon, J. R. (2015) 'UV-polymerisable, phosphorus-containing, flame-retardant surface coatings for glass fibre-reinforced epoxy composites', *Progress in Organic Coatings*. Elsevier B.V., 78, pp. 73–82.

Luangtriratana, P., Kandola, B. K. and Myler, P. (2015) 'Ceramic particulate thermal barrier surface coatings for glass fibre-reinforced epoxy composites', *Materials and Design*. Elsevier Ltd, 68, pp. 232–244.

Lynch, I., Dawson, K. A., Lead, J. R., Valsami-Jones, E. (2014) 'Macromolecular Coronas and Their Importance in Nanotoxicology and Nanoecotoxicology'. 1<sup>st</sup> edition, Frontiers of Nanoscience. 1st edn. Elsevier Ltd.

Menini, R., Ghalmi, Z. and Farzaneh, M. (2011) 'Highly resistant icephobic coatings on aluminum alloys', *Cold Regions Science and Technology*. Elsevier B.V., 65(1), pp. 65–69.

Mirabedini, S. M., Behzadnasab, M. and Kabiri, K. (2012) 'Effect of various combinations of zirconia and organoclay nanoparticles on mechanical and thermal properties of an epoxy nanocomposite coating', *Composites Part A: Applied Science and Manufacturing*. Elsevier Ltd, 43(11), pp. 2095–2106.

Mitrano, D. M., Motellier, S., Clavaguera, S., Nowack, B. (2015) 'Review of nanomaterial aging and transformations through the life cycle of nano-enhanced products', *Environment International*. Elsevier Ltd, 77, pp. 132–147.

Momber, A. W., Irmer, M. and Glück, N. (2016) 'Performance characteristics of protective coatings under low-temperature offshore conditions. Part 1: Experimental set-up and corrosion protection performance', *Cold Regions Science and Technology*. Elsevier B.V., 127, pp. 76–82.

Movia, D., Gerard, V., Maguire, C. M., Jain, N., Bell, A. P., Nicolosi, V., O'Neill, T., Scholz, D., Gun'ko, Y., Volkov, Y., Prina-Mello, A. (2014) 'A safe-by-design approach to the development of gold nanoboxes as carriers for internalization into cancer cells', *Biomaterials*. Elsevier Ltd, 35 (9), pp. 2543–2557.

Mudunkotuwa, I. A. and Grassian, V. H. (2015) 'Biological and environmental media control oxide nanoparticle surface composition: the roles of biological components (proteins and amino acids), inorganic oxyanions and humic acid', *Environmental Science: Nano*. Royal Society of Chemistry, 2(5), pp. 429–439.

Nel, A., Xia, T., Mädler, L., Li, N. (2006) 'Toxic potential of materials at the nanolevel', *Science*, 311 (5761), pp. 622–627.

OECD (2003) 'Descriptions of Selected Key Generic Terms Used in Chemical Hazard/Risk Assessment'.

OECD and European Commission (2012) 'Series on the Safety of Manufactured Nanomaterials No. 33: Important Issues on Risk Assessment of Manufactured Nanomaterials'. Paris.

Olabarrieta, J., Zorita, S., Peña, I., Rioja, N., Monzón, O., Benguria, P., Scifo, L. (2012) 'Aging of photocatalytic coatings under a water flow: Long run performance and TiO<sub>2</sub> nanoparticles release', *Applied Catalysis B: Environmental*, 123–124, pp. 182–192.

Ormsby, B. and Learner, T. (2014) 'Artists' acrylic emulsion paints: materials, meaning and conservation treatment options', *AICCM bulletin*, 34 (April), pp. 57–65.

Ormsby, B., Phenix, A., Keefe, M., Learner, T. (2016) 'A productive collaboration between conservation and industry: Developing wet surface cleaning systems for unvarnished painted surfaces', *Studies in Conservation*. Routledge, 61 (sup2), pp. 313–314.

Ortelli, S., Costa, A. L., Blosi, M., Brunelli, A., Badetti, E., Bonetto, A., Hristozov, D., Marcomini, A. (2017) 'Colloidal characterization of CuO nanoparticles in biological and environmental media', *Environmental Science: Nano*. The Royal Society of Chemistry, 4, pp. 1264–1272.

Pecora, R. (2000) 'Dynamic light scattering measurement of nanometer particles in liquids', *Journal of Nanoparticle Research*, 2, pp. 123–131.

Piccinno, F., Gottschalk, F., Seeger, S., Nowack, B. (2012) 'Industrial production quantities and uses of ten engineered nanomaterials in Europe and the world', *Journal of Nanoparticle Research*, 14(9).

Praetorius, A., Labille, J., Scheringer, M., Thill, A., Hungerbühler, K., Bottero, J. Y. (2014) 'Heteroaggregation of titanium dioxide model natural colloids under environmentally relevant conditions', *Environmental Science and Technology*, 48 (18), pp. 10690–10698.

Robinson, A. and Lawson, R. (2016) 'FRONTIERS OF NANOSCIENCE. Materials and Processes for Next Generation Lithography'. Elsevier.

Rossi, S., Deflorian, F. and Risatti, M. (2006) 'Modified Taber apparatus and new test geometry to evaluate the reduction of organic coatings corrosion protective properties induced by abrasive particles', *Surface and Coatings Technology*, 201(3–4), pp. 1173–1179.

Saber, A. T., Koponen, I. K., Jensen, K. A., Jacobsen, N. R., Mikkelsen, L., Moller, P., Loft, S., Vogel, U., Wallin, H. (2012) 'Inflammatory and genotoxic effects of sanding dust generated from nanoparticle-containing paints and lacquers', *Nanotoxicology*, 6 (7), pp. 776–788.

Sayes, C. M., Alex Smith, P. and Ivanov, I. V. (2013) 'A framework for grouping nanoparticles based on their measurable characteristics', *International Journal of Nanomedicine*, 8 (Suppl 1), pp. 45–56.

Schlagenhauf, L., Chu, B.T.T., Buha, J., Nüesch, F., Wang, J. (2012) 'Release of carbon nanotubes from an epoxy-based nanocomposite during an abrasion process', *Environmental Science and Technology*, 46 (13), pp. 7366–7372.

Schoknecht, U., Sommerfeld, T., Borho, N., Bagda, E. (2013) 'Interlaboratory comparison for a laboratory leaching test procedure with façade coatings', *Progress in Organic Coatings*. Elsevier B.V., 76 (2–3), pp. 351–359.

Scott, D. A. (1990) 'Bronze Disease: A Review of Some Chemical Problems and the Role of Relative Humidity', *Journal of the American Institute for Conservation*, 29, pp. 193–206.

Scrinzi, E., Rossi, S., Kamarchik, P., Deflorian, F.. (2011) 'Evaluation of durability of nano-silica containing clear coats for automotive applications', *Progress in Organic Coatings*. Elsevier B.V., 71(4), pp. 384–390.

Shandilya, N., Le Bihan, O., Bressot, C., Morgeneyer, M. (2015) 'Emission of titanium dioxide nanoparticles from building materials to the environment by wear and weather', *Environmental Science and Technology*, 49 (4), pp. 2163–2170.

Shchukin, D. G., Zheludkevich, M. and Möhwald, H. (2006a) 'Layer-by-layer assembled

nanocontainers for self-healing corrosion protection’, *Advanced Materials*, 18 (13), pp. 1672–1678.

Shchukin, D. G., Zheludkevich, M. and Möhwald, H. (2006b) ‘Feedback active coatings based on incorporated nanocontainers’, *Journal of Materials Chemistry*, 16 (47), pp. 4561–4566.

Soucek, M. D., Dworak, D. P. and Chakraborty, R. (2007) ‘A new class of silicone resins for coatings’, *Journal of Coatings Technology Research*, 4(3), pp. 263–274.

Stepien, M., Chinga-Carrasco, G., Saarinen, J. J., Teisala, H., Tuominen, M., Aromaa, M., Haapanen, J., Kuusipalo, J., Mäkelä, J.M., Toivakka, M. (2013) ‘Wear resistance of nanoparticle coatings on paperboard’, *Wear. Elsevier*, 307(1–2), pp. 112–118.

Sung, L., Stanley, D., Gorham, J. M., Rabb, S., Gu, X., Yu, L. L., Nguyen, T. (2014) ‘A quantitative study of nanoparticle release from nanocoatings exposed to UV radiation’, *Journal of Coatings Technology Research*, 12 (1), pp. 121–135.

Sutherland, D. (2010) ‘Chapter 2 – Nanoscience in Nature’, *Nature*, (January), pp. 1–15.

Tedesco, E., Mičetić, I., Ciappellano, S. G., Micheletti, C., Venturini, M., Benetti, F. (2015) ‘Cytotoxicity and antibacterial activity of a new generation of nanoparticle-based consolidants for restoration and contribution to the safe-by-design implementation’, *Toxicology in Vitro*, 29 (7), pp. 1736–1744.

Tsuji, J. S., Maynard, A. D., Howard, P. C., James, J. T., Lam, C. W., Warheit, D. B., Santamaria, A. B. (2006) ‘Research strategies for safety evaluation of nanomaterials, part IV: Risk assessment of nanoparticles’, *Toxicological Sciences*, 89 (1), pp. 42–50.

Turk, J., Pranjić, A. M., Tomasin, P., Škrlep, L., Antelo, J., Favaro, M., Škapin, A. S., Bernardi, A., Ranogajec, J., Chiurato, M. (2017) ‘Environmental performance of three innovative calcium carbonate-based consolidants used in the field of built cultural heritage’, *International Journal of Life Cycle Assessment*, 22(9), pp. 1329–1338.

Vorbau, M., Hillemann, L. and Stintz, M. (2009) ‘Method for the characterization of the abrasion

induced nanoparticle release into air from surface coatings', *Journal of Aerosol Science*, 40(3), pp. 209–217.

Wohlleben, W., Kuhlbusch, T. A. J., Schnekenburger, Ju., Lehr, C. M. (2015) 'Safety of nanomaterials along their lifecycle: Release, Exposure, and Human Hazards'. CRC Press Taylor & Francis Group.

Wood, B. M., Coles, S. R., Maggs, S., Meredith, J., Kirwan, K. (2011) 'Use of lignin as a compatibiliser in hemp/epoxy composites', *Composites Science and Technology*. Elsevier Ltd, 71(16), pp. 1804–1810.

Xu, F., Wang, T., Chen, H.Y., Bohling, J., Maurice, A. M., Wu, L., Zhou, S. (2017) 'Preparation of photocatalytic TiO<sub>2</sub>-based self-cleaning coatings for painted surface without interlayer', *Progress in Organic Coatings*. Elsevier, 113(October 2016), pp. 15–24.

Xu, H., Zhang, H., Wang, D., Wu, L., Liu, X., Jiao, Z. (2015) 'A facile route for rapid synthesis of hollow mesoporous silica nanoparticles as pH-responsive delivery carrier', *Journal of Colloid and Interface Science*, 451, pp. 101–107.

Zhang, X., Wang, M., Guo, S., Zhang, Z., Li, H. (2017) 'Effects of weathering and rainfall conditions on the release of SiO<sub>2</sub>, Ag, and TiO<sub>2</sub> engineered nanoparticles from paints', *Journal of Nanoparticle Research*, 19 (10), pp. 5–10.

Zuin, S., Gaiani, M., Ferrari, A., Golanski, L et al. (2014) 'Leaching of nanoparticles from experimental water-borne paints under laboratory test conditions', *Journal of Nanoparticle Research*, 16 (1).

# Ringraziamenti

Per la realizzazione di questo progetto di tesi vorrei ringraziare tutte le persone che mi hanno aiutato e affiancato durante questo tirocinio e internato di tesi con la loro costante presenza e professionalità.

Vorrei iniziare dal ringraziare la mia relatrice, Dott.ssa Elena Semenzin, e la mia correlatrice Elena Badetti che mi hanno aiutata e seguita durante il progetto di tesi dedicandomi molto del loro tempo e trasmettendomi la loro passione per la ricerca. Ringrazio anche tutte le persone del gruppo di ricerca in cui ho svolto tale studio, in particolare Andrea, Alessandro e Gabrio, e tutte le persone di altri gruppo di ricerca che hanno contribuito alla realizzazione dei test ecotossicologici e i test riguardanti il rilascio, sempre molto disponibili ad aiutarmi.

Vorrei inoltre ringraziare la mia famiglia, specialmente mia sorella, mio moroso, e tutti i miei amici per avermi consigliata in tutto questo periodo di studi, manifestandomi sempre il loro supporto.